

Development of Viral Tools for CNS Gene Transfer:
Adeno-Associated Viral Vectors in Gene Therapy of Parkinson's Disease

PhD Thesis

in partial fulfilment of the requirements for the degree
“Doctor of Philosophy (PhD)/Dr. rer. nat.”
in the Neuroscience Program
at the Georg August University Göttingen,
Faculty of Biology

submitted by

Zinayida Shevtsova

born in

Dnipropetrovsk

2006

Declaration

I hereby declare that the thesis: “Development of Viral Tools for CNS Gene Transfer: Adeno-Associated Viral Vectors in Gene Therapy of Parkinson’s Disease” has been written independently and with no other sources and aids than quoted.

Zinayida Shevtsova

Göttingen, March 2006

CONTENTS

Abbreviations	7
1. Introduction	10
1.1. Neurodegeneration	10
1.2. Parkinson's disease (PD)	10
1.2.1. Prevalence and symptomatology of PD	10
1.2.2. Morpho-pathological background of PD	11
1.2.3. Genetic clues to the etiology of PD	12
1.2.4. Environmental contribution to the etiopathogenesis of PD	13
1.2.5. Mechanisms of cell death in PD	13
1.2.6. Oxidative stress and mitochondrial dysfunction in PD	14
1.2.7. Basal ganglia physiology	17
1.2.8. Animal models of PD: complete unilateral 6-OHDA rat model	19
1.3. Therapeutic approaches for PD treatment	21
1.3.1. Current therapeutical strategies and limitations	21
1.3.2. Neuroprotective gene therapy: achievements and perspectives	22
1.3.3. Glial cell line-derived neurotrophic factor (GDNF)	22
1.3.4. BclX _L , an antiapoptotic member of the bcl-2 family proteins	24
1.4. AAV vectors as tools for gene therapy	25
1.5. Semliki Forest virus (SFV) vectors	27
1.6. Epitope-tagging	28
2. Materials and Methods	29
2.1. Materials	29
2.1.1. Chemicals	29
2.1.2. Antibodies	29
2.1.3. Plasmids	30
2.1.4. Oligonucleotides (Sigma-Aldrich)	30
2.1.5. Cell lines and electrocompetent cells	32
2.1.6. Buffers and Solutions	32
2.2. Methods	33
2.2.1. Cloning procedures	33

2.2.1.1. PCR-amplification	33
2.2.1.2. <i>In vitro</i> transcription	34
2.2.1.3. Sequencing of PCR-amplified DNA	34
2.2.1.4. DNA precipitation	34
2.2.1.5. DNA restriction, electrophoresis, gel extraction, concentration determination	35
2.2.1.6. DNA ligation and transformation in <i>E. coli</i>	35
2.2.1.7. Plasmid Mini- and Maxi - Preps	36
2.2.1.8. Preparation of electrocompetent <i>E. coli</i>	36
2.2.1.9. Cloning into pSFV-plasmid	36
2.2.1.10. Cloning into pAAV-2 plasmid	38
2.2.2. Viral vectors production and purification	41
2.2.2.1. SFV vectors	41
2.2.2.2. AAV vectors	41
2.2.3. Cell culturing	44
2.2.3.1. Continuous cell culture	44
2.2.3.2. Primary culture of hippocampal neurons	44
2.2.3.3. SFV-transduction and cell lysis for western blotting	45
2.2.3.4. Indirect immunofluorescence on primary neurons	45
2.2.4. Animal procedures	45
2.2.4.1. Stereotaxic injection into the rat brain	46
2.2.4.2. Intravitreal injections and optic nerve axotomy	46
2.2.4.3. Transcardial perfusion and brain tissue processing	47
2.2.4.4. Preparation of the brain tissue lysates for WB	48
2.2.5. Indirect immunofluorescence on brain slices	48
2.2.6. Protein handling procedures	48
2.2.6.1. Protein concentration determination	49
2.2.6.2. SDS-polyacrylamide gel electrophoresis (SDS-PAGE)	49
2.2.6.3. Immune blotting	49
2.2.7. GDNF-ELISA	50
2.2.8. Microscopy and image analysis	50
2.2.9. Quantification of neuroprotection in 6-OHDA rat model of PD	51
2.2.10. Rotational behaviour test	51
2.2.11. Statistics	52

3. Results	53
3.1. Development of AAV vectors for targeting different cell types of CNS	53
3.1.1. Construction of AAV vectors	53
3.1.2. <i>In vitro</i> transduction of brain cells by AAV vectors	54
3.1.3. <i>In vivo</i> application of AAV vectors	55
3.2. Evaluation of epitope tags suitability for CNS gene transfer studies	57
3.2.1. Expression constructs of epitope tags used for <i>in vivo</i> gene transfer	57
3.2.2. Structural influence of the epitope tags	58
3.2.3. Evaluation of epitope tags in the central nervous system	59
3.2.4. Evaluation of "established" epitope tags (HA, cMyc, FLAG)	60
3.2.5. Evaluation of "new" epitope tags (AU1, EE, IRS)	60
3.2.5. Proof -of-principle: discrimination of ectopically from endogenously expressed protein	63
3.3. Long-term neuroprotection mediated by AAV gene transfer in the complete 6-OHDA rat model of PD	65
3.3.1. Targeted transduction of SNpc by stereotaxic injection of AAV-2	65
3.3.2. Establishment of the complete 6-OHDA rat model of PD	66
3.3.3. BclX _L mediated protection of DA cell bodies in 6-OHDA rat model of PD	67
3.3.4. GDNF protects DA cell bodies and dendritic protrusions from 6-OHDA toxicity	68
3.3.5. BclX _L and GDNF co-expression has additive neuroprotective effect at 2 weeks after 6-OHDA lesion	68
3.3.6. Co-expression of BclX _L with GDNF has no beneficial effect on dopaminergic neuron survival at 6 weeks after 6-OHDA lesion	70
3.3.7. Effects of delayed AAV-GDNF administration in the rat striatum after the complete 6-OHDA lesion of the MFB	70
4. Discussion	73
4.1. AAV vector targeting	73
4.2. Epitope-tagging for <i>in vivo</i> transgene detection	74
4.3. Neuroprotective therapy of PD as evaluated in the complete 6-OHDA lesion model	77
4.4. BclX _L mediated neuroprotection	78

4.5. Combination of BclX _L and GDNF for neuroprotection of DA neurons	79
4.6. GDNF mediated neurorestorative therapy	80
5. Summary	83
6. Acknowledgements	84
7. References	85
Curriculum vitae	101
Publications	102

Abbreviations

- 6-OHDA** - 6-hydroxydopamine
AAV - adeno-associated virus
ANT - adenine nucleotide transporter
AD - Alzheimer's disease
ADP - adenosine diphosphate
ATP - adenosine triphosphate
BAX - bcl-2-associated X protein
bGH - bovine growth hormone derived polyadenylation site
bp - base pairs
BPB - bromphenol blue sodium salt
BSA - bovine serum albumine
cAMP - cyclic adenosine monophosphate
CNS - central nervous system
COMT - catechol-O-methyltransferase
CPu - caudate putamen (striatum)
Cx - cortex
DA - dopaminergic
DAPI - 4',6-diamidino-2-phenylindole
DIV - day *in vitro*
DMEM - Dulbecco's modified Eagle's medium
DNA - desoxyribonucleic acid
DsRed - red fluorescent protein
DTT - dithiothreitol
EDTA - ethylenediaminetetraacetic acid
EGFP - enhanced green fluorescent protein
ELISA - enzyme-linked immunosorbent assay
ERK - same as MAPK
FA - formaldehyde
FCS - fetal calf serum
FG - fluorogold
FPLC - fast protein liquid chromatography
GABA - γ -aminobutyric acid

GDNF - glial cell line-derived neurotrophic factor
GFAP - glial fibrillary acidic protein
GFL - GDNF family ligands
GFR - GDNF family receptor
GP - globus pallidus
GPe - globus pallidus externum
GPi - globus pallidus internum
GPI - glycosyl phosphatidylinositol
GSH - glutathione
HNC - hippocampal neuron culturesSyn1 – human synapsin 1 gene promoter
HRP - horse reddish peroxidase
HSPG - heparan sulfate proteoglycan
Int - intron
LB - Luria broth
L-DOPA - 1-3,4-dihydroxyphenylalanine
MAPK - mitogen-activated protein kinase, same as ERK
MAO-A - monoamine oxidase A
MAO-B - monoamine oxidase B
mCMV - murine cytomegalovirus immediate early promoter
MFB - medial forebrain bundle
MPTP - 1-methyl-4-phenyl-1,2,3,6-tetrahydropyridine
MWCO - molecular weight cut off
NBM - neurobasal medium
NCAM - neural cell adhesion molecule
NDD - neurodegenerative disorders
NIA - National Institute on Aging (United States of America)
NGS - newborn goat serum
NS - nervous system
nsP - non-structural protein
ORF - open reading frame
PAGE - polyacrylamide gel electrophoresis
PBS - phosphate buffered saline
PCR - polymerase chain reaction
PD - Parkinson's disease
PDGFR - platelet-derived growth factor receptor

PFA - paraformaldehyde

PI3K- phosphatidylinositol 3-kinase

PLC γ - phospholypase-C γ

PNS - peripheral nervous system

PS (-N) - penicillin-streptomycin (-neomycin)

PTP - permeability transition pore

RET - receptor tyrosine kinase

RGC - retinal ganglion cell

ROS - reactive oxygen species

RT - room temperature

RT-PCR - real time PCR

SDS - sodium dodecylsulfate

SFV - Semliki-Forest virus

SN - substantia nigra of the midbrain

SNpc - substantia nigra pars compacta

STN - subthalamic nucleus

SV40 - simian virus 40 polyadenylation site

TB - synthetic transcription blocker

TBS - tris-buffered saline

TBS-T - TBS-tween

TCA - tricyclic aminoacids

TEMED - tetraeminethylendiamine

TH - tyrosine hydroxylase

TH-IR - TH immunoreactive

TNF - tumour necrosis factor

TRAIL - tumour necrosis factor-related apoptosis-inducing ligand

VTA - ventral tegmental area of the midbrain

WPRE - woodchuck hepatitis virus posttranscriptional regulatory element

WB - western blotting

XIAP - X-linked inhibitor of apoptosis protein

1. Introduction

1.1. Neurodegeneration

Nervous system disorders are a major cause of morbidity in the western society, which impair quality of life to a degree rarely affected by other diseases. More than 1% of the population suffer from Parkinson's disease after reaching 55 years of age (de Rijk, M. C. *et al.*, 1997) and nearly half of those who reach the age of 85 years and older suffer from Alzheimer's disease (excerpt from NIA's Progress Report on Alzheimer's Disease, 1998: NIA). Among the factors contributing to the burdensome cost of managing neurodegenerative diseases is the fact that only few symptomatic and no causative therapies are currently available. Despite considerable efforts in basic research, novel diagnostic approaches and effective therapies have yet to be developed.

The majority of human neurodegenerative diseases is not related to inherited mutations of specific proteins but develops with aging as a multifactorial pathology. It is often characterized by features of oxidative stress (Tretter, L. *et al.*, 2004) and axonal degeneration preceding neuronal cell loss, as demonstrated for Alzheimer's disease (Stokin, G. B. *et al.*, 2005), Parkinson's disease (Dauer, W. *et al.*, 2003), Huntington's and other polyglutamine diseases (Gunawardena, S. *et al.*, 2005; Li, H. *et al.*, 2001). Various experimental animal models of neurodegenerative diseases have been developed to provide a better understanding of the complex mechanisms involved in neurodegeneration and to serve for the preclinical evaluation of prospective diagnostic tools and therapies. However, every model can reflect only certain aspects of the complex aetiology of respective diseases in humans. Thus, the evaluation of neuroprotective strategies aiming at generalized inhibition of neurodegeneration should be performed in more than one particular model system. Furthermore, considering the diversity of mechanisms leading to neurodegeneration, effective human therapy may necessitate targeting of more than one neurodegenerative pathway.

1.2. Parkinson's disease (PD)

1.2.1. Prevalence and symptomatology of PD

Parkinson's disease is the second most common neurodegenerative disorder, which affects more than 1% of 55-year-old individuals and more than 3% of those over 75 years of age (de Rijk, M. C. *et al.*, 1997). The overall age- and gender-adjusted incidence rate is 13.4 per 100,000, with a higher prevalence among males (19.0 per 100,000) than females (9.9 per 100,000)(Van Den Eeden, S. K. *et al.*, 2003). It was initially described by James Parkinson in 1817 and characterized by a typical triad of symptoms: 1) poverty and slowness of movement

without paralysis (bradykinesia), 2) changes in posture and muscle tone towards rigidity and 3) resting tremor. In most cases these symptoms are sufficient for the diagnosis of the disease (Hughes, A. J. *et al.*, 2001). Psychological symptoms and autonomic nervous system dysfunction typically develop as the disease progresses and often become a major cause of disability.

1.2.2. Morpho-pathological background of PD

The pathological basis of the disease remained unknown for over 100 years, although the clinical features have been well-described. The importance of the substantia nigra (SN) was emphasized by Tretiakoff in 1919, who studied the substantia nigra in thirteen cases of parkinsonism and found lesions in this nucleus in all cases. The SN, named so because of the native content of the neuromelanin pigment, was noted to show depigmentation, loss of nerve cells, and gliosis. Tretiakoff also confirmed the earlier observation of Lewy (1914), who had found the presence of lipophytic cytoplasmic inclusions in Parkinson's disease, now referred to as *Lewy bodies* and recognized as the pathologic hallmark of the disorder. In 1959, at the International Catecholamine Symposium, Carlsson suggested that Parkinson's disease was related to brain dopamine. In 1960, Ehringer and Hornykiewicz, using Carlsson's methodology, measured greatly reduced DA concentrations, to about one-tenth of normal, in the caudate, putamen and substantia nigra in brains from parkinsonian patients. The underlying key morphopathological feature is the progressive loss of dopaminergic (DA) neurons in the substantia nigra pars compacta (SNpc) of the midbrain, with intracytoplasmic inclusions (Lewy bodies) in the remaining intact nigral neurons (Braak, H. *et al.*, 2000; Forno, L. S., 1996). It is believed that the disease becomes symptomatic when 50-60% of DA neurons in SNpc and more than 70-80% of their projections in the striatum are lost (Deumens, R. *et al.*, 2002). Moreover, the severity and the stage of the disease are correlated with the extent of neurodegeneration (Riederer, P. *et al.*, 1976; Fearnley, J. M. *et al.*, 1991; Foley, P. *et al.*, 1999). DA neurons of SNpc also have a tendency to degenerate with aging at a rate of approximately 5% per decade (Fearnley, J. M. *et al.*, 1991). In PD patients, however, both the rate and the pattern of DA neurodegeneration significantly differ from that observed during normal aging. Thus, the DA neuronal loss in PD in contrast to normal aging is uneven and occurs mainly in the ventro-lateral part of SNpc. While during normal aging the rate of neurodegeneration is about 5 % per decade, it is about 10 fold faster in PD patients.

1.2.3. Genetic clues to the etiology of PD

Despite the early descriptions of clinical and pathomorphological features of PD the etiology of the disease remains unclear. Several genes which are implicated in rare familial forms of PD have been identified over the last decade and revealed novel proteins and pathways that may induce parkinsonism as a result of nigral neurodegeneration. The genetic load of known mutations in PD is small, accounting for less than 5% of the overall PD population. However, the typical and extremely consistent phenotype of both idiopathic and familial PD suggests that one common molecular mechanism may underlie PD. Similar pathways underlying familial forms of the disease might be strongly implicated in the pathogenesis of the sporadic forms. Understanding the pathogenesis of the sporadic form of PD will have the greatest impact on advancing novel therapies for this common incurable neurodegenerative disorder. Five disease genes (*SNCA*, *PARK2*, *PINK1*, *DJ-1*, *LRRK2*) have been conclusively implicated in PD (Abou-Sleiman, P. M. *et al.*, 2006), out of which the most studied are the mutations in the gene encoding for α -synuclein. This protein has also been detected as a major component of the Lewy bodies suggesting its unequivocal role in DA neurons degeneration. The only genetic evidence associating a single mutation in *UCHL1* gene with PD was not sufficient for the conclusive linkage (Abou-Sleiman, P. M. *et al.*, 2006; Leroy, E. *et al.*, 1998).

Data obtained from studies on *DJ-1* and *PINK1* mutations may serve as an indirect evidence of the seminal role of mitochondrial dysfunction and oxidative stress in PD pathogenesis. Endogenous DJ-1 is localised to the mitochondrial matrix and the mitochondrial intermembrane space in addition to its cytoplasmic pool (Zhang, L. *et al.*, 2005), and may act as an antioxidant since it can be oxidized at the cysteine residue C106. Furthermore, a quantitative proteomic study of the SN of mice treated with MPTP revealed a significant increase in the protein DJ-1 in mitochondrial fraction of the SN (Jin, J. *et al.*, 2005). These data suggest that DJ-1 may be involved in neuroprotection of DA neurons from oxidative damage. Another protein implicated in PD, PINK1, consists of a highly conserved kinase domain (Unoki, M. *et al.*, 2001; Nakajima, A. *et al.*, 2003) and a mitochondrial targeting motif (Valente, E. M. *et al.*, 2004). Together with the study showing localization of PINK1 to mitochondria in transfected cells (Beilina, A. *et al.*, 2005), this data may suggest that PINK1 may also act as a protein protecting from oxidative stress (Valente, E. M. *et al.*, 2004). Mutation and polymorphism in another gene, encoding the mitochondrial protease HtrA2/ Omi have been recently associated with PD (Strauss, K. M. *et al.*, 2005).

In addition, possible susceptibility genes (e.g. *NR4A2*, *SNCAIP*) that may increase, or decrease the risk of an individual to develop PD have been identified. However, since only a

minor group of PD patients reveal a genetic predisposition, external factors influencing the initiation and progression of the disease must be examined.

1.2.4. Environmental contribution to the etiopathogenesis of PD

One of the earliest hypotheses of PD pathogenesis was based on the finding that three inhibitors of mitochondrial complex I, namely MPTP, rotenone and paraquat, were able to reproduce parkinsonism with selective DA neuronal loss in mice and primate models (Seniuk, N. A. *et al.*, 1990). The first toxic models of PD did not fully reproduce the features of the disease, mainly because of the absence of one of the major pathological hallmark of PD, the Lewy body. Later, a chronic infusion of either rotenone (Betarbet, R. *et al.*, 2000) or MPTP (Fornai, F. *et al.*, 2005) in rodents was shown to induce the formation of α -synuclein positive aggregates. These data support the theory that sporadic PD may be caused by a combination of genetic predisposition and environmental toxins, which act via inhibition of the mitochondrial complex I to produce selective DA cell loss. Inhibition of complex I may result in the depletion of ATP leading to impairment of all ATP dependent cellular processes, and in generation of free radicals responsible for oxidative stress damage. Clear evidence of increased oxidative stress was found in postmortem PD brains, as compared to the age-matching controls (Andersen, J. K., 2004; Sian, J. *et al.*, 1994). Furthermore, a reduced activity of complex I was found in the brains of idiopathic PD patients (Schapira, A. H. *et al.*, 1990; Parker, W. D., Jr. *et al.*, 1989).

1.2.5. Mechanisms of cell death in PD

The loss of dopaminergic neurons in SNpc is a characteristic feature of PD. However, mechanisms underlying this neurodegeneration are not very well understood. Different modes of cell death, apoptotic, necrotic and autophagic have been described to contribute to the neuronal loss occurring in PD (von Bohlen und Halbach O. *et al.*, 2004; Blum, D. *et al.*, 2001). Several pathogenetic mechanisms have been proposed to be implicated in cell death observed in PD: mitochondrial dysfunction and oxidative stress, defective proteolysis and proteotoxic stress, excitotoxicity, and inflammation (Gandhi, S. *et al.*, 2005; von Bohlen und Halbach O. *et al.*, 2004; Blum, D. *et al.*, 2001). It is likely that PD pathogenesis is multifactorial and all mechanisms listed above to a certain extent contribute to the PD associated degeneration of nigrostriatal neurons. However, one of the single mutations described above, being present in all cells of the body, affects specifically DA cells in SNpc and results in clinico-pathological characteristics of PD. Furthermore, the fact that mutations described in PD affect the proteins remote from each other structurally and functionally suggests the native susceptibility of DA

neurons to various types of cellular stress. In other words, independently on the original trigger, all pathogenetic pathways mentioned above may sequentially be involved in the process of neurodegeneration of SN neurons. Conversely, if various pathogenetic mechanisms may ultimately lead to the same PD phenotype, the evidence of molecular convergence of these pathways must exist. The cellular “powerhouse organelle” mitochondria is a good candidate for a subcellular localization of such a convergence (Gandhi, S. *et al.*, 2005;Beal, M. F., 2005).

1.2.6. Oxidative stress and mitochondrial dysfunction in PD

Mitochondria are important intracellular organelles that play a crucial role in various cellular processes including energy production via pyrimidine biosynthesis, fatty acid oxidation, calcium homeostasis and cell survival (Wang, H. Y. *et al.*, 1991;Elston, T. *et al.*, 1998;Thress, K. *et al.*, 1999;Newmeyer, D. D. *et al.*, 2003;Melov, S., 2004).

Oxydative phosphorylation, occurring in the mitochondria through tricyclic aminoacid (TCA) cycle and proton gradient, is the main source of high energy compounds (e.g. ATP) in the cell. Electrons derived from metabolic utilization of glucose in TCA enter the respiratory electron transport system at the inner mitochondrial membrane (Fig. 1.1). Driven by high potential energy they induce a series of oxidation-reduction reactions resulting in the final reduction of oxygen to produce water. Electron transport chain consists of 4 complexes, which use the potential energy of electrons to pump the protons through the inner mitochondrial membrane into the intermembrane space, thus increasing energy potential across the inner membrane ($\Delta\psi$). Energy created by a charge difference across the inner membrane is stored as ATP via ATP synthesis through the F_0F_1 -ATPase (complex V) or used directly for transmembrane transport. Blocking the electron transport system or reducing the availability of final acceptors like cytochrome c or oxygen can lead to excessive reduction of ubiquinone and ubisemiquinone (Staniek, K. *et al.*, 2002). These accumulated reduced quinones can directly interact with oxygen when it becomes available thus creating free oxygen radicals, which may induce intracellular modification of lipids, proteins and nucleosides.

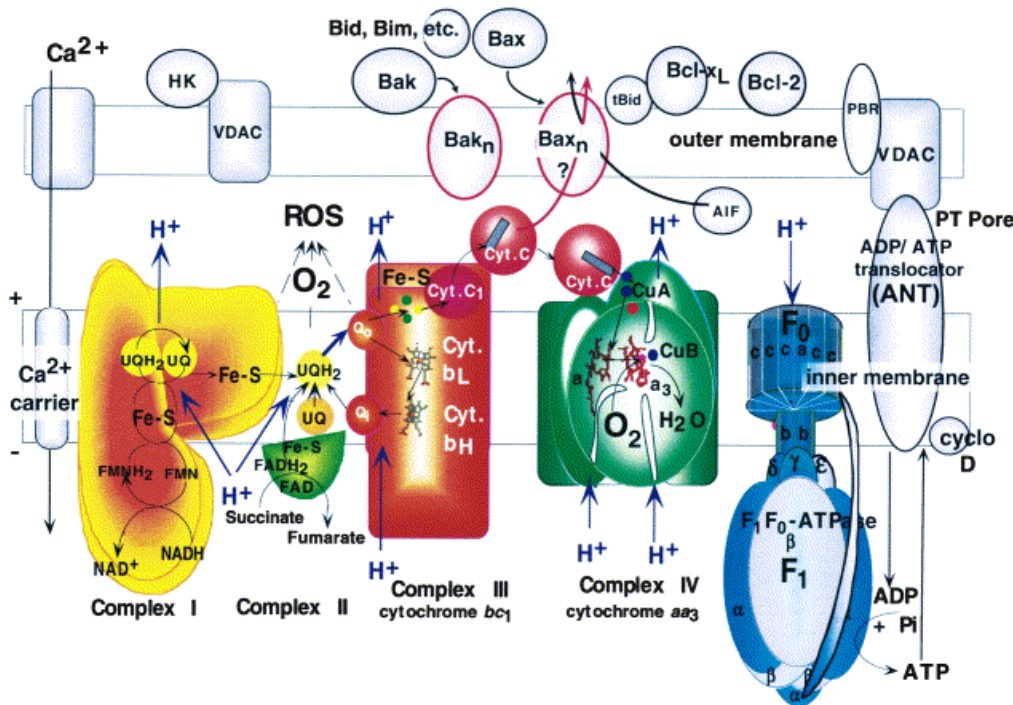


Fig.1.1. The mitochondrial electron transport chain, represented in the context of processes and proteins that may play a role in neuronal cell death. In the inner membrane of the double membrane system of mitochondria, the four respiratory chain components are shown: complexes I (yellow), II (light green), III (brown), and IV (green), with their substrates, cofactors, and the paths of electron flow (black arrows). The ATP synthase (complex V, blue) is shown using the proton gradient to drive ATP synthesis. Radical oxygen species (ROS) are indicated to be produced at the level of complexes I and III where ubiquinol (UQH₂), and ubisemiquinol are formed. In the outer membrane, the pore protein, VDAC (voltage dependent anion channel) is shown interacting with various cytosolic and mitochondrial proteins, including the ADP/ADP translocator (or ANT). The latter interaction is represented as forming the permeability transition pore often associated with loss of the inner membrane potential during apoptosis. UQ, ubiquinone; NAD+, nicotinamide adenine dinucleotide; FMN, flavin mononucleotide; FAD, flavin adenine dinucleotide; Q_o, outer quinone binding site; Q_i, inner quinone binding site; Cyt.b_L, Cyt. b_H, low and high potential cytochrome b; Cyt.c₁, Cyt.c, cytochrome c₁, c; F₀ and F₁, membrane and soluble domains of ATP synthase, with subunits designated; Bax_n = polymeric form of Bax, inserted in the outer membrane, and similarly for Bak_n. Bax, Bak Bcl-x_L, Bcl-2, tBID, AIF: apoptosis inhibitor factor. (Newmeyer, D. D. et al., 2003)

Dopaminergic neurons of SNpc are more likely to be susceptible to the oxidative stress due to the highly oxidative intracellular environment (Lotharius, J. *et al.*, 2002b; Lotharius, J. *et al.*, 2002a). The neurotransmitter dopamine is degraded in the DA cells of SNpc either by monoamine oxidase A (MAO-A) (Gotz, M. E. *et al.*, 1994) or by autoxidation (Fig.1.2). Oxidation of dopamine by MAO-A results in the production of hydrogen peroxide, which after conversion to the hydroxyl radical, leads to oxidation of cellular compounds. Autoxidation of dopamine generates both dopamine-quinones and hydrogen peroxide inside the cell (Graham, D. G. *et al.*, 1978; Sulzer, D. *et al.*, 2000). Dopamine quinones can directly modify proteins by reacting with their sulphydryl groups and

reduce the level of intracellular antioxidant glutathione (Graham, D. G. *et al.*, 1978; Stokes, A. H. *et al.*, 1999). The conversion of hydrogen peroxide to highly reactive hydroxyl radical (Fenton reaction) requires Fe²⁺ ions (Fig. 1.2, 1.3). Interestingly, the Fe²⁺ level in the SNpc is natively higher than in the other areas of the brain and, moreover, was found to be increased in PD (Sofic, E. *et al.*, 1988; Dexter, D. T. *et al.*, 1989b).

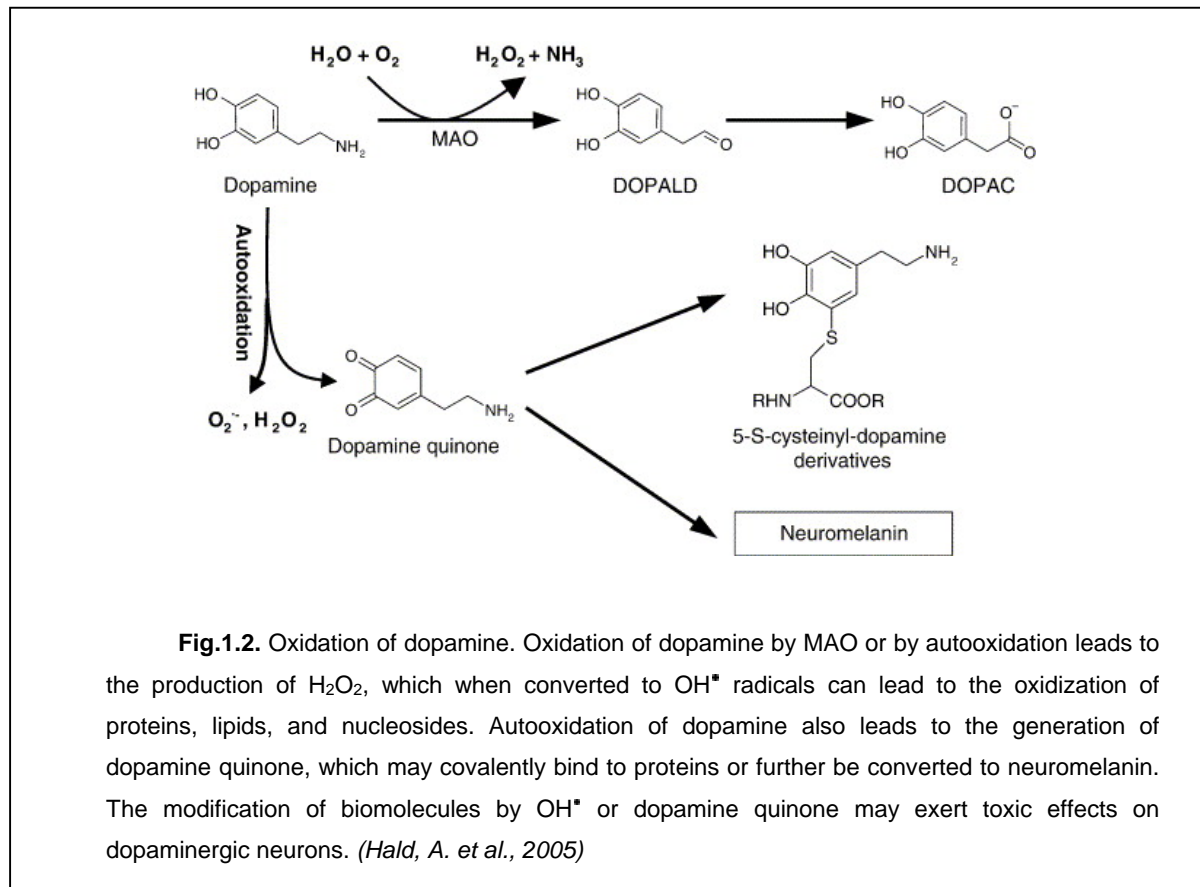


Fig.1.2. Oxidation of dopamine. Oxidation of dopamine by MAO or by autooxidation leads to the production of H₂O₂, which when converted to OH[•] radicals can lead to the oxidization of proteins, lipids, and nucleosides. Autooxidation of dopamine also leads to the generation of dopamine quinone, which may covalently bind to proteins or further be converted to neuromelanin. The modification of biomolecules by OH[•] or dopamine quinone may exert toxic effects on dopaminergic neurons. (Hald, A. *et al.*, 2005)

Excess of dopamine was reported to inhibit the complex I function in the brain (Ben Shachar, D. *et al.*, 1995). The reduced activity of the complex I of the respiratory chain was also found in PD (Schapira, A. H., 1994). Selective vulnerability of DA neurons of SNpc to the toxins (MPTP, rotenone, 6-OHDA) acting through the inhibition of the complex I activity, even when systemically applied (MPTP), suggests that these neurons are intrinsically more sensitive to the oxidative damage and mitochondrial dysfunction.

Abundant evidences of the major role of oxidative stress in the pathogenesis of PD have accumulated over the recent decades. Additionally to increased iron level, reduced levels of glutathione (GSH) and GSH-peroxidase expression (see also Fig 1.3) (Sofic, E. *et al.*, 1992; Kish, S. J. *et al.*, 1985), decrease in immunoreactivity of the reduced form of complex I (Schapira, A. H. *et al.*, 1989), and multiple signs of protein and lipid oxidation, such as 2-fold increase in carbonyl protein modifications (Floor, E. *et al.*, 1998), increased levels of thiobarbituric acid-reactive compounds (as an indicator of lipid peroxidation) and

malondialdehyde, and 8-hydroxy-2' deoxyguanosine (a nucleoside oxidation product)(Zhang, J. *et al.*, 1999; Dexter, D. T. *et al.*, 1989a) were found in SN of PD-affected brains in comparison to unaffected age-matching controls.

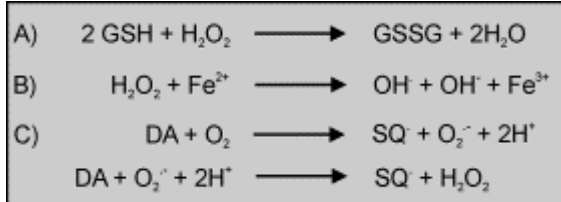


Fig.1.3. Factors leading to oxidative stress in the SNpc: (A) a deficiency in glutathione (GSH), thereby diminishing the capability to clear H_2O_2 ; (B) an increase in reactive iron, which can promote OH^\cdot formation; (C) auto-oxidation of DA into toxic dopamine-quinone species. GSSG: oxidized glutathione; SO: dopamine-quinone species.(von Bohlen und Halbach O. *et al.*, 2004)

Beside ROS generation, mitochondria are also important regulators of Ca^{2+} signalling. They actively and sensitively respond to the local increase in Ca^{2+} concentration by transient but massive uptake of the ion into the organelle (Rizzuto, R. *et al.*, 1999). Ultimately, this may lead to the loss of mitochondrial membrane potential, energy deprivation and cell death. The fluctuations of intracellular Ca^{2+} are observed in glutamate excitotoxic damage, which was suggested as one of the factors involved in DA cell death in PD, and may serve as an additional link between mitochondrial dysfunction and SNpc pathology.

1.2.7. Basal ganglia physiology

Development of new treatment strategies as well as appropriate model systems for the evaluation of their therapeutic value require a better understanding of the basal ganglia physiology, since a dysbalance in their functional circuits results in a typical for PD symptomatology. The basal ganglia consist of several interconnected nuclei which send their projections to different cortical motor areas, thalamus, certain brainstem nuclei, and indirectly to the cerebellum. The principal four nuclei of basal ganglia are the striatum, the globus pallidus (GP), subdivided into the external (GPe) and internal (GPi) segments, the substantia nigra (SN) and the subthalamic nucleus (STN) (Fig. 1.4).

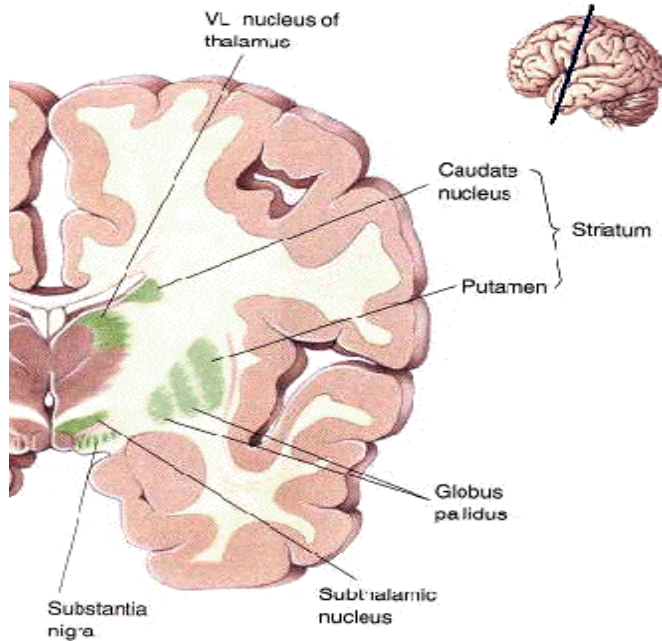


Fig.1.4. Schematic depiction of the basal ganglia of the human brain. Oblique frontal section. (Bear, M. F. et al., 2001)

Most of the intrinsic connections of the basal ganglia are GABA-ergic inhibitory. The only excitatory glutaminergic projection originates in STN. Striatum receives excitatory input from the cortex, thalamus, raphe nuclei and SN. Two major inhibitory output pathways are distinguished in the striatum: direct and indirect pathways (Fig. 1.5). The direct pathway runs from the striatum to the GPi, whereas the indirect one first passes to the GPe, then to the STN and only then to the GPi. Activation of the direct pathway, excitatory in their nature, leads to the active inhibition of the GPi output, thus reducing the thalamus inhibition and facilitating movements. Activation of the indirect pathway on the contrary, leads to the inhibition of movements. Dopamine released by nigrostriatal neurons binds to the D1 receptors facilitating the transmission through the direct pathway as well as to the D2 receptors inhibiting the transmission through the indirect pathway (Fig. 1.5). Reduction in dopamine supply in the striatum due to the loss of DA neurons in SNpc will lead to the inhibition of the direct and facilitation of the indirect pathway resulting in the hypokinetic movement disorder, of which PD is the best-studied example.

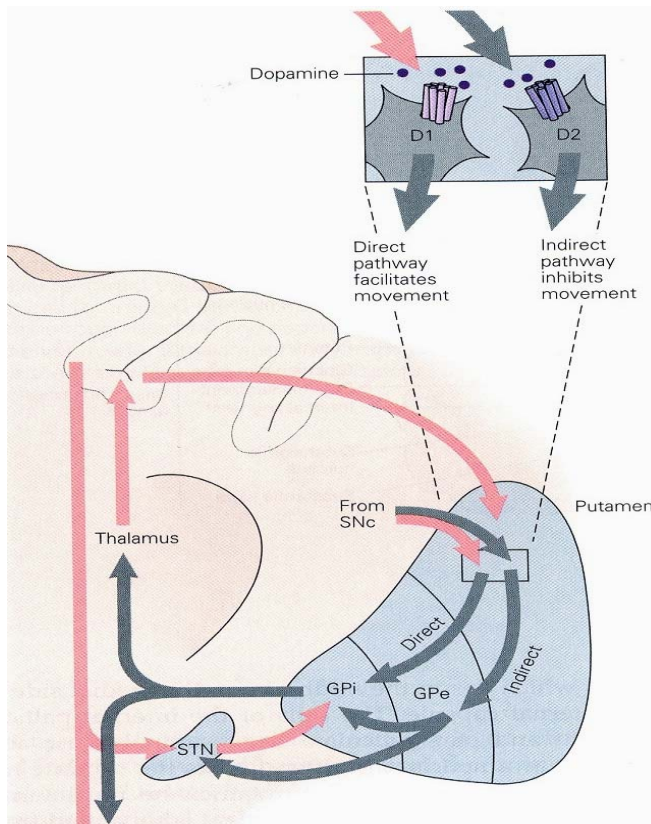


Fig.1.5. The anatomic connections of the basal ganglia-thalamocortical circuitry, indicating the parallel direct and indirect pathways from the striatum to the basal ganglia output nuclei. Two types of dopamine receptors (D1 and D2) are located on different sets of output neurons in the striatum that give rise to the direct and indirect pathways. Inhibitory pathways are shown as gray arrows, excitatory pathways, as pink arrows. GPe, external segment of the globus pallidus; GPI, internal segment of the globus pallidus; SNC, substantia nigra pars compacta; STN, subthalamic nucleus. (Kandel, E. R. et al., 2000)

1.2.8. Animal models of PD: complete unilateral 6-hydroxydopamine rat model

Modelling human neurological disorders in animals is common practice used for the study of the underlying pathogenetic mechanisms and evaluation the novel therapeutic approaches. However, they generally can only partly reproduce specific pathological and behavioural features of the particular disease. Various animal models of PD that are currently used can be subdivided into two groups: 1) genetic and 2) pharmacological (toxic) models. First group continuously enlarges due to the discovery of new mutations in PD related genes as well as due to the successful transgenic technologies, the use of different model systems (ranging from *Drosophila* to primates) and gene transfer approaches. Thus, α -synuclein transgenic *Drosophila* flies (Feany, M. B. et al., 2000) and rats (Klein, R. L. et al., 2002; Kirik, D. et al., 2002) have been created, however transgenic mouse models remain the most extensively used models of α -synucleinopathy (Fleming, S. M. et al., 2005). The

pharmacological models of PD remain a widely employed alternative, since they are easy to create and are able to reproduce the major etiopathologic features of PD induced by oxidative stress and inhibition of complex I. Several different neurotoxins, 6-hydroxydopamine (6-OHDA), MPTP, and rotenone are commonly used to this purpose (Blum, D. *et al.*, 2001; von Bohlen und Halbach O. *et al.*, 2004).

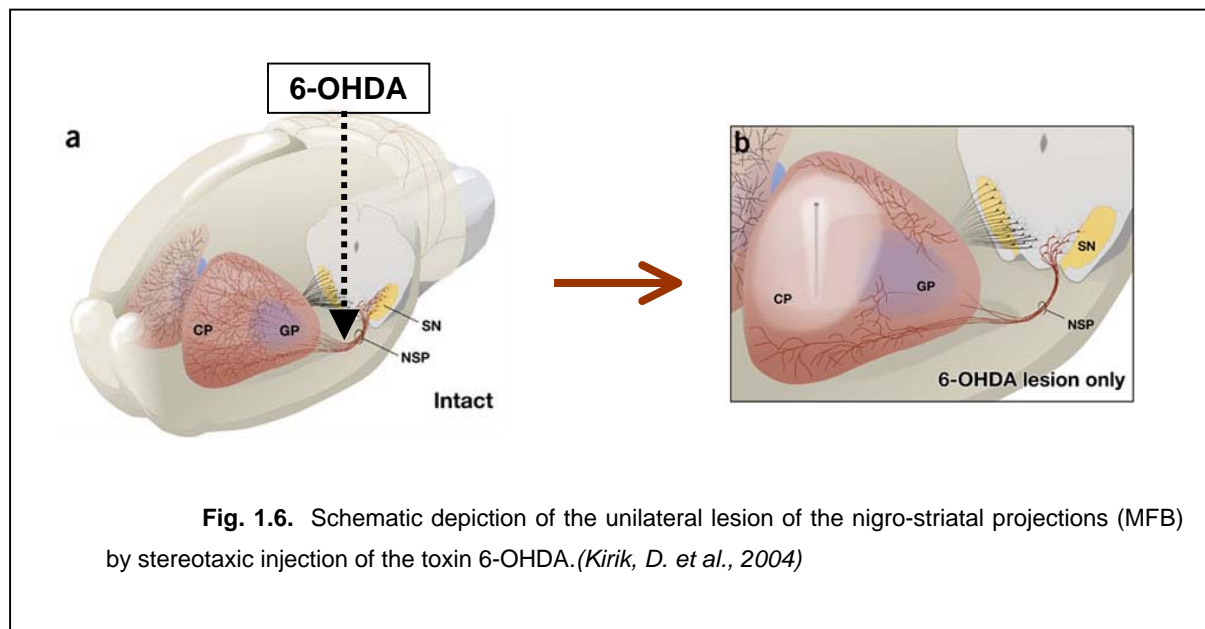


Fig. 1.6. Schematic depiction of the unilateral lesion of the nigro-striatal projections (MFB) by stereotaxic injection of the toxin 6-OHDA.(Kirik, D. *et al.*, 2004)

The first toxic model of PD was established by unilateral injection of 6-OHDA into the caudate-putamen, or striatum, or into the medial forebrain bundle (MFB) in close proximity to the SNpc of rat brain (Ungerstedt, U., 1968). Remarkable degeneration of the whole nigrostriatal dopamine neuron system associated with significant motor asymmetry was observed after the injection of the toxin into the SNpc. Usually, dopamine content in the striatum is reduced by more than 97% after this lesion (Schmidt, R. H. *et al.*, 1983; Rioux, L. *et al.*, 1991; Kirik, D. *et al.*, 1998). The expression of D₁ and D₂ receptors was shown to be upregulated in the lesioned caudate-putamen (Gagnon, C. *et al.*, 1991; Cadet, J. L. *et al.*, 1992; Dawson, T. M. *et al.*, 1991). Quantification of drug-induced rotations was later used as a simple behavioural test for estimation of the degree of the produced lesion (Ungerstedt, U. *et al.*, 1970). Typically, two drugs are used for induction of the rotational behaviour in unilaterally lesioned animals: amphetamine and apomorphine. Amphetamine acts as an agonist of dopamine inducing the fast and almost complete release of the neuromediator dopamine from the presynaptic terminals (Sulzer, D. *et al.*, 2005). Apomorphine, a short-acting dopamine D₁ and D₂ receptor agonist, functions postsynaptically (Picada, J. N. *et al.*, 2005). An animal subjected to the injection of either of the drugs will rotate away from the site of a greater

activity. This can be explained by the anatomical structure of the mammalian CNS, particularly the fact of crossing of the afferent tracts to the contralateral side at the level of either brainstem or spinal cord. However, due to the difference in mechanisms of action of the drugs, the rat exposed to amphetamine will rotate ipsilaterally, while the apomorphine-injected rat will exhibit contralateral to the lesion turns. Drug-induced rotational behaviour is often used to select the animals with complete lesions, since only those rats with complete degeneration of the nigrostriatal projections will exhibit robust turning behaviour induced by the drug.

1.3. Therapeutic approaches for PD treatment

1.3.1. Current therapeutical strategies and limitations

The pharmacological standard for the treatment of PD remains a replacement of dopamine. This is typically accomplished with the precursor of dopamine, 1-3,4-dihydroxyphenylalanine (L-DOPA). The clinical effects of L-DOPA on akinesia in parkinsonism were first presented in 1967 by Birkmayer and Hornykiewicz. L-DOPA is typically administered in a combination with carbi-dopa, an inhibitor of DOPA-decarboxylase which reduces the peripheral conversion of L-DOPA to dopamine thus allowing for considerable amount of the drug to cross the blood brain barrier and undergo decarboxylation to DA in the brain. Although the initial therapeutic effects of L-DOPA are excellent, patients develop drug-related side effects over the course of the disease, which include motor fluctuations (the so-called "wearing-off" and "on-off" phenomena) and dyskinesias (Lang, A. E. *et al.*, 1998). Other medications including anticholinergic agents, inhibitors of catechol-O-methyltransferase (COMT) or monoamine oxidase-B (MAO-B) provide only mild-to-moderate benefit (Lang, A. E. *et al.*, 1998; Hristova, A. H. *et al.*, 2000; Olanow, C. W. *et al.*, 2004; Marjama-Lyons, J. M. *et al.*, 2001). Eventually, L-DOPA or dopamine agonists are required for management of progressive disability. However, dopamine agonists usually take longer than L-DOPA to reach effective doses, and also require co-administration of L-DOPA for supervening disability after varying periods of time.

At the later stages of the disease patients developing resistance or severe side effects to pharmacological therapy may benefit from neurosurgical procedures such as pallidotomy or deep brain stimulation of the subthalamic nucleus (STN) (Esselink, R. A. *et al.*, 2004). Nevertheless, none of the currently available treatments has been proven to slow the progression of PD.

1.3.2. Neuroprotective gene therapy: achievements and perspectives

Different strategies have been employed to inhibit neurodegenerative processes: early studies aimed at blocking the executioners of apoptotic cell death, cysteine proteases of the caspase family, however, no sustained neuroprotection could be achieved (Kermer, P. *et al.*, 1999;Perrelet, D. *et al.*, 2000;Rideout, H. J. *et al.*, 2001). Most pro-apoptotic signals converge on breakdown of mitochondrial membrane potential, followed by release of pro-apoptotic factors and subsequent caspase activation (Chang, L. K. *et al.*, 2002). Thus, several studies focused on the maintenance of mitochondrial integrity by overexpression of anti-apoptotic members of the bcl-2 family of proteins (Azzouz, M. *et al.*, 2000;Malik, J. M. *et al.*, 2005;Wong, L. F. *et al.*, 2005). This strategy proved to be significantly more efficient than caspase inhibition, although in long-term studies substantial neuronal cell loss was still observed (Malik, J. M. *et al.*, 2005;Kim, R., 2005).

Neurotrophic factors in several paradigms could only shortly postpone neuronal degeneration (Cheng, H. *et al.*, 2002;van Adel, B. A. *et al.*, 2003). Glial cell line-derived neurotrophic factor (GDNF) appears to be an exception and remains a promising candidate in the treatment of Parkinson's disease.

1.3.3. Glial cell line-derived neurotrophic factor (GDNF)

GDNF was originally identified as a trophic factor promoting the survival of embryonic midbrain dopaminergic neurons (Lin, L. F. *et al.*, 1993). Subsequently, it was found to be a potent trophic factor for noradrenergic neurons of the CNS (Arenas, E. *et al.*, 1995) as well as for the moto- and sensory neurons of the PNS (Henderson, C. E. *et al.*, 1994;Ramer, M. S. *et al.*, 2000). GDNF was purified from a glioma cell line supernatant and then found to be expressed in several glial cell types of the NS (Schaar, D. G. *et al.*, 1993;Strelau, J. *et al.*, 1999). In toxicity animal models of PD, GDNF was proven to rescue DA neurons of SNpc from the neurotoxic damage and promote behavioural recovery (Grondin, R. *et al.*, 1998). However, lentiviral delivery of GDNF to SNpc failed to prevent neurodegeneration in α -synuclein transgenic rat model of PD (Lo, Bianco C. *et al.*, 2004). Furthermore, recent clinical trials demonstrated divergent outcomes (Gill, S. S. *et al.*, 2003;Nutt, J. G. *et al.*, 2003;Patel, N. K. *et al.*, 2005). GDNF has also been shown to induce resprouting of the lesioned nigrostriatal neuron system and thus may have beneficial effects on deafferentiated neurons in general (Björklund, A. *et al.*, 1997;Love, S. *et al.*, 2005).

Together with three other neurotrophic factors (neurturin, artemin, persephin) GDNF comprises a family of proteins, the so-called GDNF family ligands (GFLs). GFLs are distantly related to the transforming growth factor-beta superfamily, containing seven cysteine residues

with the same relative spacing and acquiring similar conformation as the other members of this superfamily (Ibanez, C. F., 1998). The main signalling pathway of GFLs is mediated by RET-receptor tyrosine kinase (Sariola, H. *et al.*, 2003), which was initially discovered as a protooncogen (Takahashi, M., 2001). RET is activated upon binding of GDNF dimer to GFR α 1 receptors linked to the plasma membrane via a glycosyl phosphatidylinositol (GPI) anchor (Fig. 1.7). Dimerization of RET triggers its autophosphorylation, thus initiating various intracellular signalling cascades, that regulate cell survival, proliferation, differentiation, neurite outgrowth, synaptic plasticity and morphogenesis (Airaksinen, M. S. *et al.*, 2002). For example, MAPK and phosphatidylinositol 3-kinase (PI3K) may be involved in neurite outgrowth and neuronal survival, while PLC γ regulates intracellular Ca^{2+} levels (Sariola, H. *et al.*, 2003).

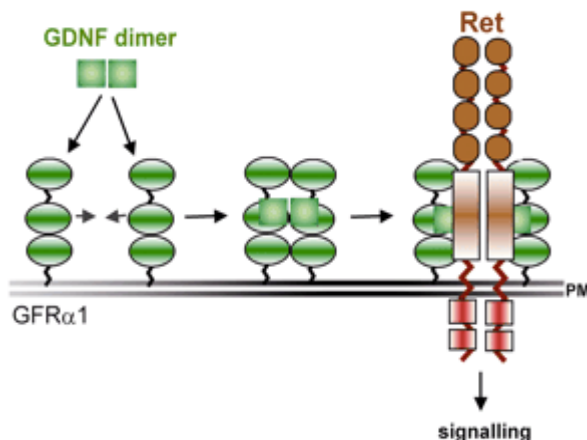


Fig. 1.7. GDNF interaction with its receptors. A dimer of GDNF brings together two molecules of GFR α 1. This complex dimerizes two molecules of Ret leading to transphosphorylation of their tyrosine kinase domains. GFR α proteins are attached to the plasma membrane through a GPI-anchor and consist of three globular cysteine-rich domains joined together by adapter sequences.(Sariola, H. *et al.*, 2003)

GDNF may also signal independently of RET but involving the same receptor GFR α 1. In RET-deficient cells GDNF may act through the Src family kinases, inducing sustained activation of the Ras/ERK and PI3K/Akt pathways, cAMP response element-binding protein phosphorylation, and increased c-fos expression (Trupp, M. *et al.*, 1999). In the absence of RET, Src-mediated cellular events may also promote neuronal survival and neurite outgrowth (Sariola, H. *et al.*, 2003).

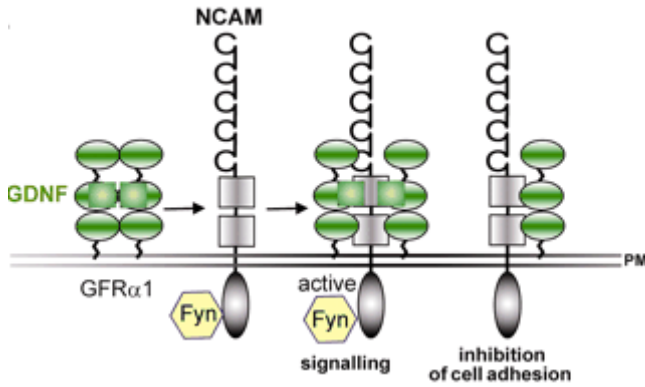


Fig. 1.8. Non-RET signalling for GDNF through NCAM. NCAM interacts with a GDNF-GFR α 1 dimer leading to activation of Fyn, a Src-like kinase, for instance. It is not known whether Fyn activates Met in NCAM-mediated GDNF signalling. (Sariola, H. et al., 2003)

NCAM has been proposed as an alternative signalling receptor for GDNF (Paratcha, G. et al., 2003). When GFR α 1 is absent, GFL associates with NCAM with low-affinity. In turn, in the presence of GFR α 1, GDNF may bind to the p140-NCAM and activate cytoplasmic Src-like Fyn and FAK kinases (Fig. 1.8) (Paratcha, G. et al., 2003). Interestingly, both *in vivo* and *in vitro* effects of GDNF, such as DA neuron survival, neurite outgrowth, DA turnover, and locomotor activity in rats were inhibited by anti-NCAM antibodies (Chao, C. C. et al., 2003).

1.3.4. BclX_L, an antiapoptotic member of the bcl-2 family proteins

The antiapoptotic member of the bcl-2 protein family, BclX_L plays an important role in the inhibition of mitochondria-dependent cell death pathways. Mouse embryos deficient in BclX_L show massive cell death of immature neurons of the CNS and dorsal root ganglia (Motoyama, N. et al., 1995). Co-deletion of BAX largely rescued the BclX_L knockout phenotype providing evidence that BclX_L serves as a negative regulator of BAX -mediated cell death *in vivo* (Shindler, K. S. et al., 1997). Together with bcl-2, BclX_L is considered a prominent native inhibitor of apoptosis and BAX and BAK function. The latter belong to the pro-apoptotic proteins of the bcl-2 family, which are believed to induce permeabilization of the mitochondrial membrane in response to both internal and external apoptotic triggers (Kim, R., 2005).

Several models have been proposed to explain the mechanism for the formation of such permeability transition pore (Hengartner, M. O., 2000). Truncated Bid, the caspase-

activated form of a "BH3-domain-only" bcl-2 family member, triggers the homooligomerization of "multidomain" conserved proapoptotic family members BAK or BAX. This interaction may lead to the formation of a channel pore, through which cytochrome *c* and other mitochondrial intermembrane proteins can escape. The recruitment of the voltage-dependent anion channel (VDAC) located at the outer leaflet of the mitochondria and the adenine nucleotide transporter (ANT) of the inner mitochondrial membrane for the formation of the permeability transition pore was also suggested (see also Fig. 1.1). Both bcl-2 and BclX_L might prevent the interaction of BAX/BAK via heterodimerization, which is achieved when the BH3 domain of one molecule binds into a hydrophobic pocket formed by the BH1, BH2 and BH3 domains of another family member (Sattler, M. *et al.*, 1997; Cheng, E. H. *et al.*, 2001).

The ability of BclX_L and bcl-2 to inhibit mitochondrial permeability transition pore (PTP) formation and cytochrome *c* release rendering cells more resistant to the oxidative stress makes these proteins attractive candidates for neuroprotective therapy. In contrast to bcl-2, BclX_L was shown to possess a C-terminal mitochondrial targeting motif which ensures its more effective localization to mitochondria and may in part explain the higher potential of BclX_L to inhibit the loss of mitochondrial membrane potential as compared to bcl-2 (Kaufmann, T. *et al.*, 2003; Kim, R., 2005). Also, overexpression of BclX_L, but not bcl-2 suppressed TNF-induced cell death in tumour cells (Marini, P. *et al.*, 2003).

1.4. AAV vectors as tools for gene therapy

In order to express transgenic proteins in the lesioned CNS, effective gene transfer tools, such as viral vectors, are needed. Adeno-associated virus (AAV) is a small dependovirus from the *Parvoviridae* family, which is replication deficient in the absence of adenovirus, herpesvirus or vaccinia virus (Buller, R. M. *et al.*, 1981). Wild-type AAV is not known to be associated with any disease in humans or mammals, which makes it an attractive tool for human gene therapy. AAV harbours a linear single-stranded genome of 4,675 nucleotides in length and contains inverted terminal repeats (ITRs) of 145 nucleotides, the first 125 nucleotides of which form a palindromic sequence (Srivastava, A. *et al.*, 1983). AAV genome possesses two large open reading frames (ORF) that do not overlap. One (*cap*) encodes for virus coat proteins, the other (*rep*), for the proteins necessary for virus replication and transcription of the viral genes. To date, ten different AAV serotypes (AAV-1 – AAV-9, and AAV-Rh10) have been identified (Cearley, C. N. *et al.*, 2006). While most AAV serotypes share certain sequence homology in *cap* genes, AAV-5 appears to be the most distantly related serotype to the other parvoviruses (Bantel-Schaal, U. *et al.*, 1999).

AAV vectors used for gene therapy are typically devoid of 96% of their genome with the exception of ITRs, the only *cis* elements which are required for packaging (Samulski, R. J. *et al.*, 1989). Therefore, recombinant AAV vectors are considered to have one of the highest biosafety ranking among the viral vectors.

Different transduction properties of the AAV serotypes have been employed using “pseudotyping”, the generation of hybrid AAV vectors which contain the genome of one serotype (typically AAV-2) packaged into the capsid of another serotype (Duan, D. *et al.*, 2001;Auricchio, A. *et al.*, 2001;Hildinger, M. *et al.*, 2001). The other technique exploiting the different serotype properties of capsid proteins is generation of chimeric rAAV vectors by cross-dressing of the virion (Hauck, B. *et al.*, 2003). By mixing helper plasmids of different AAV serotypes at different ratios, the final contribution of the serotype-specific capsid components to the mature virion can be controlled (Rabinowitz, J. E. *et al.*, 2004). Except for variations in cellular tropism, the capsid proteins of different serotypes may also influence the onset and the intensity of gene expression (Auricchio, A. *et al.*, 2001;Chao, H. *et al.*, 2000;Rabinowitz, J. E. *et al.*, 2004).

Recombinant AAV vectors are lacking the wild-type *rep* gene, which is responsible for the site-specific integration in the chromosomal DNA, and thus persist mainly in an episomal form (Duan, D. *et al.*, 1998). They can, nevertheless, mediate stable transgene expression for more than one year (Woo, Y. J. *et al.*, 2005;Stieger, K. *et al.*, 2006). Among other beneficial features of the AAV for gene transfer is the ability to infect both dividing and non-dividing cells (Flotte, T. R. *et al.*, 1994;Flotte, T. R. *et al.*, 1992). Recombinant AAV vectors have been reported to be non-toxic, non-inflammatory and inducing only a very limited immune response without any noticeable decrease in transgene expression after injection into the brain (Mastakov, M. Y. *et al.*, 2002)

Apart from the fact that neutralizing antibodies to AAV have been found in circulation of certain individuals (Moskalenko, M. *et al.*, 2000), a relatively small packaging capacity (less than 5 kb) has limited the application of rAAV for gene therapy (Dong, J. Y. *et al.*, 1996). However, by exploring a unique feature of AAV biology, the possibility of viral DNA heterodimerization and formation of head-to-tail concatemers, the expression of genes larger than 5 kb could be achieved (Duan, D. *et al.*, 2001;Sun, L. *et al.*, 2000).

1.5. Semliki Forest virus (SFV) vectors

Semliki Forest virus (SFV) is a positive-stranded enveloped RNA virus that belongs to the alphavirus genus of the *Togaviridae* family. The single-stranded, around 12 kb long genome of SFV functions directly as an mRNA encoding its own replicase, being capped at the 5' terminus and polyadenylated at the 3'terminus. The SFV genome is divided into two open reading frames (ORF). The first ORF encodes four non-structural proteins (nsP1-4) responsible for transcription and replication of viral RNA. The second ORF codes for the structural proteins required for the encapsidation of the viral genome and the assembly into enveloped particles under the control of a 26S subgenomic promoter (Lundstrom, K., 2005; Lundstrom, K. *et al.*, 2003).

Alphavirus gene expression is transient by nature due to the cytoplasmic replication and strong cytotoxicity leading to the shutdown of endogenous gene expression of the host cell. This property of alphaviruses can serve as an advantage for application in cancer gene therapy. However, the same feature makes SFV vectors non-useful for long-term gene therapy as well as for functional studies.

Alphaviruses possess certain advantages for gene transfer, known to have a very broad host range and replicating efficiently to high titres in many cells of both vertebrates and invertebrates (Strauss, J. H. *et al.*, 1994). Principally, three types of SFV vector systems have been developed so far: 1) replication-competent viral particles, 2) replication-deficient RNA vectors (replicons), and 3) DNA-based vectors. Most applications of alphavirus vector systems have been attributed to the replicon vectors, in which the genome for the viral structural proteins has been replaced by a multiple cloning site (Liljestrom, P. *et al.*, 1991). However, they retain the entire non-structural region as well as the natural subgenomic promoter. Considerable efforts have been made over the recent years to generate novel alphavirus vectors with reduced cytotoxicity and prolonged expression profiles. Thus, the SFV(PD) vector, which bears two point mutations in nsP2, shows lower host cell toxicity, probably due to the decreased replication (Lundstrom, K. *et al.*, 2003). On the basis of SFV(PD) vector, a triple mutant which substantially prolongs transgene expression in cell cultures for more than 20 days was generated (Lundstrom, K. *et al.*, 2003). Typically, SFV vectors infect both neurons and glial cells in the CNS (Atkins, G. J. *et al.*, 1999). However, generation of novel vector based on the avirulent A7 strain exhibit a temperature dependent expression pattern in organotypic hippocampal cultures in that the expression pattern was mainly restricted to glial cells at 37°C, and was neuron-specific at 31°C (Ehrengreuber, M. U. *et al.*, 2003).

Taken together, these novel rapid-to-generate mutant SFV vectors with reduced cytotoxicity are excellent tools for fast evaluation of epitope tags applicability for *in vivo* transgene tracing in the brain.

1.6. Epitope-tagging

In the post-genomic era it will be a major task to assign cellular functions to proteins. Recent estimations of the number of protein-coding genes in complex eukaryotic organisms like mice and humans have been between 25,000 to 35,000 (Ewing, B. *et al.*, 2000) which would be only one-third more than that of simple organisms like *C. elegans* with 19,000 genes. Alternative splice variants of genes and posttranslational modifications of proteins may thus significantly contribute to the higher complexity of higher eucaryotes (Liu, S. *et al.*, 2003). Assessing the functional diversity of proteins may require the ability to trace multiple variants of a protein. This task may be one of the major applications for epitope tagging techniques, which allow for a specific recognition of short peptides (epitopes), fused to a protein under investigation, by commercially available antibodies. This will greatly facilitate studies in fields such as sub-cellular tracing, protein-protein interactions, or the effects of dominant negative mutants *in vitro* and *in vivo*. Another prominent field for using epitope tagging technology is the evaluation of proteins to which no antibodies for immunodetection exist yet. Furthermore, gene transfer studies seeking to overexpress a protein, or its dominant-negative mutants, may encounter an intrinsically expressed equivalent in either the transduced cell type or in cells near to the site of transduction. Therefore, unequivocal identification of the overexpressed transgene is required and benefits substantially from an epitope tag.

While epitope tagging is frequently used for *in vitro* applications (Terpe, K., 2003), no attempt has been made so far to elucidate the properties of the different available epitope tag / antibody combinations in tissue sections derived from animals expressing respectively tagged proteins. In the present study we approached this question by overexpressing several epitope tags fused to the fluorescent reporter protein EGFP in different areas of the central nervous system, e. g. striatum, retina and primary hippocampal cultures, by means of viral vector based gene transfer.

2. Materials and Methods

2.1. Materials

2.1.1. Chemicals

Applichem: 2-Propanol, Acetone, Agarose, Ethanol absolute, Boric acid, Glycine, HEPES, LB medium (powder), LB agar (powder), Magnesium chloride ($MgCl_2$), Methanol, Paraformaldehyde, PBS (1x Dulbecco's, powder), Potassium chloride (KCl), Sodium chloride (NaCl), Sodium dodecylsulfate (SDS), Sodium hydroxide pellets, D(+)-Sucrose, Tris.

BIO-RAD: Avidin-HRPO.

Calbiochem: Moviol, Sodium citrate.

Gibco: B27 Supplement, DMEM, DMEM: F12 (1:1), Neurobasal medium (NBM), OptiMEM, PS-N

Fluka: Chloral hydrate, Coumaric acid, Sodium acetate, Tween 20.

Merck: Agar, Ammonium peroxide, Formaldehyde, Hydrogen peroxide (H_2O_2).

PAA (cell culture company): NGS, FCS, penicillin/streptomycin (PS).

QIAGEN: QIAGEN Plasmid Maxi Kit, QIAprep spin MiniPrep kit, QIAquick Gel Extraction Kit, RNeasy QIAGEN Kit

Roche: DNase I

Roth: Glycerol, Milk powder, Rothiphorese.

Riedel-deHaen: Diethylether.

Seromed: L-glutamine

Serva: Bromphenol blue sodium salt (BPB), TEMED.

Sigma: 2-mercaptoethanol, 6-hydroxydopamine hydrochloride, α -chymotrypsin, Ampicillin (Sodium salt), Bactotryptone, Bezonase, Biotinylated SDS Molecular Weight Standard Mixture for SDS-PAGE (Molecular Weight Range 14,300 - 97,000 Da), Bradford reagent, BSA D(+)-glucose, Dithiothreitol (DTT), EDTA, Ethidium bromide, Laminin, L-ascorbic acid, Luminol, MOPS, Poly-L-Ornithine, Sodium azide, Sodium bicarbonate (Na_2CO_3), Streptavidin-Peroxydase, Transferrin, Triton X-100, Trypsin, Yeast extract.

2.1.2. Antibodies

Anti-HA, mouse monoclonal (Covance, # MMS-101R)

Anti-FLAG M2, mouse monoclonal (Sigma, # F3165)

Anti-c-Myc, rabbit polyclonal (Cell Signalling Technologies, # 2272)

Anti-EE (Glu-Glu), rabbit polyclonal (Covance, # PRB-115C)

Anti-AU1, mouse monoclonal (Covance, # MMS-130R)

Anti-IRS, mouse monoclonal (Covance, # MMS-166R)
Anti-TH, rabbit polyclonal (Advanced Immunochemicals, RATH 4-6b)
Anti-BclX, rabbit polyclonal (BD Transduction Laboratories, # 610211)
Anti-cabindin D_{28K}, rabbit polyclonal (Swant, # CB38a)
Anti-GFP, rabbit polyclonal (Clontech, # 8367-1)
Anti-GFAP, rabbit polyclonal (DAKO A/S, #Z0334)
Anti-NeuN, mouse monoclonal (Chemicon, # MAB377)
Anti-Tubulin, rabbit polyclonal (Sigma, #T3526)
Secondary antibodies for immunofluorescence were Cy3-coupled anti-mouse or anti-rabbit IgGs (Dianova), for western blotting - HRP-coupled anti-mouse and anti-rabbit IgGs (Santa Cruz Biotechnology).

2.1.3. Plasmids

pAAV-6p1-TB, kindly provided by S. Kügler
pAdV-hGDNF, kindly provided by S. Kügler
pBluescript-II-KS (Stratagene)
pDG, kindly provided by Kleinschmidt
pDP5, kindly provided by Kleinschmidt
pDsRed2 (Clontech)
pEGFP (Clontech)
pMH4 (Microbix Biosystems)
pSFV-PD, a generous gift of K. Lundström
pSFV-helper2, a generous gift of K. Lundström

2.1.4. Oligonucleotides (Sigma-Aldrich)

5'-BamHI-HA-EGFP:

AAAAAAAGGATCCACCATGGGATACCCATATGACGTACCAAGACTACGCAGGC
AGTGAGCAAGGGCGAGGAGCTGTT

3'-XhoI-HA-EGFP:

AAAAAAACTCGAGTTATGCGTAGTCTGGTACGTACATGGGTATCCGCCCTTGA
CAGCTCGTCCATGCCGAGAG

3'-XhoI-IRS-EGFP:

AAAAAAACTCGAGTTATGAGCGTATATATCGGCCTCCCTGTACAGCTCGTCCAT
GCCGAGAG

5'-BamHI-AU1-EGFP:

AAAAAAAGGATCCACCATGGGAGACACATATCGATAACATAGGCAGGTGAGCA
AGGGCGAGGAGGTCTTC

3'-XhoI-EE-EGFP:

AAAAAAACTCGAGTTATTCCATTGGCATGTATTCTCCGCCCTGTACAGCTCGTC
CATGCCGAGAG

5'-BamHI-Myc-EGFP:

AAAAAAAGGATCCACCATGGAGCAGAAACTCATCTCTGAAGAGGATCTGGCG
GAGTG AGCAAGGGCGAGGAGCTGTT

3'-XhoI-FLAG-EGFP:

AAAAAAACTCGAGTTACTTATCGTCGTACCTCTGTAATCTCCGCCCTGTACAG
CTCGTCCATGC CGAGAG

5'-PstI-Intron-SV40pA-w/oEcoRV:

AAAAAAACTGCAGCTGCTGGGCTCACTCTCAGTCGGAAG

3'-EcoRI-Intron-SV40pA-w/oEcoRV:

AAAAAAAGAACATTACCGCGACATATCTCGATGCTAGACGAT

pBS-woMCS-oligo:

AAAAAGAGCTCACTAGTAGTGATACTAGGACGCGTGGTACCTTTT

5'-MfeI-GDNF:

AAAAACAATTGAAGCTGCTAGCAAGGATCCACCGGTCGCCACCATGGAAAGT
TATGGGATGTCGTGG

3'-NotI-GDNF:

AAAAAGCGGCCGCTCATGCGTAGTCTGGTACGTCATA

RT- calbindin D_{28K}:

GATACAATGTATCACTAGCAAGTGG

5'-calbindin D_{28K} -cDNA:

CTCTAACTAGCCGCTGCACCATGG

3'-calbindin D_{28K} -cDNA:

AGTGGTTGTGCCACCAACTCTA

5'-hSyn1-MfeI-AU1-calbindin D_{28K}:

AAAAACAATTGAAGCTGCTAGCAAGGATCCACCGGTCGCCACCATGGAGACA
CATATCGATAACATAGGCGGA

3'-NotI-calbindin D_{28K}:

AAAAAGCGGCCGCTAGTTGTCCCCAGCAGAGAG

5'-BamHI-AgeI-DsRed2:

AAAAAAAGGATCCACCGGTATGGCCTCCTCCGAGAACGTC

3'- HindIII-BsrgI-DsRed2:

AAAAAAAAAGCTTGTACACTACAGGAACAGGTGGTGGCG

5'-SpeI-mCMV:

AAAAACTAGTCTGACTAGAGATATCTGAGTCATT

3'-NotI-MfeI-mCMV:

AAAAAGCGGCCGCAATTATCCAATTGCGACC GGATCCTTGCTAG

2.1.5. Cell lines and electrocompetent cells

BHK-21 (Sigma)

HEK 293 (ATCC)

AAV-293 (STRATAGENE)

DH5 α and SURE E. coli strains (STRATAGENE)

2.1.6. Buffers and Solutions

Blocking solution for IHC: 10% NGS, 0.3% Triton X-100 in PBS.

Blocking solution for WB: 10% Milk in TBS-T (see below).

Citric saline (1 x): 135 mM potassium chloride, 15 mM sodium citrate.

DNA loading buffer (6 x): 2% glycerol, 60 mM Na₂EDTA, pH 8; 0.6% SDS, 0.003% BPB

ECL-1: 2.5 mM Luminol, 0.4 mM p-Coumar acid, 0.1 M Tris-HCl, pH 8.5.

ECL-2: 18% H₂O₂, 0.1 M Tris, pH 8.5.

Electrophoresis buffer: 192 mM Glycine, 0.1% SDS, 25 mM Tris-HCl, pH 8.3.

HBS (2 x): 280 mM NaCl, 1.5 mM Na₂HPO₄, 50 mM HEPES, pH 7.1.

Incubation solution -1 for immunofluorescence (IF): 2% NGS, 0.3% Triton X-100 in PBS

Incubation solution -2 for immunofluorescence (IF): 2% NGS in PBS.

Lysis buffer I (cell culture): 0.5% SDS, 1 mM DTT, 50 mM Tris-HCl, pH 8.0.

Lysis buffer II (tissue): 150 mM NaCl, 1% Triton X-100, 50 mM Tris-HCl, pH 8.0.

MOPS (10x): 0.2 M MOPS, 50 mM Na acetate, 10 mM EDTA, pH 7.0.

PBS: 9.55 g of PBS powder in 1 L millipore H₂O, autoclaved.

RNA loading buffer: 62.5% Formamide, 8% Formaldehyde, 12.5% 10xMOPS, 0.025% BPB, 0.017% Ethidium bromide.

SDS-Sample buffer (2x): 0.125 M Tris-HCl, pH 6.8, 4% SDS, 0.15 M DTT, 20% Glycerol, 0.01% Bromphenolblue.

TE: 0.01 M Tris-HCl, pH 7.4, 1 mM EDTA, pH 8.0.

TBE: 42 mM Boric Acid, 10 mM EDTA, 50 mM Tris-HCl, pH 8.0.

TBS: 150 mM NaCl, 10 mM Tris-HCl, pH 9.0 (for antigen retrieval).

TBS-T: 0.1% Tween in TBS, pH 7.6 (for WB).

Transfer buffer: 192 mM Glycine, 20% Methanol, 25 mM Tris-HCl, pH 8.3.

Trypsin solution (0.25%) for primary culture: 25 mg Trypsin, 10 ml CMF.

2.2. Methods

2.2.1. Cloning procedures

Primer design and all major cloning steps were first simulated using SECentral software. Restriction sites, necessary for cloning of the DNA fragments into respective plasmids, as well as epitope sequences were added to the cDNA by using corresponding primers via PCR. All basic DNA procedures were essentially performed according to the protocols described in Molecular Cloning Laboratory Manual, 2nd edition (Sambrook, J. *et al.*, 1989).

2.2.1.1. PCR-amplification

Before amplification of the cDNA sequences of interest, the most suitable PCR conditions were checked. Thus, different concentrations (2 mM, 4 mM and 6 mM) of magnesium sulfate salt ($MgSO_4$) in the buffer and annealing temperatures (usually 50°C and 60°C) were used for initial amplification. Those conditions that resulted in the best yield of PCR-product were chosen for further amplification. PCR reaction mix typically contained: the ThermoPol Reaction Buffer (20 mM Tris-HCl, pH 8.8, 10 mM $(NH_4)_2SO_4$, 10 mM KCl, 2 mM $MgSO_4$, 0.1 % Triton X-100; *BioLabs*), 2-6 mM of $MgSO_4$, 400 nM of sense and antisense primers, 200 μ M of dATP, dCTP, dGTP, dTTP (*BioLabs*), 5-10ng of the template DNA, 0.5 unit of the Vent DNA Polymerase (2,000 units/ml; *BioLabs*), and millipore H₂O to achieve a total volume of 50 μ l. The amplification was performed on PCR machine from MJ Research Biozym (Hessisch Oldendorf, Germany). The amplification was started with 1 min incubation at 95°C followed by 30 cycles of amplification (annealing – 30 sec at 50°C or 60°C, elongation – 45 sec at 72°C, separation of DNA strands – 30 sec at 95°C). The amplified fragments were purified from the 1% agarose gel by DNA electrophoresis using the Gel Extraction Kit (QIAGEN).

2.2.1.2. *In vitro* transcription

Calbindin D_{28K} cDNA was obtained through reverse transcription amplification from total RNA extract from a rat brain. RNA was extracted using RNA Extraction Kit (QIAGEN)

according to the protocol of the manufacturer. 500 ng of total RNA, 2 pmol of RT-calbindin D_{28K} primer, 1 µl of dNTP mix (10 mM each; *BioLabs*) and RNase-free sterile H₂O were mixed in a total volume of 12 µl, heated to 65°C for 5 min and quickly chilled on ice. After collecting the content of the tube by a brief centrifugation 4 µl of 5 x First-Strand Buffer (250 mM Tris-HCl, pH 8.3, 375 mM KCl, 15 mM MgCl₂, Invitrogen) and 2 µl of 0.1 M DTT were added, and the reaction mix was incubated at 42°C for 2 min. SuperScript II reverse transcriptase (1 µl or 200 units; Invitrogen) was added and mixed with the content of the tube by gentle pipetting up and down. The final reaction mix was incubated for 50 min at 42°C. The transcription reaction was stopped by heating at 72°C for 15 min. To remove RNA complementary to the cDNA 1µl of *E. coli* RNase H (Invitrogen) was added and the mix was incubated at 37°C for 20 min.

2.2.1.3. Sequencing of PCR-amplified DNA

The sequencing reactions were carried out using the ‘ABI PRISM® BigDye™ Terminator Cycle Sequencing Ready Reaction Kit’ (Perkin Elmer Applied Biosystems Division, Foster City, CA) according to the manufacturer’s protocol. The Terminator Ready Reaction Mix contained the four dNTPs with different fluorescence labels (BigDye™ Terminators), unlabeled dNTPs, AmpliTaq DNA Polymerase FS, MgCl₂, Tris-HCl buffer (pH 9.0). Template DNA (10 ng) and 3.2 pmol of the sequencing primer (universal T7 or T3 promoter primers for sequencing of cDNA inserted in pBluescript vector) and 8 µl of the Terminator Ready Reaction Mix were used in a 20 µl sequencing reaction. The sequencing reaction mixes were subjected to 25 linear amplification cycles. Each cycle consisted of 30 sec at 95°C, 45 sec at 50°C and 1 min at 60°C. The amplified probes were then precipitated as described in DNA precipitation section (3.2.1.4.), resuspended in 20 µl of template suppression reagent (Applied Biosystems) and subjected to DNA capillary electrophoresis on the ABI PRISM™ 310 Genetic Analyzer. Sequence analysis and alignment with reference cDNA were performed using ABI PRISM™ (Applied Biosystems) 3100 and SECentral softwares.

2.2.1.4. DNA precipitation

One tenth volume of 3 M Sodium Acetate buffer (pH = 5.0 -5.3) was added to the DNA solution to equalize ion concentrations. Two volumes of ice-cold 100 % ethanol were added to the mix, then the mix was briefly vortexed and left on dry ice for 5 min. The sample mix was then centrifuged for 30 min at highest speed in a 4°C microcentrifuge. The supernatant was removed and 200 µl of ice-cold 70 % ethanol were added to the precipitate. The mix was centrifuged again for 10 minutes in a 4°C centrifuge. The supernatant was

carefully removed and the precipitate left for drying at room temperature for 5-10 min. The DNA pellet was resuspended in desired volume of water or TE buffer.

2.2.1.5. DNA restriction, electrophoresis, gel extraction, concentration determination

For restriction digest 5-10 µg of plasmid DNA and 0.5-3 µg of PCR product were used. Appropriate endonucleases in corresponding buffers (*BioLabs*) were mixed with DNA and left for (us. 1 - 1.5 h) restriction digest at the temperature specified for each enzyme in the instruction manual of *BioLabs*. Analysis of the DNA size was performed by agarose gel electrophoresis. To prepare the gel 1% agarose was dissolved in TBE buffer in a microwave oven and 0.3µg/ml ethidium bromide solution was added then. DNA samples were mixed with DNA loading buffer and millipore sterile water to reach a final volume of 12.5 µl for loading the gel. The gel was run in 1 x TBE buffer. The DNA bands were visualized by UV-light of 302 nm at Gel Documentation 2000™ UV-transilluminator (Bio-Rad) using the Quantity One software (version 4.2.1). DNA extraction after gel electrophoresis was performed in accordance with QIAquick Gel Extraction Kit (QIAGEN) protocol. To increase the purity and the concentration of DNA in the final solution DNA precipitation step typically followed the extraction procedure. The concentration of DNA in the final solution was measured at the Biophotometer (Eppendorf) at 260 nm.

2.2.1.6. DNA ligation and transformation in *E. coli*

For ligation vector DNA and cDNA fragment were mixed in a molar ratio of 1:1 and 1:3 with ligation buffer (10 mM MgCl₂, 1 mM ATP, 10 mM dithiothreitol, 25 µg/ml BSA, 50 mM Tris-HCl, pH 7.5 @ 25°C), millipore sterile water and T4 DNA ligase (1µl = 2 000 units, *BioLabs*) in a total volume of 10 µl. The ligation reaction was performed for 1 h at room temperature. The DNA ligation product (3 - 5 ng DNA) was added to 50 µl of de-frozen and kept on ice electrocompetent *E.coli* cells. The mixture was transferred to a prechilled on ice cuvette and subjected to the electroporation pulse procedure at Bio-Rad Gene Pulser II (Voltage = 1.8 kV, pulse controller- low resistance = 200 Ohm, capacitance = 25 µF). Immediately after the pulse 1 ml SOC medium (2% bacto-tryptone, 0.5% yeast extract, 10 mM NaCl, 10 mM KCl, 20 mM MgCl₂ and 2 mM glucose) was added and the cells transferred to a sterile culture tube. The transformed cells were incubated for 40 min with moderate shaking at 37°C and then plated on LB agar plates containing ampicillin (100µg/ml) for the selection of the clones.

2.2.1.7. Plasmid Mini- and Maxi - Preps

Small- and large-scale DNA plasmid extractions were performed using the QIAGEN Plasmid Mini and Maxi kits according to the protocol of the manufacturer. Briefly, the procedure consists of alkaline lysis of the bacterial cell wall, removing the cell debris while keeping the supernatant containing the nucleic acids, degradation of RNA by RNase, binding of plasmid DNA to a silica-gel matrix and washing with high-salt solution (to remove the chromosomal DNA and proteins) and elution of plasmid DNA.

2.2.1.8. Preparation of electrocompetent *E. coli*

One liter of LB medium was inoculated with 10 ml of a fresh overnight culture of *E. coli* (DH5 α or SURE strains). The cultures were grown at 37 °C with shaking to an O.D. 600 = 0.5 - 0.8 and chilled on ice for 1 h. The cells were transferred to a prechilled centrifuge bottles and harvested by centrifugation (10 minutes, 5,000 x g, 4°C). The pellets were resuspended in the original culture volume of ice-cold water. After a second centrifugation step (15 minutes, 5,000 x g, 4°C) the pellets were resuspended again in a 10 ml of ice-cold water and washed with an original culture half-volume of ice-cold water. The cells were centrifuged again (15 minutes, 5,000 x g, 4°C). Bacterial pellets now were re-suspended in 30 ml ice-cold 10% Glycerol in water and transferred to 30 ml centrifugation tubes (Beckmann). Following the last centrifugation (15 minutes, 5,000 x g, 4°C), the pellets were now re-suspended in 1.5 ml of ice-cold 10% Glycerol in water, aliquoted and quickly frozen in dry ice-ethanol bath and stored at -80 °C. The cells were kept ice-cold during the entire procedure.

2.2.1.9. Cloning into pSFV-plasmid

Epitope tags were fused to EGFP by PCR based cloning. The following amino acid sequences were used for the tags: HA = YPYDVPDYA; c-Myc = EQKLISEEDL; FLAG = DYKDDDDK; AU1 = DTYRYI; EE (also called Glu-Glu) = EYMPME; IRS = RYIRS. N-terminal tags were separated by one glycine residue from the initiator methionine and by two glycine residues from EGFP. C-terminal tags were separated by two glycine residues from EGFP (Fig. 2.1). *BamHI* and *XhoI* restriction sites were inserted in the primers at the N- and C-terminus respectively to allow subcloning into pSFV-PD plasmid (Fig. 2.2) as well as into pBluescript-II-KS vector (Fig. 2.3) for sequencing of the subcloned PCR product. All primers are listed in the materials section.

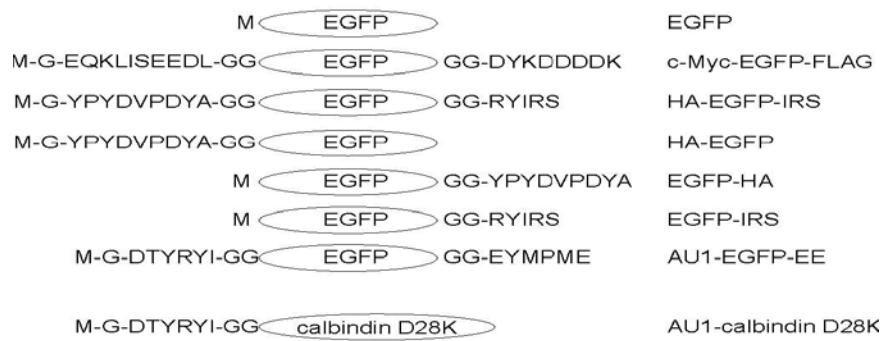


Fig.2.1. Schematic depiction of the epitope tag peptides fused to EGFP and calbindin D_{28K}.

The amino acids sequences of various tags fused to EGFP and calbindin D_{28K} via glycine linkers (GG), shown in one letter code. All C-terminal fusion proteins retain the genuine EGFP start codon, while in N-terminal fusions the initiator methionine of EGFP or calbindin D_{28K} is replaced by the glycine linkers.

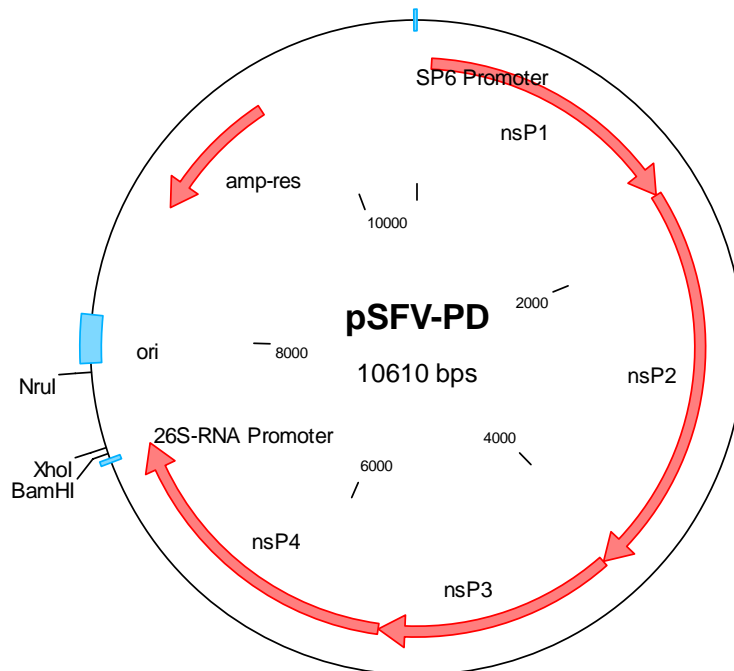
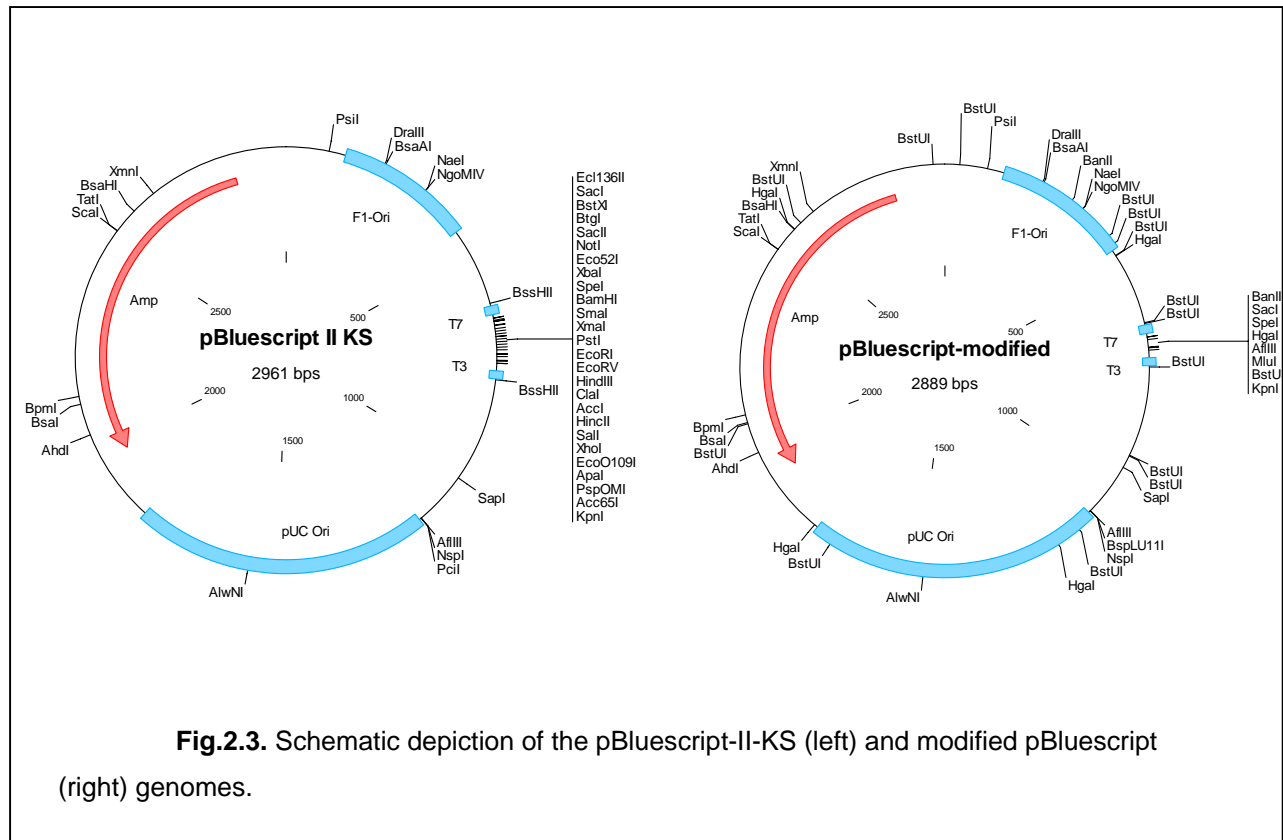
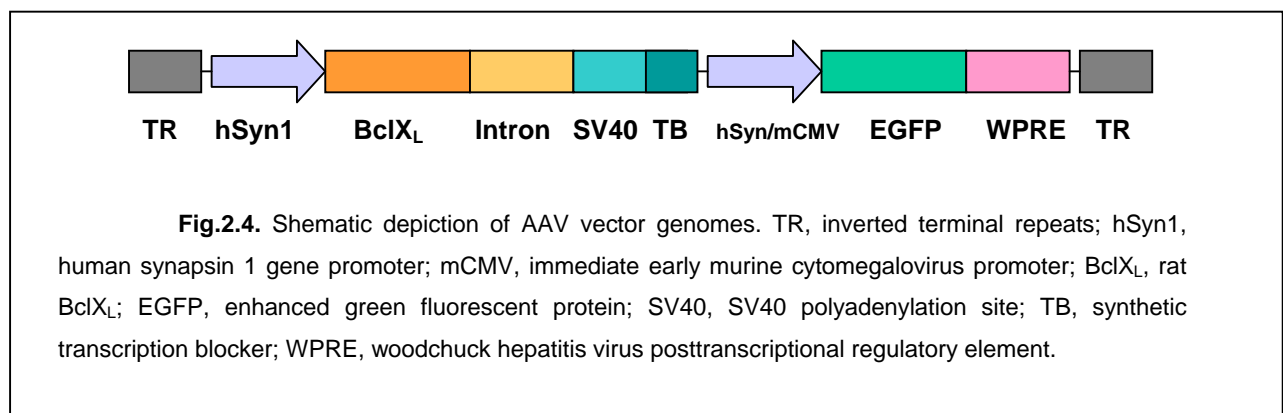


Fig.2.2. Schematic depiction of the pSFV-PD genome.



2.2.1.10. Cloning into pAAV-2 plasmid

Construction of adeno-associated virus (AAV) vectors has been described previously (Kügler, S. *et al.*, 2003b). For this study we employed a bi-cistronic vector expressing the functional transgene and a fluorescent reporter from two independent human synapsin 1 gene promoters (Fig. 2.4). We used pAAV-6p1-TB plasmid (Fig. 2.5) as a backbone for subsequent cloning.



First, BclX_L cDNA was substituted by GDNF and calbindin D_{28K} cDNA. GDNF was amplified with 5'-*MfeI*-GDNF and 3'-*NotI*-GDNF primers from pAdV-hGDNF by PCR. Calbindin D_{28K} cDNA was obtained via reverse transcription from a rat brain lysate (see

reverse transcription). For this, RT- calbindin D_{28K} primer was used initially, followed by specific amplification of calbindin cDNA using 5'-calbindin D_{28K}-cDNA and 3'-calbindin D_{28K}-cDNA primer set. Finally the required restriction sites and AU1-epitope tag were inserted through the third amplification step with 5'-hSyn1-*MfeI*-AU1-calbindin D_{28K} and 3'-*NotI*-calbindin D_{28K} primer set. The sequences of the PCR products were verified in the modified version pBluescript-II-KS (pBS-II-KS) plasmid. Since original pBS-II-KS vector (Fig. 2.3) does not contain *MluI* and *SpeI* restriction sites, we designed the oligo (pBS-woMCS-oligo), which bore these sites. The obtained pBluescript-modified (pBS-m) vector was devoid of a large part of MCS, but included *MluI* and *SpeI* restriction sites (Fig. 2.3). First expression cassette of the bi-cistronic AAV-6p1-TB vector (hSyn1-FLAG-BclX_L-Intron-SV40pA) was cut out by *MluI* and *SpeI* and inserted into pBluescript-modified version. The obtained plasmid was cut with *EcoRI* and *NotI* to allow for the insertion of the PCR products cut with the same enzymes or with *MfeI* and *NotI*, since *MfeI* and *EcoRI* generate compatible ends upon cut. The ligated into pBS-m fragments were subjected to sequencing procedure to verify the absence of any mutations generated through PCR amplification. After the sequencing the whole expression cassette was cut out by *MluI* and *SpeI* and transferred to AAV-6p1-TB cut at the same restriction sites. Thus, we obtained pAAV-GDNF-EGFP and pAAV-calbindin D_{28K}-EGFP vectors.

Second, we replaced EGFP in the second expression cassette of pAAV-6p1-TB by DsRed-2 cDNA to obtain pAAV-6pRed plasmid. DsRed2 was amplified from DsRed2 plasmid (Clontech) using 5'-*BamHI*-*AgeI*-DsRed2 and 3'-*HindIII*-*BsrgI*-DsRed2 primers. The PCR product was subcloned via *BamHI* and *HindIII* restriction sites into pBS-II-KS vector and sequenced and then inserted into pAAV-6p1-TB vector through ligation at *BsrgI* and *AgeI* sites.

Finally, we substituted hSyn-1 promoter in the second expression cassette of the bi-cistronic AAV vector by mCMV promoter (Addison, C. L. *et al.*, 1997; Gerdes, C. A. *et al.*, 2000). To this purpose we amplified mCMV from pMH4-I vector using 5'-*SpeI*-mCMV and 3'-*NotI*-*MfeI*-mCMV primers. The plasmid for sequencing was prepared as follows: the first expression cassette was inserted into pBS-m as described above and then the fragment was cut out by *SpeI* and *NotI* endonucleases and replaced by mCMV cut at the same restriction sites. After confirming the sequence the promoter was cut out by *SpeI* and *MfeI* and inserted into AAV-vector backbone after cutting pAAV-6p1-TB with *SpeI* and *EcoRI*. Thus, the obtained AAV-mCMV-EGFP vector contained only one expression cassette where EGFP was driven by mCMV promoter.

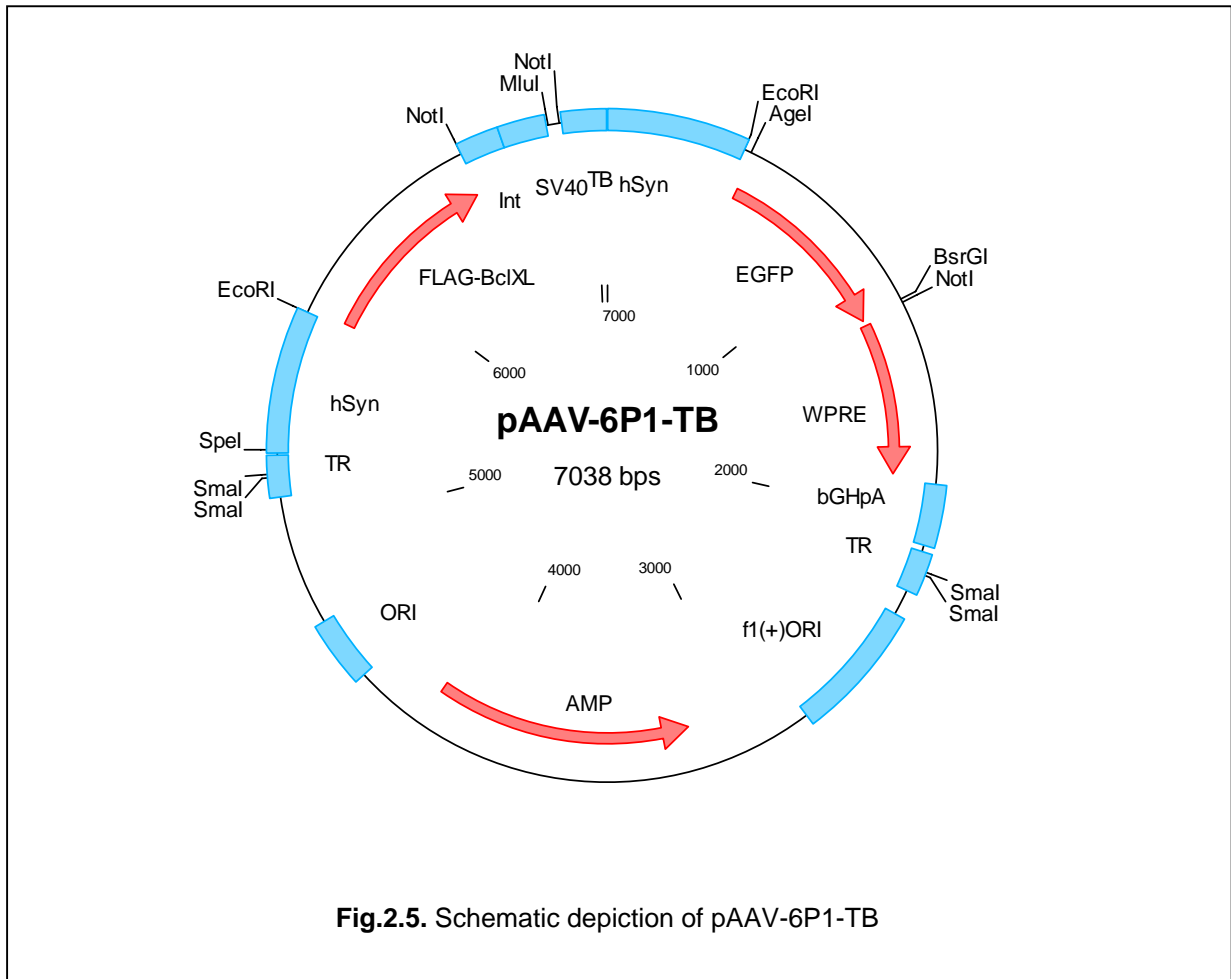


Fig.2.5. Schematic depiction of pAAV-6P1-TB

We also constructed the control vector, which expressed only a reporter EGFP, but no functional transgene. For this, we amplified Intron-SV40pA fragment from pBS-m-hSyn-BclXL-Int-SV40pA via PCR using 5'-*PstI*-Intron-SV40pA-w/oEcoRV and 3'-*EcoRI*-Intron-SV40pA-w/oEcoRV primers. The PCR product was then cut with *PstI* and *EcoRI* and inserted on the place of hSyn-1 promoter, which was cut out with the same enzymes from pBS-m-hSyn-BclXL-Int-SV40 plasmid. The first expression cassette in the pAAV-6p1-TB vector was replaced by the fragment which was cut out from resulted pBS-m-Int-SV40-BclXL-Int-SV40 plasmid with *MluI* and *SpeI*. Thus, the control vector retained only one active expression cassette of the reporter EGFP.

AAV vectors are characterized by inherently high recombination probability due to the presence of ITRs. Therefore all AAV plasmids were propagated in the SURE strain of *E. coli*, and the integrity of AAV vector genome was confirmed by a *SmaI* digest (cutting the vector plasmid in the ITR regions) was performed before using it for AAV vector production.

2.2.2. Viral vectors production and purification

2.2.2.1. SFV vectors

Recombinant Semliki-Forest virus (SFV) vectors with reduced cytotoxicity and conditionally infective particles were generated as described (Lundstrom, K. *et al.*, 2003). pSFV-PD vector, containing epitope-tagged EGFP was linearized with *NruI*, while pSFV-helper2 plasmid was linearized with *SpeI* endonuclease. Linearization of the plasmids was necessary for *in vitro* transcription step that followed. The reaction conditions were following: 3-5 µg DNA was mixed with 5 µl of rNTPs (10 mM each), 5 µl of Cap structure (Ribo m⁷G Cap Analog, Promega), 5 µl of 10 x SP6-transcription buffer, 1.5 µl of RNasin, 3.5 µl of SP6 polymerase (Promega) and millipore sterile water to achieve a volume of 50 µl, and the reaction mix was incubated for 1 h at 37°C. RNA was purified using RNeasy QIAGEN Kit, precipitated as described above for DNA, and run in the denaturing RNA agarose gel (1% agarose, 20 mM MOPS , 5 mM Na acetate, 1 mM EDTA, pH 7.0; 2% Formaldehyde) to check for the purity. RNA concentration was determined at a photometer as described above for DNA. Each vector production run required 30 µg of SFV-RNA , 15 µg of SFV-helper2 RNA and only 2 x 10⁷ BHK-21 cells, which after electroporation (Bio-Rad Gene Pulser II: voltage = 0.36 kV, pulse controller- high resistance = 500 Ohm, capacitance = 75 µF) were seeded in one 6-well plate (Sarstedt) and cultured for 24 h at 31°C. Electroporation medium contained 1:1 DMEM/F12, 10% FCS, 4 mM glutamate, 1% PS. The supernatants containing the virus particles were collected twice at 24 (2 ml/well) and 48 h (1 ml/well) after the transfection, sterile filtered to remove the cell debris and stored at -20°C until processed further. Viral particles were precipitated by ultracentrifugation of the activated by addition of α-chymotrypsin treatment supernatants in a Beckman SW41 rotor (39,000 rpm, 1 h, 4°C) and resuspended in a small volume of phosphate buffered saline (PBS). Titration of transducing units was performed on BHK-21 cells by counting EGFP positive cells.

2.2.2.2. AAV vectors

AAV-293 cells were harvested after they reached ca. 50% confluency in 175 cm² culture flasks and then seeded in cell factories (Nunc) at 1.1 x 10⁸ cells per factory in 700 to 800 ml of medium (see cell culturing). Typically 6 culture flasks are required for seeding of one cell factory. When the cells reached 50-60% confluency (ca. 24 h), they were subjected to calcium-phosphate transfection. Cells were first washed with ca. 400 ml of DMEM. The transfection mix contained 265 µg of AAV-plasmid, 1 mg of helper plasmid (pDG for AAV-2 and pDP5 for AAV-5), 0.25M CaCl₂ in 16.5 ml of deionized sterile water. 16.5 ml of 2 x HBS (pH 7.05) were added to 16.5 ml of transfection mix and incubated for 1 min at 25°C. The

mixture was added to 315 ml of DMEM/ 2%FCS and the obtained transfection medium was equally distributed through the layers of the cell factory. For the transfection the cell factories were incubated overnight (12-14 h) at 37°C, 5% CO₂, 95% humidity. The medium was changed then to 10% FCS/ 1% PS/ DMEM (ca. 750 ml/ cell factory). At ca. 36-40 h after transfection the cells were checked for reporter fluorescence at the microscope and then harvested. After removing the medium from the cell factory, the cells were briefly washed 300 ml with citric saline (CS). Then 200 ml of CS were added and the cells incubated at 37°C for several min until detached and then collected to a sterile bottle. The remaining cells were collected by a second rinse with ca. 100 ml of CS. Collected cells were centrifuged then for 5-10 min at 1,300 rpm at RT. The cell pellets (the volume of the pellet was noted) were resuspended in total volume of 20 ml of Tris-buffered saline (150 mM NaCl, 50 mM Tris, pH 8.5) and stored at -80°C until further processing. For virus gradient centrifugation the virus-containing cells were first thawed and frozen 3 times in an ethanol/ dry ice bath. 1.6 µl of Bezonase (300 U/ml) was added to the cells and incubated for 30 min at 37°C water bath. The cell mix was slightly shaken every 5-10 min during incubation. Following incubation, the cell mix was centrifuged at 4000 rpm 18°C for 30 min. The supernatants were carefully transferred to new 50 ml falcon tube and adjusted to a 30 ml volume by addition of ca. 10 ml of Tris-buffered saline. After washing the pump catheter connected to a 20G needle placed into a 50 ml falcon tube pump with millipore sterile water, the iodixanol (Opti Prep™ Fresenius Kabi, Norge, Axis-Shield, Oslo, Norway) step gradient was performed. For this, the following solutions were prepared first:

B = 10 x PBS-MK (80g NaCl + 2 g KCl + 14.4 g Na₂HPO₄ + 2.4 g KH₂PO₄ dissolved in 990 ml millipore sterile water, pH 7.4; and then 5 ml 2,5 M KCl and 5 ml 1 M MgCl₂ were added and the solution sterile filtered).

C = 1x PBS-MK (500 µl 2.5 M KCl; 500 µl 1M MgCl₂ in 499 ml PBS)

D = 2 M NaCl in 1x PBS-MK

E = 54 % working solution: (45 ml iodixanol + 5 ml **B**).

For obtaining different iodixanol gradient solutions the solutions C, D, E, iodixanol and phenol red were intermixed as it is shown in the following table:

4 tubes	E	D	C	phenol red (0.05 % in water)	iodixanol
15 % gradient	15 ml	27 ml	12 ml	150 µl	
25 % gradient	2,25 ml		14,5 ml		
40 % gradient	20 ml		7 ml		
60 % gradient				150 µl	25 ml

The diluted supernatant containing the virus particles was transferred to "Quick Seal Tubes" (Beckmann; 1x 3.5 inch [25x 89 mm]) in a volume of 15 ml per tube, by using a 20 ml a syringe connected to the spinal needle (20G x 2^{3/4}). Using the pump, the iodixanol gradient solutions were added consequentially (10 ml of the 15% gradient, 6 ml of the 25% gradient, 4 ml of the 40% gradient, 6 ml or more of the 60% gradient to fill up the tube) into the Beckmann tubes underneath the virus solution. Every next gradient solution was placed underneath the previous one. The tubes were heat-sealed and the gradients were run at the ultracentrifuge (SORVALL® Discovery 90SE). The settings for ultracentrifugation were: speed 68,000 rpm (310,000 g), 1 h 15 min, 18 °C, acceleration was set to "5", deceleration to "0". After centrifugation the phase containing the concentrated and relatively pure virus solution was removed by inserting the needle connected to a 5 ml syringe slightly underneath the border between 40% and 60% iodixanol gradient and aspirating the 40% gradient solution containing the virus vectors (3-4 ml). The virus-containing gradient solution was collected in a 50 ml falcon tube and stored frozen at -20°C. The virus was further purified and concentrated by collecting the "peak" elution phase on Äkta-FPLC system FPLC using HiTrap™ Heparin HP 1 ml column for rAAV-2 (Amersham) and HiTrap™ QFF 1 ml column (Amersham) for rAAV-5 vectors. Further concentration and purification of rAAV-2 particles was done by dialysis using Slide-A-Lyzer, (MWCO = 10,000, before using) in 1 L PBS for 1 h. The final virus solution was subjected to real-time PCR (RT-PCR) quantification of the rAAV-vector genome titre. Purity of the vectors was determined by SDS-gel electrophoresis and infectious titres by transduction of cultured primary hippocampal neurons. Genome particles to transducing units (t.u.) ratio typically was 25:1 - 35:1. The AAV vectors were aliquoted and stored at -80°C until required. During all procedures dealing with AAV vectors, 0.5% SDS solution in water was used for disinfection.

2.2.3. Cell culturing

2.2.3.1. Continuous cell culture

Working with continuous cell culture was always performed under sterile conditions. Mammalian AAV-293 were cultured in DMEM supplemented with 10% FCS and 1% PS and BHK-21 cells in DMEM/F12 1:1 supplemented with 10% FCS, 4 mM glutamine, 1% PS in 175 cm² culture flasks (Sarstedt) at 37°C, 5% CO₂ supply, 95 % humidity. After reaching approximately 70% confluence, the cells were split 1:4 (every 2-4 days). For this, the medium was removed, 4 ml of pre-warmed to 37°C 0.05% trypsin/ 0.02% EDTA solution were added to the culture and left in the incubator at 37% for 5-12 min until detached from the flask. Trypsin activity was stopped by addition of 7 ml of the cell culture medium to the flask. The mix containing detached cells was carefully transferred to a 15 ml Falcon tube and spun down at 4,000 g, 4°C, 5 min. After removing the supernatant a cell pellet was resuspended in 100 ml of the fresh medium and seeded in 4 (175cm²) flasks.

2.2.3.2. Primary culture of hippocampal neurons

Coating of 24-well plates (Nunc) or coverslips with polyornithine/ laminin is particularly useful for culturing CNS neurons. For this, ethanol-soaked and flamed coverslips (\varnothing 10 mm) incubated with polyornithine solution (500 µl/well, 100 µg/ml in millipore sterile water) for 12-24 h at RT, then washed twice with 1 ml/well of millipore sterile water and coated with laminin (500 µl/well, 1µg/ml in NBM) by incubation at 37°C, 5% CO₂, 95 % humidity overnight. Before the preparation of the hippocampi, the coverslips were washed twice with NBM and then 500 µl of hippocampus medium (1% PS-N, 0.5 mM L-glutamine, 0.05% Transferrin, 2% B27 Supplement in NBM) was added and the plates kept at 37°C. To obtain primary hippocampal neurons, hippocampi were dissected from Wistar rat embryos (embryonic day 18) and further processed for establishing dissociated cell cultures. All surgical procedures were performed on ice. In brief, hippocampal tissue pieces were collected in ice-cold hippocampus medium and centrifuged at 1,000 rpm for 4 min. The medium was removed and the tissue pellet was incubated in 750 µl trypsin (0.25%, 15 min, 37°C). Trypsin was inactivated by addition of 750 µl ice-cold FCS. The pellet was then dissociated by gentle trituration using a fire-polished Pasteur pipette. After centrifugation at 1,000 rpm for 4 min, the pellet was resuspended in warm hippocampus culture medium. Cells were seeded in poly-L-ornithine/laminin 24-well culture plates (Nunc) at a density 250,000 cells/well. Cultures were maintained at 37°C in a humidified atmosphere and 5% CO₂ in hippocampus medium.

2.2.3.3. SFV-transduction and cell lysis for western blotting

After reaching 70% confluence HEK-293 cells seeded in a 6-well plate were transduced by addition of 5×10^5 SFV t.u. per well in a 500 μ l volume of OptiMEM and kept at 31°C, 5% CO₂, 95% humidity for 1 h. Then 1.5 ml of OptiMEM was added to each well and the plates were transferred to a 35°C, 5% CO₂, 95% humidity for overnight incubation (12-13 h). After removing the medium the cells were washed twice with PBS, the lysis buffer for cells was added (250 μ l/well) and the cells scraped from the plate and transferred to a 1.5 ml eppendorf tube. The lysates were boiled for 5 min and chilled on ice. After addition of protease inhibitor mix the lysates were centrifuged at 4°C at maximum speed for 20 min. The supernatant was collected, aliquoted and frozen at -20°C.

2.2.3.4. Indirect immunofluorescence on primary neurons

For transduction of primary hippocampal neurons seeded in 24-well plates 1×10^8 t.u. of AAV-2 vector in 500 μ l of hippocampal medium were used per well. After the reporter gene fluorescence (either EGFP or DsRed2) could be clearly detected by microscopy (us. 4-5 days after AAV-2 transduction), the cultured neurons were subjected to indirect immunofluorescence assay. The coverslips with primary hippocampal neurons were rinsed with PBS and fixed by incubation in 4% formaldehyde for 10 min at room temperature. After washing 2 times for 5 min with PBS the cells were subjected to permeabilization procedure by incubation with ice-cold acetone at -20°C for 5 min. Following a second washing with PBS (3 x 5 min), blocking solution (10% NGS in PBS) was applied for 30 min at room temperature to block unspecific binding of the antibodies. Incubation with a primary antibody (all anti-tag antibodies were used in a dilution of 1:500) was performed for 1 h at 37°C. The cells were rinsed with PBS 3 x 5 min and then incubated for 1 h at room temperature with a secondary antibody coupled to a fluorescent reporter cy3 (1:200). The cells were washed again 3 x 5 min with PBS and mounted on the glass slides embedded in Moviol mounting medium (16 % Moviol in 30 % Glycerol/ PBS, 0.02 % sodium azide) to protect immunofluorescence from bleaching.

2.2.4. Animal procedures

Adult female Wistar rats (University Hospital Animal Facility, Göttingen) of 250-280g of weight were housed at 12h/12h of light/dark cycle, provided with food and water *ad libitum*. Animals were deeply anaesthetised by 7% chloral hydrate intraperitoneally (340mg/kg) before the respective surgery. All animal procedures were performed in

accordance to German guidelines for care and use of laboratory animals and to the respective European Community Council Directive 86/609/EEC.

2.2.4.1. Stereotaxic injection into the rat brain

The head of the rat was fixed by ear bars and a jaw holder in a stereotaxic frame (“Kopf” Instruments) after the appropriate anaesthesia. A skin covering the skull was longitudinally cut from the imaginary line connecting the eyes in front till the imaginary line connecting the auditory channels in the back. Remaining connective tissue was carefully removed aside by scalpel in order to achieve appropriate visualisation of the skull sutures and to define the bregma (a crossing point of parasagittal with coronal sutures) on the surface of the skull as “zero” or “start” point. After achieving flat positioning of the skull, the coordinates for the injection were calculated related to bregma. For the injection into the SNpc, the following coordinates were used according to Paxinos and Watson atlas of a rat brain: antero-posterior (AP): -0.53; medio-lateral (ML): +0.22; dorso-ventral (DV): -0.78. The coordinates for the injection into the LMFB were the following: AP: -0.2; ML: +0.2; DV: -0.85; into the striatum: AP: +0.2 mm; ML: -2.8 mm; DV: -5.6 mm; and into hippocampus: AP: -4.3; ML: +3.0; DV: -3.4 mm. Glass capillaries (World Precision Instruments, WPI), filled with mineral oil and the solution for the injection were attached to the nanoliter injector (WPI). The injector was connected to a microprocessor-based controller, Micro4 smart controller (WPI), which allows for setting the operating parameters, such as the volume and the speed (nl/min) of the injection. AAV-vectors were injected into SNpc in a volume of 2 µl and in the striatum in a volume of 2-4 µl depending on the original infectious titre of the virus. The volume 3 µl of 5mg/ml of 6-hydroxydopamine hydrochloride in 0.2% ascorbic acid/PBS was injected in LMFB to produce the unilateral PD lesion model. The speed for all injections was set to 500nl/min.

2.2.4.2. Intravitreal injections and optic nerve axotomy

Wistar rats of 200-270g were anesthetized with 7% chloral hydrate (340mg/kg body weight). Pupillary dilatation for better visualisation of the lens was achieved with subsequent surface application of 1% tropicamide and 2% mepivacaine. Injections into the eye were performed by a fine bore glass capillary with a tip diameter of 30 µm attached to a catheter on a Hamilton syringe. 2 µl (1×10^5 transducing units of SFV, 1×10^7 transducing units of AAV) of viral suspension were injected intravitreally by puncturing the eyeball below the cornea-sclera junction. Due to pupillary dilatation, the tip could be observed during the injection and care was taken to avoid contact with the lens. Vector injections were performed 3 weeks before

the optic nerve axotomy. After skin incision close to the superior orbital rim, the orbita was opened and lacrimal gland was partially removed to achieve a better visualisation of the optical nerve and surrounding vessels. Following the spreading of superior extraocular muscle by a small retractor, the optical nerve was exposed by longitudinal incision of the perineurium. Optic nerve was transected at a distance of ca. 2 mm from the posterior pole of the eye leaving the retinal blood supply intact. Retrograde fluorogold (FG) labelling of RGCs was performed by putting a small sponge soaked with FG tracer onto the proximal to the eyeball optic nerve stump. Animals with retinal ischemia, as verified after the surgery fundoscopically, have been excluded from the study.

2.2.4.3. Transcardial perfusion and brain tissue processing

Transcardial perfusion under terminal anaesthesia is a commonly used method for tissue fixation in immunohistochemical protocols. This method takes advantage of the animal's circulatory system to deliver the fixative solution evenly throughout the body tissues, with optimal penetration of the brain. Fixation preserves the ultrastructure, stabilizes protein and peptide conformation so that antibodies can bind to antigen sites. We used 4% paraformaldehyde (PFA) in phosphate buffer solution (PBS) as a fixative since it is optimal for visualization using fluorescent dyes.

After a deep anaesthesia with 7% chlral hydrate (800 mg/ml) the rat was fixed on rack, the abdominal cavity was opened with sharp scissors, and the diaphragm was cut to allow access to the thorax. With large scissors, blunt side down, ribs were bilaterally cut and the rib cage was open to allow access to the heart. While holding heart steady, the left ventricle was cut and the catheter blunt-ended needle inserted through the ventricle and atrium into aorta. Needle position was secured by clamping in place. The liver was cut then to allow a large part of blood volume to leave the body. The abdominal aorta was clamped to restrict perfusion to the upper par of the body. The nose was cut for the control of procedure. Thus, if fluid was flowing freely from the cut nose the needle was considered to be appropriately positioned. The syringe containing ice-cold PBS and connected to the catheter was operated with a speed of 15–20 ml/min. When blood has been cleared from body (ca. 200 ml of PBS is usually required), PBS was replaced with ice-cold 4% PFA solution (200 ml). The rat was decapitated and the brain carefully removed from the skull and placed into 4% PFA overnight at 4°C for post-fixation. The brain was cryoprotected by dehydration in 30% sucrose solution in PBS, frozen on dry ice and cut on a cryostat (*Leica CM 3050 S*) to 18 µm coronary sections.

2.2.4.4. Preparation of the brain tissue lysates for Western Blotting

Rats were sacrificed by an overdose of chloral hydrate (1mg/kg) and transcardially perfused with 150 ml ice-cold PBS. The brain was removed and quickly frozen on dry ice. 3 mm thick coronal section containing the *substantia nigra* was cut out and subjected to biopsy in the SNpc region by using a small biopsy needle with 2 mm inner diameter. The excised tissue was weighted and homogenized in a tissue lysis buffer by sonication and incubated on ice for 15 min. The lysates were then centrifuged twice at 4°C with maximum speed for 15 min to remove the debris. The supernatants were aliquoted and kept frozen at -20°C.

2.2.5. Indirect immunofluorescence on brain slices

Brain slices were dried for 1 h at 37°C, then rehydrated in PBS for 45 min and exposed to antigen retrieval in TBS (pH 9.0) for 5 h in a water bath at 60°C. While regular antigen retrieval destroys EGFP fluorescence, this procedure allows for keeping it intact. The slides were shortly washed with PBS and incubated in a blocking solution for 30 min at room temperature to avoid unspecific binding of the antibodies. Incubation with primary antibody (anti-TH, 1:600; anti-calbindin 1:1000, anti-GFAP, 1:500; anti-NeuN 1:200; all anti-tag antibodies were used in 1:500 dilution after testing different dilutions, ranging from 1:200 to 1:5,000) was performed overnight at 4°C in incubation solution -1 for IF. After washing 3 x 5 min with PBS the secondary cy3-coupled antibody (1:250 in incubation solution -2 for IF) was applied for 1 h at room temperature. The secondary antibody was washed out with PBS (3 x 5 min). Slides were embedded in Moviol, coated by coverslips and kept at 4°C until microscopy.

2.2.6. Protein handling procedures

Western Blotting or immunoblotting allows for determination, with a specific primary antibody, the relative amounts of the protein present in different samples. Briefly, 1) samples are prepared from tissues or cells that are homogenized in a buffer that protects the protein of interest from degradation; 2) the sample is separated using SDS-PAGE and then transferred to a membrane for detection; 3) the membrane is incubated with a generic protein (such as milk proteins) to bind to any remaining sticky places on the membrane. A primary antibody is then added to the solution which is able to bind to its specific protein; 4) a secondary antibody-enzyme conjugate, which recognizes the primary antibody, is added to find locations where the primary antibody bound.

2.2.6.1. Protein concentration determination

Protein concentration was determined by Bradford assay. The assay is based on the observation that the absorbance maximum for an acidic solution of Coomassie Brilliant Blue G-250 shifts from 465 nm to 595 nm when binding to protein occurs. Both hydrophobic and ionic interactions stabilize the anionic form of the dye, causing a visible colour change. The reaction was performed in a 96-well plate at room temperature. Protein standards were prepared in PBS in a concentration range between 0.1-1.4 mg/ml. Unknown protein samples were diluted to 1:2, 1:10 and 1:100. 5 µl of protein standards or diluted unknowns were mixed with 250 µl of Bradford reagent in each well and incubated for 15 min. The absorbance of the samples was measured at 595 nm on a TECAN *Rainbow* plate reader using the easyWINbasic software (SLT Company). Plotting of the absorbance vs. the protein concentration for protein standards to obtain a standard curve and calculation of the unknown samples protein concentration was done using the Microsoft Office 2003 Excel software.

2.2.6.2. SDS-polyacrylamide gel electrophoresis (SDS-PAGE)

SDS-PAGE is based on separation of a large range of proteins of varying molecular weights and charges under the influence of the electrical field within the continuous cross-linked polymer matrix polyacrylamide/ bis-acrylamide (Rothiphorese). Cross-linking is catalysed by free radicals produced upon addition of ammonium peroxide and TEMED. Two-phase gels were used for collection and separation of the proteins according to their molecular weight. Usually, 12% resolving gel and 5% stacking gel were used to separate the proteins of interest. To define a molecular weight of loaded proteins the molecular weight marker was loaded and separated in parallel. The protein concentration in the samples was adjusted by dilution of more concentrated samples in PBS. Equal volumes of protein samples and 2 x SDS-loading buffer were mixed, subjected to heating at 95°C for 5 min, chilled on ice and loaded in the gel combs. SDS-PAGE was run at 4°C in ice-cold electrophoresis buffer. All equipment used for SDS-PAGE and WB was purchased from Bio-Rad. Electric field of 70 V was applied for 15 min to allow samples to enter the gel and collect without a smearing and then increased to 100 V and kept constant until the bromophenol blue reached the bottom of the resolving gel.

2.2.6.3. Immune blotting

For the western blot procedure a Mini Trans-Blot Cell setup (Bio-Rad) was employed. After electrophoresis completion the polyacrylamide gel was placed between two sheets of Whatman filter paper and a nitrocellulose membrane (Protran), all preliminary soaked in transfer buffer. Two additional Whatman filter papers were placed on the top on the

membrane and the “sandwich” was placed in the Mini Tans-Blot Cell. A voltage of 100 V was applied for 1 h at 4°C.

After the completion of the transfer the membrane was treated with blocking solution for 1 h at room temperature to avoid unspecific binding of the antibody. Incubation with both primary and secondary antibodies was performed in 2% Milk/TBS-T solution for 1 h at room temperature. The membrane was washed 3 x 10 min with TBS-T between primary and secondary antibody application and 3 x 15 min with TBS-T after the incubation with secondary antibody. The following dilutions of the primary antibodies were used: anti-EGFP, 1:1,000; anti-FLAG 1:500; anti BclX, 1:2,000. All secondary antibodies coupled to HRP were used in dilution 1:3000. Together with a secondary antibody streptavidin peroxidase was applied in dilution 1:3000 to allow for later visualization of biotinylated molecular weight protein marker (Sigma). For developing the membrane equal volumes of ECL-1 and ECL-2 reagents were mixed, applied for 1 min in the dark onto the membrane and imaged at Fluor-S-Max Gel Imager (Bio-Rad) and Quantity One software (version 4.2.1).

2.2.7. GDNF-ELISA

Quantification of GDNF tissue levels in transduced and contralateral SNpc was determined by ELISA (GDNF Emax® ImmunoAssay System, Promega) according to the instructions of the manufacturer. Tissue samples of SNpc were obtained from 3 mm thick tissue slices by means of small biopsy needles with inner diameter of 2 mm and lysed according to the procedure described in section 2.2.4.4. After an overnight coating of a 96 well plate, the specific protein is detected using an antibody sandwich format. To this purpose 96 well plates are coated with anti-GDNF monoclonal antibody, which binds soluble GDNF. The captured GDNF is then bound by a second, specific polyclonal antibody. After several washing steps, the amount of specifically bound polyclonal antibody is detected using a species-specific antibody conjugated to horseradish peroxidase as a tertiary reactant. The unbound conjugate is removed by washing, and after incubation with a chromogenic substrate, the colour change is detected. The amount of GDNF in the test solutions corresponds to the colour generated in the oxidation-reduction reaction. Using this system, GDNF in tissue culture supernatants or tissue homogenates can be quantitatively measured.

2.2.8. Microscopy and image analysis

Fluorescence from tissue sections and fixed cultured cells was recorded on a Zeiss Axioplan-2 microscope equipped with a 16 bit greyscale CCD camera (Zeiss). Narrow band filter sets specific for EGFP and cy3 fluorescence were used. For all recorded EGFP images

exposure time was 3 000 ms, except for pictures taken from HA-tag transduced sections which are labelled EGFP x 5. These images were recorded with an exposure time of 15,000ms. cy3 fluorescence was recorded with an exposure time of 500 ms. Images from individual fluorescences were recorded separately as greyscales. Pseudo-colouring of images, generation of overlays and quantification of EGFP / cy3 co-localization was performed with AxioVision 3 software package (Zeiss).

2.2.9. Quantification of neuroprotection in 6-OHDA rat model of PD

At the respective time points after 6-OHDA injection into medial forebrain bundle (MFB), rats ($n = 5$ per condition) were sacrificed by an overdose of chloral hydrate and transcardially perfused with 4% PFA. Brains were processed to 18 μm slices, and immunofluorescent visualization of dopaminergic neurons in SNpc was performed with primary rabbit antibody against tyrosine hydroxylase (anti-TH, 1:500, Advanced ImmunoChemicals Inc., USA; overnight incubation at 4°C) followed by 1h incubation at RT with secondary cy3-conjugated goat anti-rabbit antibody (Dianova). Images of brain sections were recorded as described above. TH-immunoreactive (TH-IR) cells were counted in every 8th brain section in the region anatomically correspondent to SNpc. TH-IR cells of the ventral tegmental area (VTA) area were excluded from counting. To obtain the corresponding total DA cell numbers the counted values were multiplied by 8, assuming that the average diameter of the adult rat DA-neuron is 16-18 μm (Juraska, J. M. *et al.*, 1977).

2.2.10. Rotational behaviour test

One of the most simple to perform and widely used test for evaluation of the unilateral 6-hydroxydopamine lesion is drug-induced rotational behaviour test (Ungerstedt, U. *et al.*, 1970). Disbalance in dopamine secretion in the brain results in preferable turning of the animal to the side of the lesion. When the rat is challenged with certain drugs (apomorphine, amphetamine), this rotation tendency is greatly increased and leads to a typical “rotational behaviour” when an animal “tries to catch its own tail”. The more complete the lesion is- the more complete rotations to one side per min will be counted. To evaluate the degree of the lesion of dopaminergic system each rat was subjected to intraperitoneal apomorphine hydrochloride injection (0.2 mg/kg, Teclafarm) at 2 weeks after the lesion. If a rat exhibited 5 or more rotations per min toward the contralateral to the lesion side during one hour after apomorphine injection, the lesion was considered to be complete. This typically corresponded to the $\geq 80\%$ loss of dopaminergic neurons in SNpc and almost absolute loss of dopaminergic

projections of these neurons to the striatum of a rat brain as revealed by indirect TH-immunofluorescence.

2.2.11. Statistics

RGC and TH-IR cell counts are presented as means \pm standard deviations. For each time point and experimental condition $n = 5$ were used. For retinas, 3 independent fields per retina were counted, for TH-IR cells of SNpc region at least 13 sections were counted per animal. Statistical significance was assessed by split-plot analysis of variance and alpha-adjusting for multiplicity (Bonferroni-Holm sequentially rejective procedure) and, at the 1% level, revealed $p < 0.001$ for either BclX_L or GDNF transduced areas vs. untransduced and versus the control AAV-EGFP-transduced SNpc at all time points. Analysis of variance (factor 1 - BclX_L, factor 2 - GDNF, interaction 1 / 2 = BclX_L + GDNF) revealed that interaction was not additive ($p < 0.001$), but more than additive (= synergistic) for retina, but not for the brain, where it is additive at 2 weeks, but not significant at 6 weeks after lesion when compared to the GDNF-treated group. Pairwise comparisons of values were performed by paired, one-tailed Student's t-test.

3. Results

3.1. Development of AAV vectors for targeting different cell types of CNS

3.1.1. Construction of AAV vectors

AAV vectors hold a great promise as tools for long-term gene transfer in the brain. Specific targeting of transgene expression to either neurons or glial cells would expand the usability of AAV vectors. In this study, in order to produce AAV vectors with different expression profiles in CNS cells several strategies have been employed.

First, to overcome the inherent limitations of AAV vectors for transgene accommodation, small transcriptional regulatory elements have been used. The fluorescent reporter gene was expressed from either short neuron-specific hSyn1 gene promoter or ubiquitously active murine cytomegalovirus immediate early promoter (mCMV). In figure 3.1.1 vector genomes as used in this study are schematically depicted: here, small transcriptional control elements allowed for the construction of bi-cistronic vectors, which express both a functional transgene and a fluorescent reporter gene, and thus demarcate successfully transduced cells.

Second, we cross-packaged AAV-2 vector genomes in AAV-5 capsid shell, since these two AAV serotypes require different cell-surface receptors for successful entry into the cell, and thus are being predicted to have different transduction patterns (Davidson, B. L. *et al.*, 2000; Di Pasquale, G. *et al.*, 2003; Walters, R. W. *et al.*, 2001; Opie, S. R. *et al.*, 2003).

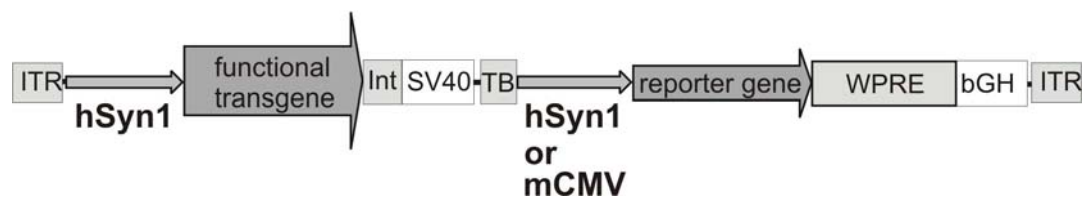


Fig.3.1.1. Schematic representation of bi-cistronic vector genomes used in this study. Vectors used for the expression of a functional transgene also carry a second, independent expression cassette for a reporter gene EGFP (green fluorescent protein) or DsRed2 (red fluorescent protein). Functional transgenes expressed from these bi-cistronic vectors may be up to 1500 bp in size. ITR, inverted terminal repeats of AAV-2; hSyn1, human synapsin 1 gene promoter; mCMV, murine cytomegalovirus immediate early promoter; Int, 146 bp chimeric intron, WPRE, woodchuck hepatitis virus posttranscriptional control element; SV40, simian virus 40 derived polyadenylation site; bGH, bovine growth hormone derived polyadenylation site; TB, synthetic transcription blocker.

3.1.2. *In vitro* transduction of brain cells by AAV vectors

Following the construction of recombinant AAV vectors, we first investigated their transduction properties in primary hippocampal cultures. As shown in figure 3.1.2, different combinations of AAV serotypes and promoters allow for targeting the transgene expression either exclusively to neurons or to astrocytes. Types of cells transduced by the respective virus vector were identified by typical morphology and confirmed by immunofluorescent co-labeling with either NeuN or GFAP (data not shown).

In order to achieve quantitative transduction of cultured neurons (90 - 95 % transduction efficacy), cells were grown on coverslips in 24 well plates. Transduction was performed at 12 hours after seeding, in a culture volume of 250 µl. $1.5 - 3 \times 10^9$ vector genomes as determined by quantitative PCR are used for each well. This corresponds to $0.5 - 1 \times 10^8$ transducing vector units, as the ratio of infective vs. total viral particles routinely obtained was 1:30. After overnight incubation, culture medium was filled up to 750 µl. This procedure allows for the generation of "transgenic" cultures of primary brain cells (Fig. 3.1.2 d, e), which are routinely maintained for about 4 weeks without any signs of cytotoxicity (Kügler, S. *et al.*, 2003b).

The onset of transgene expression after AAV vector transduction is often claimed to be "slow", supposedly due to the necessity of conversion of the single stranded genome into double-stranded DNA, especially in non-dividing cells. However, when primary hippocampal cultures were infected by AAV-2-hSyn-EGFP vectors at the time of seeding, readily detectable transgene expression emerged in neurons at 2-3 days after transduction, reaching almost 100% transduction efficacy at 5-7 days after transduction (Fig. 3.1.2 a).

Transgene expression was also completely restricted to neurons as identified by anti-NeuN staining if the AAV-2 vector genomes containing the expression cassettes were cross-packaged into the AAV-5 capsid. However, expression levels were substantially reduced (Fig. 3.1.2 b), indicating that receptors for AAV-5 capsids (PDGFR and sialic acids (Di Pasquale, G. *et al.*, 2003)) are less abundant on primary hippocampal neurons as compared to the receptors necessary for AAV-2 entry (heparansulphate proteoglycan moieties (Opie, S. R. *et al.*, 2003)). Intriguingly, replacing the hSyn1 gene promoter by the mCMV promoter in the AAV-5 vector drastically changed the transgene expression pattern: rapid onset of transgene expression is detected in fibrous astrocytes as identified by anti-GFAP immunofluorescence (Fig. 3.1.2 c) and remained confined to this cell type throughout the lifetime of the culture. Thus, AAV-5 vectors can transduce both neurons and astrocytes in primary cultures, and can be efficiently targeted to either of cell types by choosing the appropriate promoter.

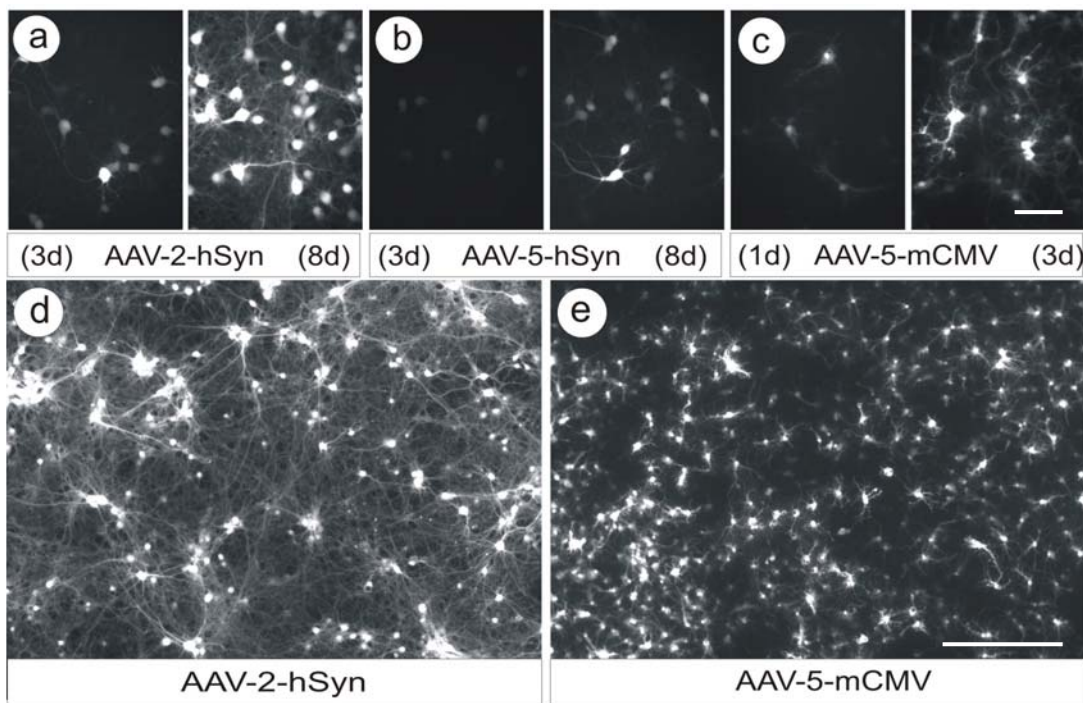


Fig.3.1.2. Neuron- or astrocyte-specific transduction of primary neuronal cultures. AAV vectors expressing EGFP from different promoters, packaged into either AAV-2 or AAV-5 capsids, were used to transduce primary hippocampal neurons at times of preparation (DIV 0). Transduction of astrocytes was performed at DIV 7 of the same culture. EGFP fluorescence of living cultures was recorded at an inverse fluorescent microscope at either day 3 or day 8 after transduction for neurons, or at day 1 or day 3 after transduction for astrocytes. Parts (a) to (c) show high power magnifications of cultures transduced with (a) an AAV-2 vector expressing EGFP from the hSyn1 promoter, (b) an AAV-5 vector expressing EGFP from the hSyn1 promoter, and (c) an AAV-5 vector expressing EGFP from the mCMV promoter. Low power micrographs showing quantitative transduction of either neurons or astrocytes derived from the same culture are shown in (d) and (e). Scale bar, 100µm in c, 400µm in e.

3.1.3. *In vivo* application of AAV vectors

As discussed above, AAV vectors packaged into the serotype-5 capsid are relatively inefficient in transducing neurons in primary hippocampal cultures but are excellent for astrocyte-specific transgene expression. Since the production of neurotrophins may be more effective if secreted from astrocytes in the brain (e.g. in model systems of neuronal de- and regeneration), the AAV-5-mCMV-EGFP vector was tested for its transduction properties in the adult rat brain. In contrast to the results obtained in cultured cells prepared from the embryonic rat brain, we detected striatal transgene expression mainly in cells which co-localized with neither the astrocyte specific GFAP marker, nor with the neuron specific NeuN marker (Fig 3.1.3 a, b).

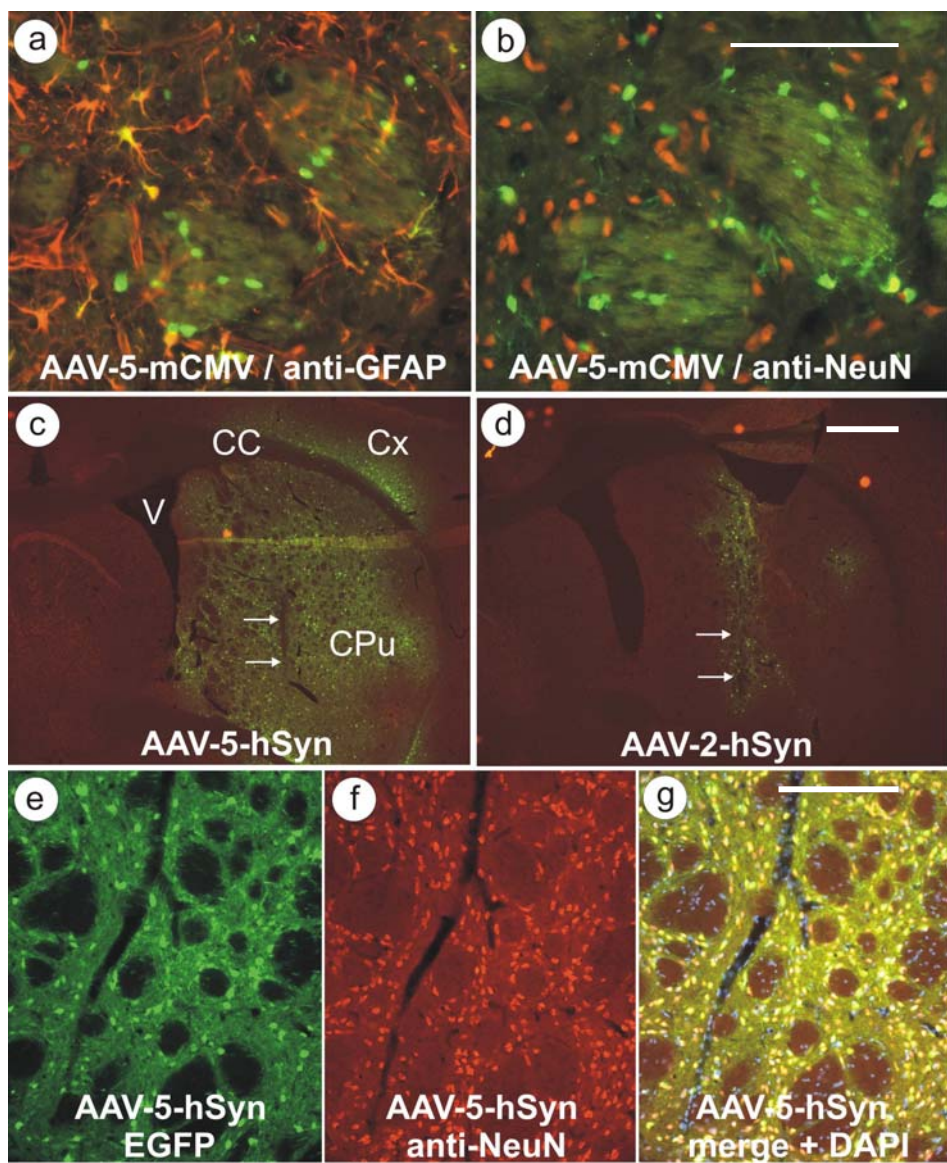


Fig.3.1.3. AAV-5 vector targeting in the brain. An attempt to target transgene expression from an AAV-5 vector to astrocytes in the rat brain is shown in (a) and (b). EGFP expression driven by the mCMV promoter is shown as an overlay with the astrocyte-specific anti-GFAP stain (red (a)) or the neuron-specific anti-NeuN stain (red (b)). Note that EGFP expression (green) was only rarely co-localized (yellow) with these markers. However, AAV-5 vectors expressing EGFP from the hSyn1 promoter very efficiently expressed EGFP in neurons of the striatum (c). This expression was neuron specific as demonstrated by the co-localization of EGFP expression with the neuronal marker NeuN (e - g). An AAV-2 vector used at the same titre showed transgene expression closely confined to the injection tract (arrows). V = ventricle, CC = corpus callosum, Cx = cortex, CPu = caudate putamen. Scale bar, 200 μ m in b, 500 μ m in d, 300 μ m in g.

Although the combination of mCMV promoter and serotype-5 capsid failed to do the intended task in the brain, AAV-5 vector in combination with hSyn1 promoter offered very promising features. While AAV vectors packaged into the most widely used serotype-2 capsid show transduction of brain tissue fairly restricted to areas near the injection site (Fig. 3.1.3 d), a much larger transduction area was obtained when the serotype-5 capsid was used (Fig. 3.1.3 c). In combination with the neuron specific hSyn1 promoter, transgene expression was found exclusively in neurons (Fig. 3.1.3 e-g), over large areas in the striatum. Quantification of transduced neurons versus total neuron number (as revealed by NeuN staining) showed that in a volume of ca. 15 mm³ about 40% of the striatal neurons expressed the transgene EGFP after a single injection of 2 µl containing 1 x 10⁸ transducing vector units (3 x 10⁹ genomes). While the AAV-5-mCMV-EGFP vector demonstrated that AAV-5 is not a neuron specific vector *per se*, targeting the vector to neurons by the hSyn promoter allowed for efficient and wide spread neuronal transduction.

Since co-expression of several interacting proteins may be desirable, AAV genome size may constitute restrictions even if small transcriptional control units are used. Therefore, we demonstrate that this problem may be readily overcome by the use of a double transduction approach: after stereotaxic injection of two different AAV-2 vectors, one expressing EGFP, the other DsRed (1 x 10⁸ transducing units / 3 x 10⁹ genomes each) the majority of neurons (>90%) was found to express both transgenes (more details are given in section 3.3, Fig. 3.3.2)

3.2. Evaluation of epitope tags suitability for CNS gene transfer studies

3.2.1. Expression constructs of epitope tags used for *in vivo* gene transfer

Although the vector genomes used in this study contained the fluorescent reporter gene to demarcate the transduced cells, unambiguous detection of transgenic protein expression may be required. This may become necessary when reporter gene has to be removed to increase the capacity for accomodation of relatively large transgene, or when the intracellular localization of the transgenic protein has to be determined.

Since in this study we aimed to overexpress proteins that are endogenously present in the brain, discrimination of the transgenic protein from the endogenously expressed is necessary and can be successfully accomplished by the epitope-tagging. Although extensively used *in vitro*, little information is currently available on the effective detection of the established epitopes by available antibodies. In order to investigate epitope tags and respective antibodies in tissue sections, the short peptide sequences were fused to the fluorescent protein

EGFP for demarcation of the transduced cells. Gene transfer of the respective constructs was achieved by viral vectors based on either Semliki-Forest virus (SFV) or adeno-associated virus (AAV). If EGFP fluorescence was detected in cells not recognized by the epitope-specific antibody, then *sensitivity* of tag detection was considered to be insufficient. If immunoreactivity was detected in cells not transduced by the vector (EGFP negative) then *specificity* of the tag detection was considered to be inappropriate.

3.2.2. Structural influence of the epitope tags

Denaturing SDS-PAGE revealed that epitopes might have considerable influence on the tagged protein (Fig. 3.2.1). First, fusion of the cMyc- and the FLAG-tags to EGFP resulted in more pronounced gel mobility retardation than could be expected from addition of the respective amino acids alone (EGFP = 26.9 kDa; expected for cMyc-EGFP-FLAG = 29.4 kDa, observed for cMyc-EGFP-FLAG = 34 kDa). Analysis of the amino acid sequences of the cMyc and the FLAG-tags by the neural network trained NetPhos 2.0 server (Blom, N. *et al.*, 2004) revealed that (cMyc : EQKL~~I~~SEEDL) or a tyrosine (FLAG : D~~Y~~KDDDDK) residue, which both have a high probability to be phosphorylated in the context of the EGFP fusion protein (scores = 0.997 for serine in cMyc and 0.937 for tyrosine in FLAG, with 1.0 being the highest probability score possible). Although tyrosine residues are present in the HA-, AU1-, IRS- and EE-tags as well, their scores were close to or significantly lower than a threshold value of 0.5 and thus, phosphorylation of these residues is unlikely to occur (first and second tyrosine in HA below 0.1, third tyrosine in HA = 0.515; tyrosine in AU1 = 0.671; tyrosine in IRS = below 0.1; tyrosine in EE = 0.564).

Second, fusion of the HA-tag to EGFP resulted in distinctly different migration patterns, depending on whether the tag was fused to either the amino- or the carboxy-terminus. Two distinct protein bands were detected with the amino-terminal HA-tag, by using two independent constructs (HA-EGFP and HA-EGFP-IRS). Conversely, only one protein band was detected after the expression of the carboxy-terminally fused HA-tag. Intriguingly, all HA-tagged EGFP constructs also showed "functional" impairment: regardless of the position of the HA-tag at either the amino- or the carboxy-terminus of EGFP, fluorescence of EGFP was reduced considerably as compared to EGFP alone or to EGFP fused to the other epitope tags. Using the same exposure time for recording EGFP fluorescence from all tagged constructs, we found that the HA-tagged EGFP yielded only 20 - 25 % of the brightness that was obtained from EGFP tagged with the other epitopes. Only when we used 5 times longer exposure time for recording EGFP fluorescence (i.e. 15,000 vs. 3,000 ms), the greyscale fluorescence level of HA - tagged EGFP reached that of the other constructs, suggesting a roughly 4 to 5 fold

reduction of EGFP fluorescence due to the fusion to the HA-tag (compare Fig. 3.2.2 c with a, b and d).

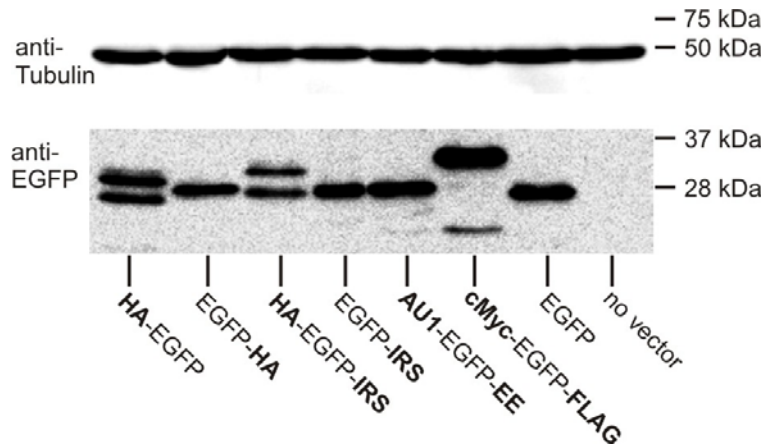


Fig.3.2.1. Analysis of the various tag-EGFP constructs by SDS-PAGE. Cell lysates of SFV-vector transduced primary neuron cultures were consecutively probed on the same membrane with an anti-tubulin antibody for loading and migration control and with an anti-EGFP antibody to demonstrate different gel retardation properties of the respective EGFP-tag fusion proteins. Size standards are shown on the right.

3.2.3. Evaluation of epitope tags in the central nervous system

For *in vivo* CNS applications, epitope tags were evaluated in striatum and retina. Injection of 2×10^5 infective particles of recombinant SFV vectors into striatum of adult rats resulted in transgene expression in different cell types. These were categorized by morphological criteria (Kügler, S. *et al.*, 2003a) to be predominantly neurons, some oligodendroglia (inside striosomes) and some astrocytes or resting microglial cells (heavily ramified cells). Brains were prepared at 16h after transduction in order to avoid inappropriately high levels of transgene expression due to the self-replication of SFV genomes, and to prevent any possible adverse tissue reactions due to vector administration. No such tissue reactions were observed, either by DAPI staining to detect cellular infiltrates or by staining for activated microglia (not shown).

In a series of pilot experiments, the dilution of antibodies that resulted in the best signal-to-noise ratio (typically in the range of 1:500 – 1:1,000) was determined first. All pictures were taken using the optimal dilution for the respective antibody.

3.2.4. Evaluation of "established" epitope tags (HA, cMyc, FLAG)

The FLAG-tag is readily detected in SFV-cMyc-EGFP-FLAG transduced cells (Fig. 3.2.2 c). However, in control brain transduced with SFV-EGFP or without any transduction, the anti-FLAG M2 antibody moderately but reproducibly stained the cytoplasm of cells with neuronal morphology (Fig. 3.2.2 a). Even more pronounced background staining was observed using anti-FLAG M2 antibody in the retinal ganglion cell layer (Fig. 3.2.2 b). Further dilution of the antibody reduced both background staining and specific signal detection, but did not enhance signal-to-noise ratio. Despite sensitive detection of the FLAG epitope in the brain, we noticed that a subpopulation (about 10-20%) of EGFP expressing cells was not stained by anti-FLAG antibody (Fig. 3.2.2 c).

Detection of the cMyc-tag was highly sensitive and specific in the brain, but not in the retina, where we noticed that about 20-30% of cells, which showed cMyc immunoreactivity were not EGFP-positive (Fig. 3.2.2 d). This finding suggests that endogenous cMyc protein (of which 10 amino acids represent the cMyc epitope peptide, corresponding to residues 423 - 432 of human cMyc or residues 424 - 433 of rat cMyc) was detected in these cells rather than the vector expressed cMyc epitope tagged transgene. Since cMyc is a protein crucial for cell cycle progression but also is upregulated in several paradigms of neuronal degeneration (Qin, Z. H. *et al.*, 1999; Di Giovanni, S. *et al.*, 2003), our finding emphasizes that physiological tissue reactions may readily result in the false-positive detection of the cMyc-tag.

The anti-HA antibody sensitively and specifically detected the HA-tag, however, EGFP fluorescence of the fusion proteins (HA-EGFP, HA-EGFP-IRS, EGFP-HA) was considerably reduced in brain sections and in cultured brain cells as compared to other tagged EGFP constructs (compare Fig. 3.2.2 e with a-d and f). Regardless, the remaining EGFP fluorescence was still sufficient to detect the fusion protein by using longer exposure times (approximately 5 times longer than for the other constructs).

Taken together, all "established" epitope tag / antibody combinations allowed for sensitive detection of the expressed transgene, although we also document either structural influence of the epitope tag on the fusion partner (HA - tag) or problems with background staining, depending on either tissue composition (FLAG - tag) or potential physiological tissue reactions as in case of cMyc - tag.

3.2.5. Evaluation of "new" epitope tags (AU1, EE, IRS)

The very short IRS-tag was detected specifically by its respective antibody. However, this detection was limited to cells expressing high levels of EGFP. Cells expressing lower levels of EGFP were not detected by the antibody in brain sections (Fig. 3.2.3 a), or in cultured

brain cells (Fig. 3.2.3 c). Increasing antibody concentration or changing the permeabilization protocol did not improve IRS detection (not shown).

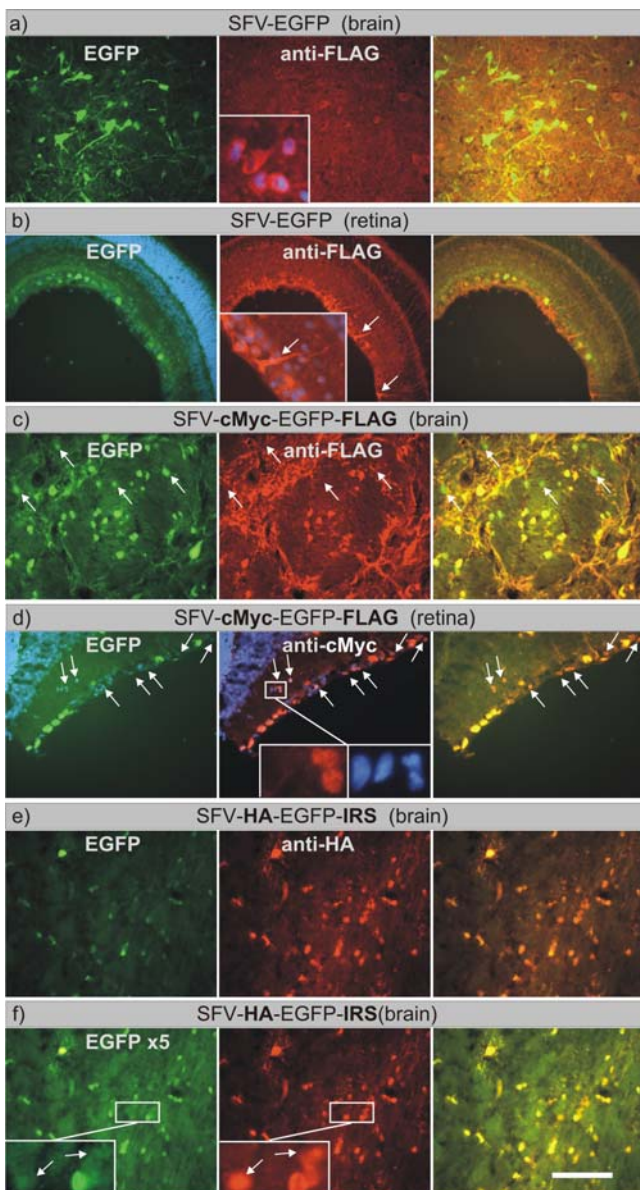


Fig.3.2.2. Evaluation of FLAG-, cMyc-, and HA-tags in striatum and retina. Recombinant SFV-vectors (2×10^5 infective units each) were either stereotactically injected into the striatum (a, c, e, f), or into the eye (b, d). Vectors expressed either EGFP alone (a, b), or EGFP coupled to the cMyc- and the FLAG-tags (c, d), or EGFP coupled to the HA- and the IRS-tags (e, f). Each sub-panel of the figure shows EGFP fluorescence in the left (green), antibody staining (visualized by a cy3-coupled secondary antibody) in the middle part (red) and an overlay in the right part. Retinal sections are shown as overlays with nuclear DAPI stain to demonstrate tissue composition. Inlays in (a), (b), (d) and (f) show higher magnifications of the respective pictures. Arrows in (b) denote a Müller glia cell clearly recognizable by its longitudinal morphology with extended endfeet in the ganglion cell layer. Arrows in (c) denote EGFP expressing cells which are not recognized by the anti-FLAG antibody. Arrows in (d) denote retinal cells, which are not transduced by the SFV-vectors (EGFP-negative) but positively stained for the cMyc antigen. Arrows in (f) denote cells showing levels of EGFP expression barely above background but nonetheless properly detected by the anti-HA antibody. Note that (e) and (f) show the same specimen, for which in (f) five times longer exposure time (15,000 ms) was used to record EGFP fluorescence than for all other specimen shown in this figure (3,000 ms). Scale bar, 100 μ m.

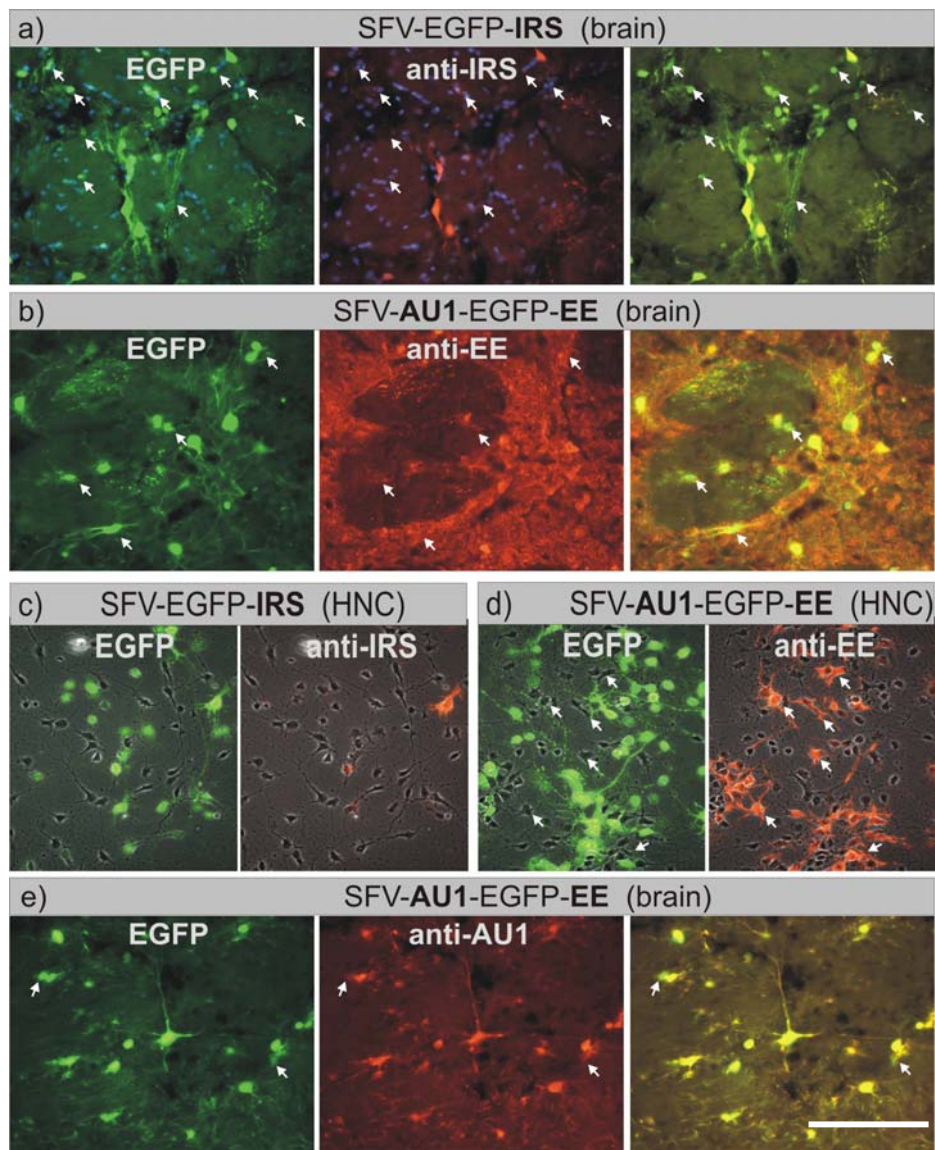


Fig.3.2.3. Evaluation of IRS-, EE- and AU1- epitope tags in striatum and primary neuron cultures. Recombinant SFV-vectors (2×10^5 infective units each) were either stereotactically injected into the striatum ("brain", a, b, e), or used for transduction of primary hippocampal neuron cultures ("HNC", c, d). Vectors expressed either EGFP coupled to the IRS-tag (a, c), or EGFP coupled to the AU1- and EE-tags (b, d, e). Each sub-panel of the figure shows EGFP fluorescence in the left (green), antibody staining (visualized by a cy3-coupled secondary antibody) in the middle part (red) and the overlay in the right part, except for (c) and (d), which show EGFP fluorescence in the left and cy3 fluorescence in the right part of the panel. Sections in (a) are shown as overlays with nuclear DAPI stain to demonstrate that no accumulation of blood-borne immune cells were observed in these specimen. Arrows in (a) denote cells expressing EGFP but not stained by the anti-IRS antibody. Arrows in (b) denote EGFP expressing cells which are not recognized by the anti-EE antibody. Arrows in (d) denote cultured brain cells not transduced by the SFV-vectors (no EGFP fluorescence) but positively stained for the EE-antigen. Arrows in (e) denote a few cells expressing EGFP but not stained by the anti-AU1 antibody. Scale bar, 150 μ m.

Since this epitope tag is the shortest (only 5 amino acids in length) of all epitope peptides evaluated in this study, it may not be possible to develop more sensitive antibodies in order to increase the otherwise highly specific detection due to its low immunogenicity.

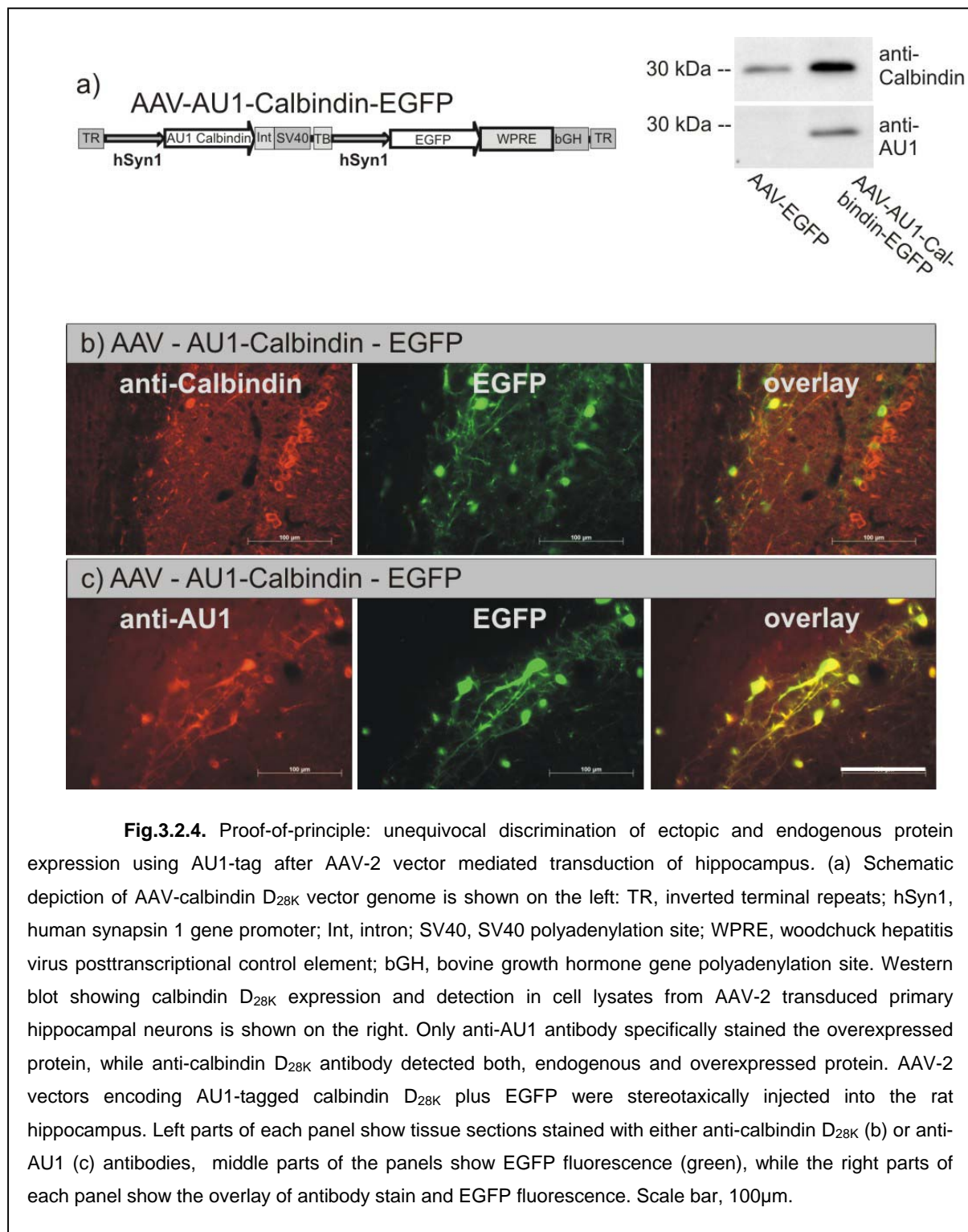
In contrast, we were unable to determine appropriate conditions for using the anti-EE antibody to detect specific immunoreactivity of its respective tag. Brain sections exhibited dramatic background staining of fibrous structures and even of those cells which strongly express EGFP, only a subset was detected by the anti - EE antibody (Fig. 3.2.3 b). Some cells in primary hippocampal cultures were stained by the antibody, however most cells which were transduced by the respective SFV-vector, were not detected (Fig. 3.2.3 d).

Apparently, the best results were achieved by using the anti-AU1 antibody to detect the AU1-EGFP-EE fusion protein. In the brain sections the AU1-tagged EGFP was sensitively and specifically detected (Fig. 3.2.3 e). EGFP and cy3 co-localization was observed in > 95 % of cells as judged from counting respectively labelled cells in sections of SFV-AU1-EGFP-EE-transduced brain. Taken together, detection of the IRS - and EE - tags was hindered by either low sensitivity or a complete lack of specificity. Only the AU1 - tag was detected both sensitively and specifically.

3.2.6. Proof-of-principle: discrimination of ectopically from endogenously expressed protein

Gene transfer of proteins with potentially neuroprotective function is a rapidly developing field aiming at therapeutic intervention in animal models of neurodegenerative diseases. In order to prove efficacy of such attempts it is crucial to target expression of the respective protein to the affected neuronal populations, but also to be able to trace transgene expression appropriately. As SFV vectors are not suited for long-term gene transfer, we used a bicistronic adeno-associated virus vector (AAV-2) to express AU1-tagged calbindin D_{28K} together with EGFP (Fig. 3.2.4 a) in the brain hippocampus, where high endogenous level of calbindin D_{28K} expression was reported (Lomri, N. *et al.*, 1989). After control vector (AAV-EGFP) injection or in untransduced hippocampi, pronounced endogenous calbindin D_{28K} expression was detected (Fig. 3.2.4 b). Thus, a specific cellular localization of the overexpressed protein would be almost impossible by using a calbindin-specific antibody. After stereotaxic injection of an AAV-2 vector expressing both, EGFP and AU1-tagged calbindin D_{28K}, and after staining with the anti-AU1 antibody, only those cells transduced by the vector (as demarcated by EGFP fluorescence) were found to be immunoreactive for AU1-tagged calbindin D_{28K} (Fig. 3.2.4 c). Appropriate discrimination of endogenous from overexpressed calbindin D_{28K} was also achieved by western blotting of the transduced with

either AAV-EGFP or AAV-AU1-calbindin-EGFP hippocampal cell lysates by using anti-AU1 but not by anti-calbindin antibody (Fig. 3.2.4 a). Thus, proper discrimination of neuronal populations endogenously expressing calbindin D_{28K} from those overexpressing the transgene after viral vector-mediated gene transfer was accomplished unambiguously.



3.3. Long-term neuroprotection mediated by AAV gene transfer in the complete 6-OHDA rat model of PD

3.3.1. Targeted transduction of SNpc by stereotaxic injection of AAV-2 vectors

After establishing effective means for gene transfer in CNS, we overexpressed BclX_L or GDNF, or BclX_L plus GDNF in the substantia nigra pars compacta (SNpc) aiming to achieve efficient neuroprotection of DA neurons in rat model of PD. To this purpose, AAV-2 viral vectors expressing BclX_L or GDNF plus a fluorescent reporter protein (EGFP or DsRed2; Fig. 3.3.1) have been constructed. Fluorescent reporters simplified tracing of transduced neuronal populations. We also constructed a control vector containing a fluorescent reporter EGFP but no functional transgene (Fig. 4.3.1). After stereotaxic co-injection of 1.4×10^8 transducing units (t.u.) of AAV-GDNF-EGFP and AAV-BclX_L-DsRed vectors into the substantia nigra, we detected highly efficient co-expression from both vectors (Fig. 3.3.2 a-c). Efficient transduction of dopaminergic neurons was documented by staining transduced sections for tyrosine-hydroxylase immunoreactivity, demonstrating almost quantitative transduction of dopaminergic neurons (Fig. 3.3.2 d-f).

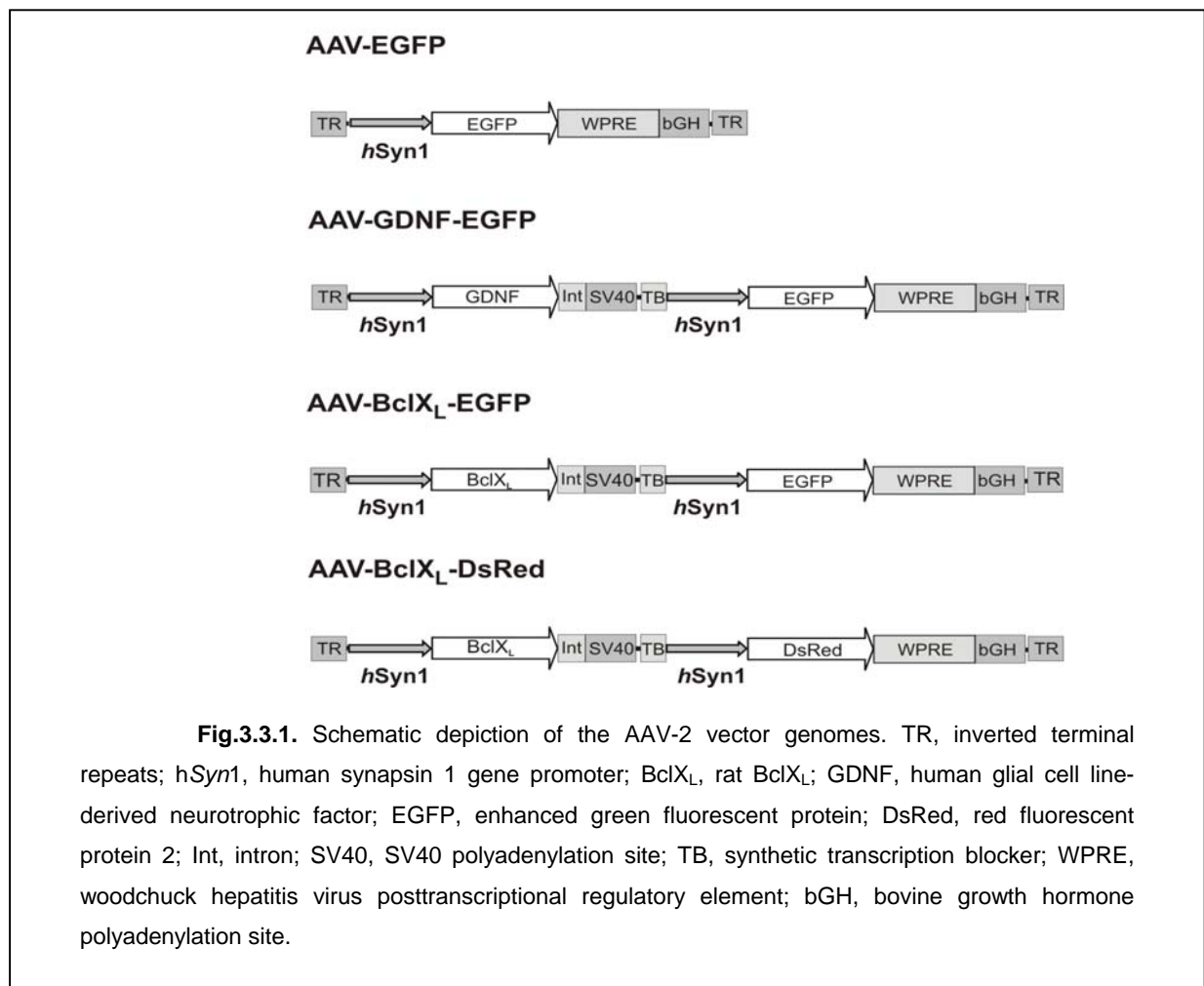


Fig.3.3.1. Schematic depiction of the AAV-2 vector genomes. TR, inverted terminal repeats; hSyn1, human synapsin 1 gene promoter; BclX_L, rat BclX_L; GDNF, human glial cell line-derived neurotrophic factor; EGFP, enhanced green fluorescent protein; DsRed, red fluorescent protein 2; Int, intron; SV40, SV40 polyadenylation site; TB, synthetic transcription blocker; WPRE, woodchuck hepatitis virus posttranscriptional regulatory element; bGH, bovine growth hormone polyadenylation site.

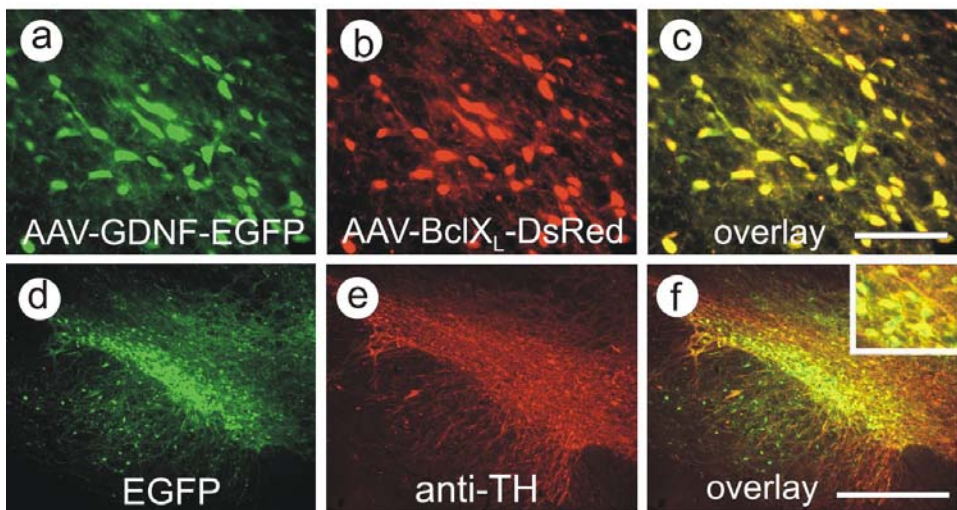


Fig.3.3.2. Transduction of a rat brain by AAV-2 vectors. Co-transduction of SNpc neurons by AAV-GDNF-EGFP (a) and AAV-BclXL-DsRed (b) is shown as an overlay image in (c). Representative transduction of SNpc dopaminergic neurons after injection of 1.4×10^8 t.u. of AAV vector as demarcated by EGFP-fluorescence (d), where dopaminergic neurons are visualised by TH immunoreactivity (e), is shown as an overlay in (f). Scale bar, 100 μ m in (c) and 400 μ m in (f).

3.3.2. Establishment of the complete 6-OHDA rat model of PD

Since unilateral 6-OHDA lesion of the nigrostriatal projection was chosen as a model system for the evaluation of neuroprotective effects of BclXL and GDNF, the criteria for successful surgery and appropriateness of the produced lesion had to be developed first. Wistar rats of 250-280g were found to be the best suited for effective and reproducible stereotaxic targeting of the medial forebrain bundle. The minimal effective dose of 6-OHDA was used to achieve the complete lesion of the nigrostriatal system. In order to evaluate the degree of the lesion rotational behaviour test and tyrosine hydroxylase (TH) immunofluorescent staining of the brain slices have been performed at different time points after the lesion. The 6-OHDA injected rats were subjected to the apomorphine test at 1, 2, 3 and 4 weeks after brain surgery, followed by perfusion and evaluation of remaining TH-immunoreactivity (TH-IR) in the striatum and SNpc brain regions. More reproducible data in terms of correlation between the number of rotations and the loss of TH-IR have been obtained at 3 and 4 weeks after the lesion. Although some rats did not show pronounced rotational behaviour at 2 weeks after the injury (e.g. ≤ 3 rotations/min), they often developed a strong response to apomorphine by 3 weeks time point which then remained stable. However, those rats which at 2 weeks after the lesion showed 5 or more rotations per min typically presented with more than 85 % reduction of TH-IR cells in the SNpc as well as almost complete loss of TH positive terminals in the striatum.

All the rats in the study were subjected to the rotational test at 2 weeks after the 6-OHDA lesion to confirm that the lesion was complete and to exclude from the study those rats which exhibited less than 5 rotations per min.

3.3.3. BclXL mediated protection of DA cell bodies in 6-OHDA rat model of PD

In animals injected with a control virus expressing only EGFP, 25% of nigral dopaminergic neurons survived for 2 weeks after the 6-OHDA lesion, while only 7% survived for 6 weeks following the lesion (Fig. 3.3.4 c, d; Fig. 3.3.5 a and Table 3.3.1). Care was taken to exclude TH-positive neurons of the ventral tegmental area (VTA) from counting, as these neurons were not directly affected by the lesion. BclXL overexpression significantly improved survival of DA neurons, which constituted 61% at 2 weeks after lesion and 31% at 6 weeks after lesion (Fig. 3.3.4 f, g; Fig. 3.3.5 a, Table 3.3.1). Importantly, the protection from neurodegeneration was restricted predominantly to the DA cell bodies, since the dense neuritic network of these neurons present under normal conditions was lost to a large extent (compare Fig. 3.3.4 f and g with h). It should be noted that the decline in numbers of TH-positive neurons was accompanied by a respective decline in numbers of neurons showing EGFP fluorescence in both, EGFP and BclXL / EGFP transduced SNpc. These data indicate that not only a downregulation of TH expression, but a real loss of DA neurons was observed after 6-OHDA lesion in our paradigm. The rate of decline in TH-positive neuron numbers in either BclXL / EGFP or in EGFP transduced SNpc was similar, indicating that BclXL overexpression failed to protect against the slowly progressive cell death at later time points after 6-OHDA intoxication.

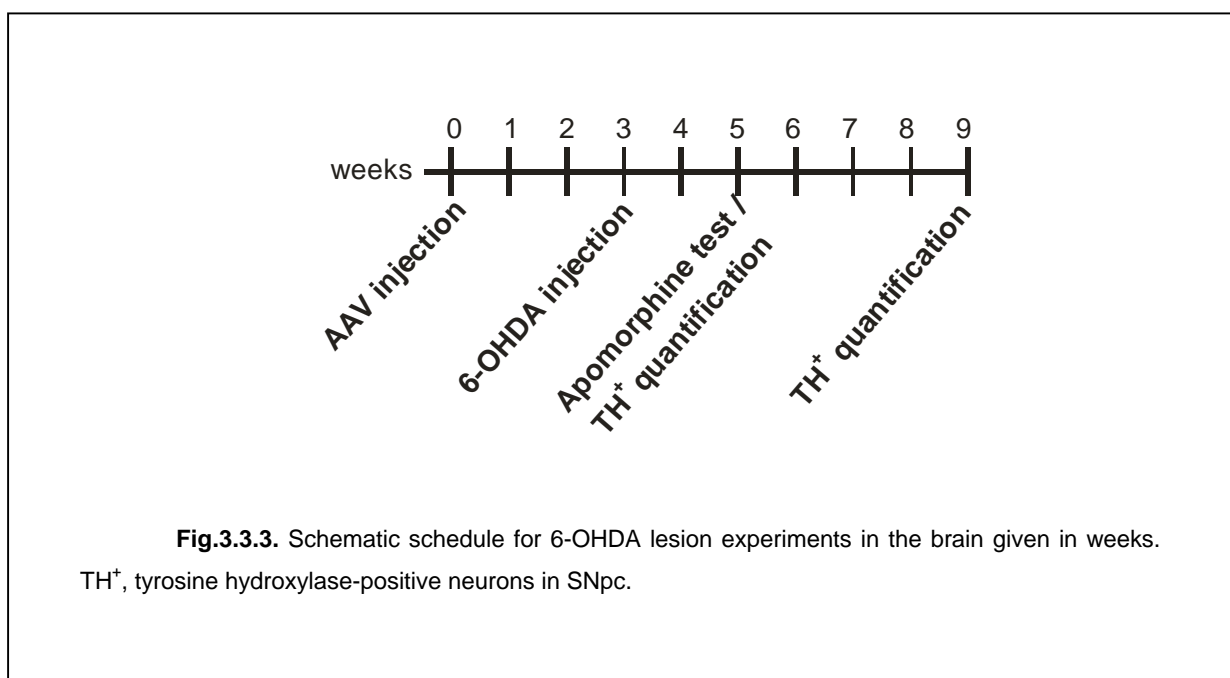


Fig.3.3.3. Schematic schedule for 6-OHDA lesion experiments in the brain given in weeks.
TH⁺, tyrosine hydroxylase-positive neurons in SNpc.

3.3.4. GDNF protects DA cell bodies and dendritic protrusions from 6-OHDA toxicity

At 2 weeks after 6-OHDA lesion, DA neurons in GDNF transduced SNpc were substantially protected from degeneration in that 77% survived at this time (Fig. 3.3.4 i, Table 3.3.1). In contrast to BclX_L-mediated neuroprotection, surviving DA neurons showed a dense network of dendritic arborisations throughout the SNpc, indicating that GDNF not only protects DA cell bodies but also their neurites from 6-OHDA toxicity. At 6 weeks after 6-OHDA lesion, no significant decline in TH-positive cell numbers has taken place (76% surviving DA neurons, Fig. 3.3.4 j, Table 3.3.1), indicating that GDNF can inhibit and not only postpone 6-OHDA-induced neurodegeneration. No obvious difference in the density of neuritic arborisations of TH-positive neurons in either unlesioned controls or GDNF transduced SNpc at 2 or 6 weeks after 6-OHDA lesion were detectable (Fig. 3.3.4 j-k).

As it was demonstrated earlier, high levels of GDNF expression may result in disturbances of dopaminergic metabolism and some aberrant sprouting of dopaminergic fibres (Georgievska, B. *et al.*, 2002b). Therefore, the GDNF expression cassette used in our vector construct did not contain transcriptional control elements which strongly enhance transgene expression, such as the WPRE. GDNF expression levels in AAV-EGFP and in AAV-GDNF transduced SNpc quantified by ELISA were 11pg/mg and 190pg/mg, respectively.

3.3.5. BclX_L and GDNF co-expression has additive neuroprotective effects at 2 weeks after 6-OHDA lesion

Co-expression of BclX_L and GDNF resulted in almost complete protection of SNpc DA neurons from 6-OHDA toxicity at 2 weeks after lesion: 96 % of DA neurons survive at this time (Fig. 3.3.4 l; Table 3.3.1). When compared to 77 % surviving neurons through GDNF alone and 61 % surviving neurons through BclX_L alone, these data represent a statistically significant additive neuroprotective effect ($p < 0.001$; Fig. 3.3.4; Table 3.3.1). Moreover, no obvious morphological differences were detected between unlesioned control DA neurons and DA neurons under combination therapy (Fig. 3.3.4 l, n).

	AAV-EGFP	AAV-BclX _L	AAV-GDNF	AAV-BclX _L +AAV-GDNF	unlesioned
2 weeks	2792 ± 301	6947 ± 783	8690 ± 998	10876 ± 392	11356 ± 569
6 weeks	841 ± 249	3496 ± 780	8598 ± 528	8840 ± 262	

* $n = 5$ for each group

Table 3.3.1. Quantification of surviving TH⁺-neurons in SNpc at 2 and 6 weeks after 6-OHDA lesion of MFB. The numbers of surviving TH⁺-neurons in AAV-BclX_L, -GDNF, -BclX_L +GDNF transduced SNpc regions are presented along with the numbers of surviving TH⁺-neurons in a control-vector (AAV-EGFP) transduced SNpc and the numbers of TH⁺-neurons in unlesioned contralateral SNpc.

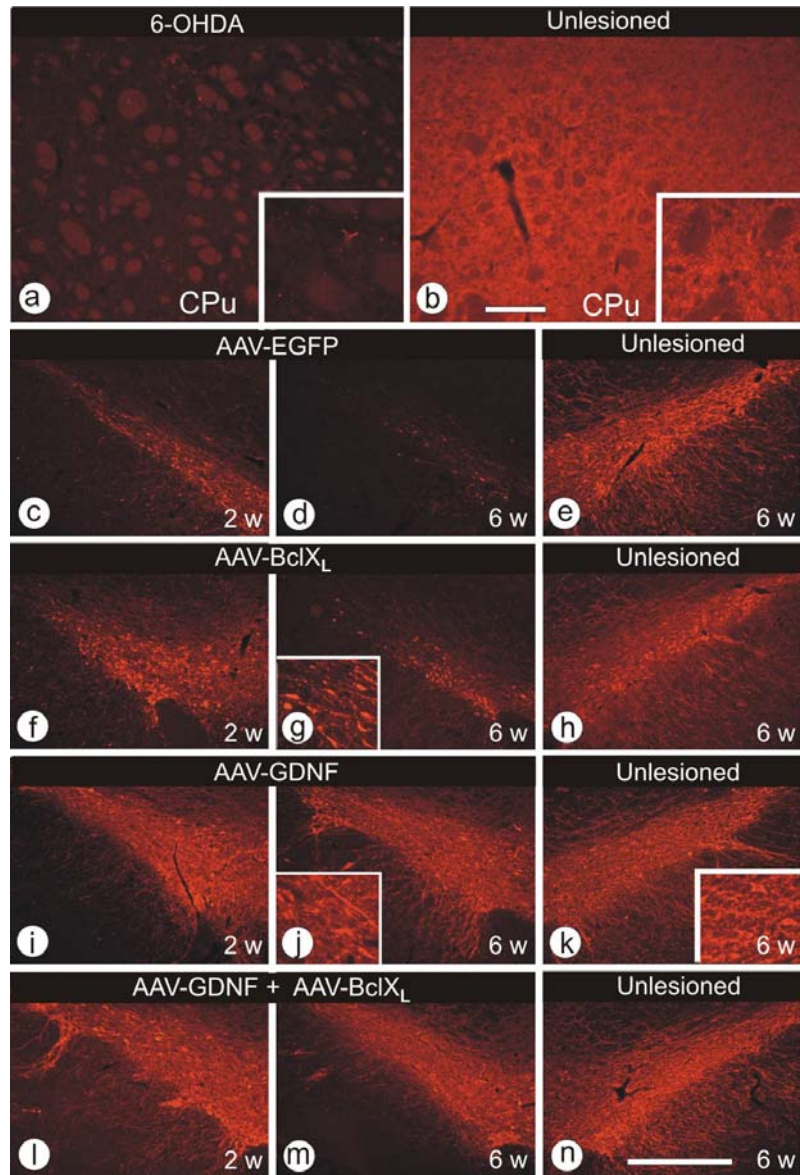


Fig.3.3.4. TH-immunoreactivity in rat brain after unilateral 6-OHDA lesion. Representative CPU regions show the TH-immunoreactive projections of the DA-neurons (a) at 3 weeks after 6-OHDA injection into MFB and, (b) on contralateral (unlesioned) side. The insets in (a) and (b) depict the magnified views on the TH⁺- fibre density in the corresponding areas. Immunohistochemical visualisation of surviving DA-neurons by TH-immunostaining in AAV-transduced SNpc (c, d, f, g, i, j, l, m) at 2 and 6 weeks after the MFB lesion compared to the unlesioned side of the same animal (e, h, k, n) at 6 weeks after the lesion. The AAV-EGFP transduced SNpc is shown at 2 and 6 weeks after 6-OHDA lesion in (c) and (d). TH⁺ neurons transduced by AAV-BclXL are shown in (f), at 2 weeks after lesion, and in (g), at 6 weeks after lesion. The inset in (g) shows the predominant morphology of surviving DA-neurons transduced by AAV-BclXL at 6 weeks after the lesion. Note that most cell bodies of the remaining TH⁺-neurons are devoid of processes. The AAV-GDNF transduced nigrae are shown at 2 and 6 weeks after the 6-OHDA lesion in (i) and (j); the S. nigrae co-transduced with AAV-GDNF and AAV-BclXL at 2 and 6 weeks after the MFB lesion are shown in (l) and (m). The inset in (j) shows the morphology of the majority of surviving DA-neurons in AAV-GDNF transduced SNpc at 6 weeks after the 6-OHDA lesion, while the inset in (k) depicts the native morphology of neurons in untreated SNpc. Note that the fibre density of the DA-neurons protected by GDNF at 6 weeks after the 6-OHDA lesion (inset in (j)) is indistinguishable from that of unlesioned side (inset in (k)). Scale bar, 200μm in (b) and 400μm in (n).

3.3.6. Co-expression of BclX_L with GDNF has no beneficial effect on dopaminergic neuron survival at 6 weeks after 6-OHDA lesion

Although BclX_L expression alone resulted in significant neuroprotection from 6-OHDA toxicity at 6 weeks after lesion, its co-expression with GDNF at this time did not result in any additive neuroprotective effect. It rather appeared that the neuroprotection at this time is exclusively mediated by GDNF, since the numbers of TH-positive (TH⁺) neurons in the GDNF group were almost identical to the numbers in the GDNF plus BclX_L group (Fig. 3.3.5 a; Table 3.3.1). In order to rule out that 6-OHDA lesion might have any effect on BclX_L expression from the viral vector genome, AAV-BclX_L transduced nigrae were stained for BclX_L. In DA-neurons surviving for up to 6 weeks after 6-OHDA intoxication we detected the same level of immunoreactivity for BclX_L as in unlesioned controls (Fig. 3.3.5 b-d). In contrast, we could not detect any obvious upregulation of BclX_L (Fig. 3.3.5 e-g) or bcl-2 expression (not shown) in AAV-GDNF transduced DA-neurons. These latter results demonstrate that the long-lasting neuroprotective effect of GDNF on survival of DA-neurons was independent from BclX_L.

3.3.7. Effects of delayed AAV-GDNF administration in the rat striatum after the complete 6-OHDA lesion of the MFB

In agreement with several other studies (Björklund, A. *et al.*, 1997; Eslamboli, A. *et al.*, 2003; Georgievska, B. *et al.*, 2002b) we have shown here that the overexpression of GDNF alone allows for sustained protection of dopaminergic cell bodies of SNpc as well as their neuritic arbour from 6-OHDA toxicity. However, the primary pathologic background that results in movement disorders typically observed in PD patients is believed to be a disbalance in dopamine release in the striatum.

Therefore, we overexpressed GDNF in the lesioned striatum *late after* the complete lesion of nigrostriatal projections was achieved. To this purpose, we first induced the lesion by 6-OHDA injection in the MFB and introduced GDNF three weeks after the lesion by stereotaxic injection of the AAV-5-hSyn-GDNF into the ipsilateral to the lesion striatum (for schematic timetable see Fig. 3.3.6 a). AAV-5 serotype was used in this experiment for GDNF delivery since it allows for transduction of a large area in the brain (Fig. 3.1.3 c). Neither at 6 weeks nor at 4 months after the AAV injection we observed behavioural or immunohistochemical recovery in lesioned animals. The striatum on the side of the lesion was almost completely devoid of TH-immunoreactive terminals in both GDNF- and EGFP-expressing animals (Fig. 3.3.6 b, c).

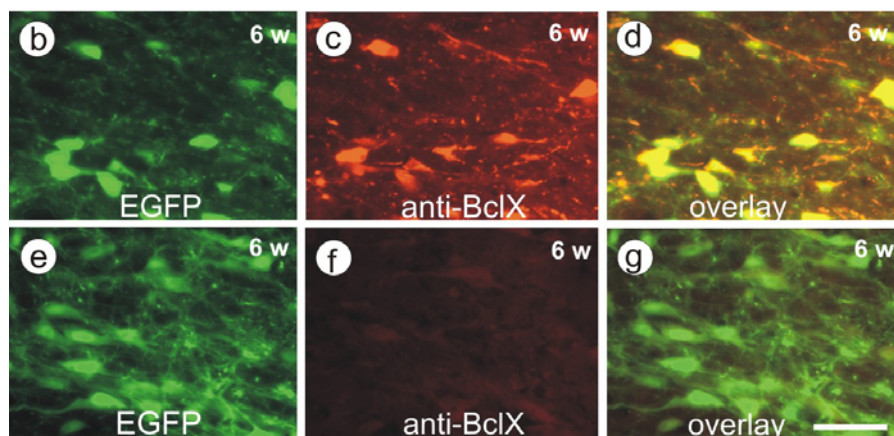
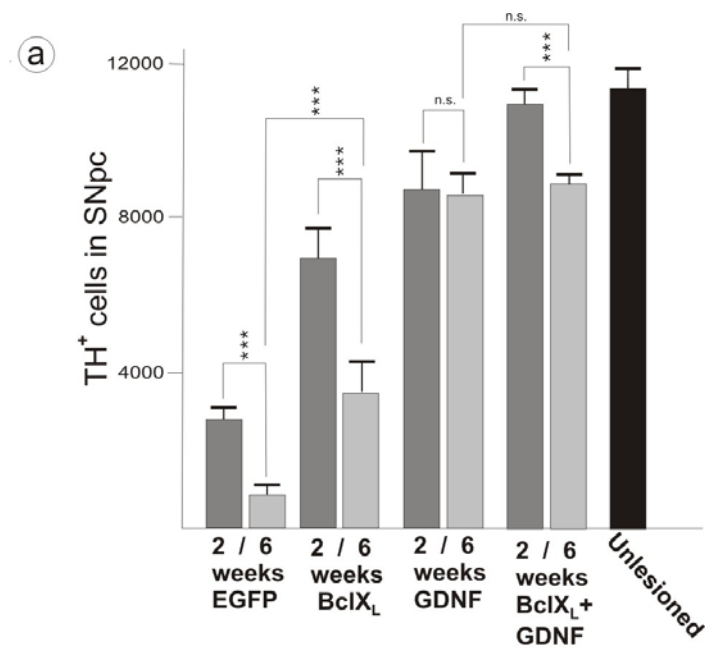
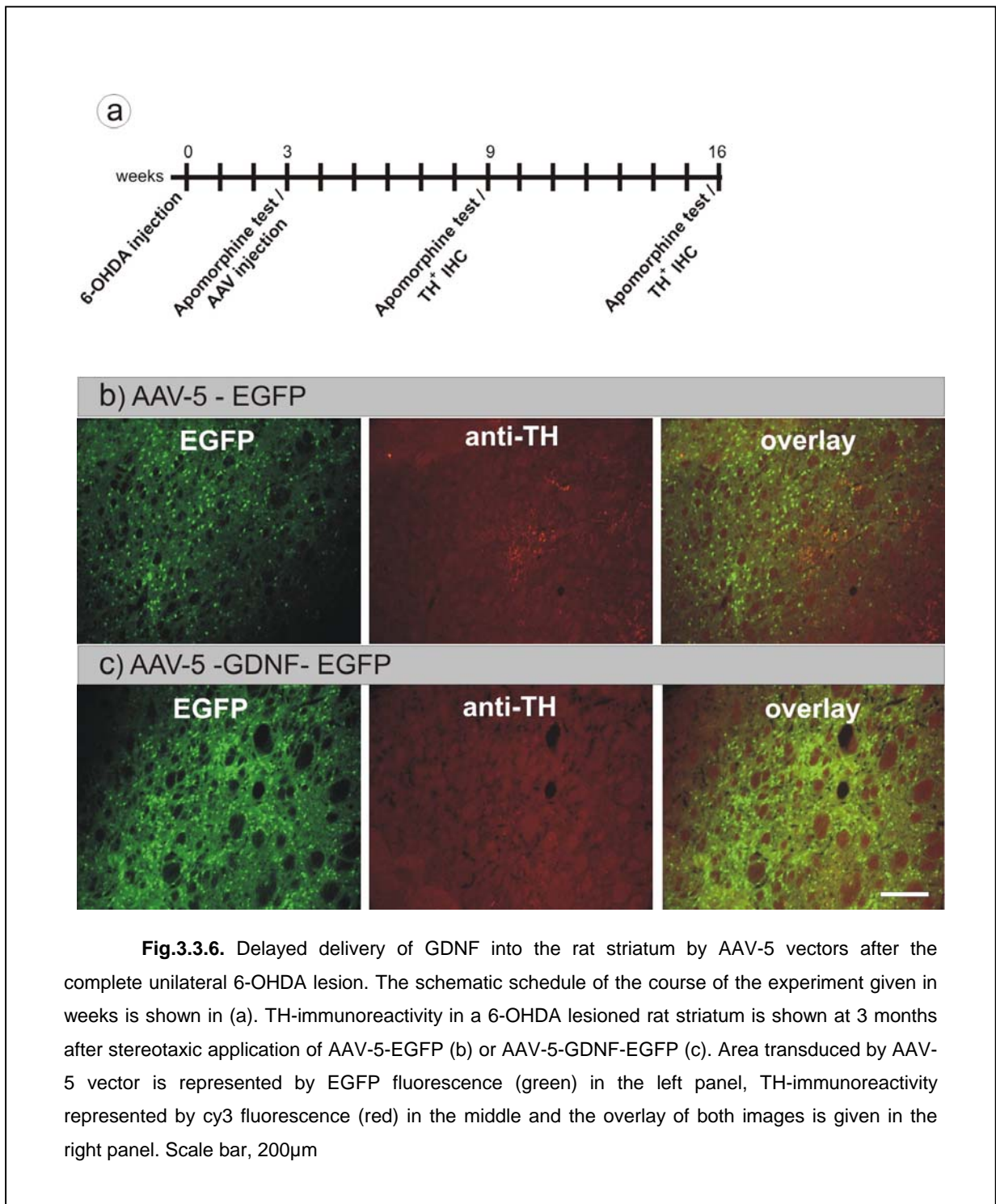


Fig.3.3.5. Quantification of DA-neuron survival in SNpc after 6-OHDA lesion. In (a) the number of surviving TH⁺-neurons was determined after the control vector injection (AAV-EGFP) and after the injection of AAV-BclX_L, or AAV-GDNF, or AAV-BclX_L plus AAV-GDNF (gray bars). Dark-gray bars represent the mean values of surviving TH⁺-neurons in SNpc at 2 weeks after 6-OHDA lesion, light-gray bars represent mean values of surviving TH⁺-neurons at 6 weeks after 6-OHDA lesion. The mean number of TH⁺-neurons in unlesioned SNpc is shown by black bar. Bars represent mean values \pm standard deviations (**p < 0.001, n.s., non-significant). Immunohistochemical staining for BclX_L in SNpc neurons transduced by AAV-BclX_L confirmed that BclX_L expression is not downregulated in the course of the experiment (b - d). Immunohistochemical staining for BclX_L was also used to demonstrate that GDNF expression did not result in BclX_L upregulation in SNpc neurons after AAV-GDNF transduction (e - g). Scale bar, 40 μ m.

These data suggest that GDNF alone is not sufficient to induce resprouting of a few remaining after the lesion of the nigrostriatal projections. Neurorestorative effect of GDNF rather depends on the presence of sufficient dopaminergic “template” terminals in the lesioned striatum.



4. Discussion

In the work presented here the following aims have been pursued: 1) to evaluate the neuroprotective and neurorestorative properties of BclX_L and GDNF in the rat model of Parkinson's disease; 2) to develop appropriate adeno-associated viral vectors for efficient gene transfer to the target regions in the brain; 3) to improve detection the transgene for ongoing and future gene transfer studies by epitope-tagging approach.

4.1. AAV vector targeting

In this study we aimed to overexpress BclX_L and GDNF in the substantia nigra and GDNF in the striatum. The purpose of nigral gene transfer was to achieve efficient and long-lasting neuroprotection of DA cells. AAV-2 serotype was employed as a gene transfer tool, since it preferentially transduces neurons in the CNS and has especially high affinity to DA neurons of SNpc (Paterna, J. C. *et al.*, 2004). This property of AAV-2 vectors can be explained by high density of HSPG receptors, necessary for virus entry, on nigral neurons (Fuxe, K. *et al.*, 1994). To further restrict the expression of the transgene to neurons, hSyn1 promoter was used. However, protecting the DA cell bodies in SNpc may not be sufficient for maintenance of the basal ganglia circuit in the brain. To achieve reconstruction of functional connections of DA cell bodies to the striatum, striatal overexpression of GDNF may be required (Kirik, D. *et al.*, 2004). GDNF was found to be expressed primarily from astrocytes in the brain. Therefore, we attempted to redirect the AAV-mediated transgene expression from neurons to astrocytes. Previous studies aiming to restrict the transduction by AAV vectors to either astrocytes or oligodendroglia using the glial cell type specific promoters GFAP and myelin basic protein promoter failed (Peel, A. L. *et al.*, 1997; Peel, A. L. *et al.*, 2000). In this study we used ubiquitously active mCMV promoter which has been shown to target the transgene expression to astrocytes after adenoviral transduction of the CNS (Kügler, S. *et al.*, 2001). Moreover we made use of the AAV-5 capsid for packaging since this AAV serotype was shown to equally transduce neurons and astrocytes (Tenenbaum, L. *et al.*, 2004). With this approach, efficient astroglia-specific transgene expression was achieved in primary hippocampal culture. Incorporation of EGFP into AAV vector genome greatly simplified visualization of the transduced cells. However, when the same promoter/capsid (mCMV/AAV-5) combination was utilized for AAV-mediated gene transfer into the brain, a different cellular transduction pattern was observed as compared to *in vitro* results. Instead of predominant localization of EGFP to astrocytes as it would be expected after the *in vitro* experiments, some neurons and cells of

unidentified origin, which were negative to both astroglial and microglial immunological markers have been transduced. These apparently divergent data obtained from *in vitro* and *in vivo* studies on AAV vector targeting may be explained by variable expression of receptors required for successful entry of the recombinant virus into the cell in embryonic and adult brain. In neonatal mice intraventricular brain injection of AAV-2 or AAV-1 has been shown to result in widespread neuronal transduction, whereas AAV-5 injection led to a very limited transgene expression (Passini, M. A. *et al.*, 2003). In the brain of adult animals, however, AAV-2 transduction is localized while AAV-5 transgene expression is typically widespread (Davidson, B. L. *et al.*, 2000;Shevtsova, Z. *et al.*, 2005). Moreover, the extracellular environment and tissue composition which may contribute to the successful entry of the virus into the cell are very different in primary cultures and in the living organism. For example, in addition to glycosamynoglycans AAV-2 serotype requires fibroblast growth factor receptor and integrins as co-receptors for effective transduction (Qing, K. *et al.*, 1999;Summerford, C. *et al.*, 1999), which appear to be differentially expressed in neonate and adult brain. On the contrary, AAV-5 mediated transduction does not require heparan sulfate proteoglycan (HSPG), but α -2,3- or α -2,6-N-linked sialic acid (Kaludov, N. *et al.*, 2001;Walters, R. W. *et al.*, 2001) and platelet-derived growth factor receptor (PDGFR) (Di Pasquale, G. *et al.*, 2003). In addition, mCMV promoter activity in mature and in non-differentiated CNS cells may also influence the observed difference in expression patterns.

Consistent with the results obtained by others (Burger, C. *et al.*, 2004), the area of virus transduction in the brain was restricted to the injection site after stereotaxic application of AAV-2 vector and was spread beyond the striatum borders (ca. 10x larger) after injecting the same titre of AAV-5 vector. These serotype properties of AAV can define the choice of the vector for gene transfer: when the transduction of a relatively small-size region is intended, the use of AAV-2 serotype is appropriate. For effective transduction of a large structure in the brain (e.g. striatum), AAV-5 would be the vector of choice. Thus, AAV-2 serotype was selected for gene transfer into the small nucleus SNpc whereas AAV-5 was used to deliver GDNF into the striatum.

4.2. Epitope-tagging for *in vivo* transgene detection

Difficulties in detection of transgenic protein expression by respective antibodies and in its discrimination from the endogenously expressed analogue in a living organism (Weise, J. *et al.*, 2000;Wagenknecht, B. *et al.*, 1999) necessitate the search for alternative confirmation of transgene expression. Advanced viral gene transfer systems have made it possible to express almost every protein of interest not only in rodent but also in the more complex primate brain

(Gerdes, C. A. *et al.*, 2000; Kirik, D. *et al.*, 2003). Gene transfer studies directed towards therapeutic interventions in disease models or towards basic research on protein functions require the unambiguous verification of the transgene expression. An antibody, specific for the respective protein may be used, but this antibody might not be able to discriminate intrinsically expressed proteins from the ectopically or overexpressed one. Additionally, for dominant-negative or constitutively activated variants of a protein, or for splice variants as well as for many proteins investigated for the first time specific antibodies may not be available. Thus, epitope tags, short peptides which can be fused to the protein under investigation and specifically detected by well-characterized antibodies, appear to be an attractive alternative. Although proven to be useful for protein tracing in cell-free systems or in cultured cells *in vitro* (Terpe, K., 2003), thus far there has been no systematic attempt to characterize different epitope tags for *in vivo* gene transfer applications.

The study presented here is the first systematic evaluation of different epitope tags in the CNS. The data demonstrate that all "established" tags (HA-, cMyc-, FLAG-tag) were detected by their respective antibodies with high sensitivity, but in all cases significant drawbacks have also been observed. The anti-FLAG and the anti-cMyc antibodies showed significant background staining of distinct CNS structures, and at least one of these tags was responsible for pronounced gel mobility retardation of the tagged EGFP, probably due to the introduction of an odd phosphorylation site. Fusion of the HA-tag to EGFP resulted in pronounced reduction of EGFP fluorescence, and the N-terminally tagged EGFP showed altered mobility in SDS gel electrophoresis while the C-terminally tagged version did not. Among the "new" tags evaluated, the very short IRS tag (5 amino acids in length) was specifically detected, but not with sufficient sensitivity for routine use. In contrast, the antibody used to detect the EE-tag proved to be inoperative in brain sections due to tremendous background staining. Only AU1-tag detection was accomplished with high specificity *and* sensitivity, both on brain sections and in cultured neurons, and did not show any obvious influence on the tagged protein.

Subtle to moderate changes in protein structure and function due to the addition of extra amino acids may be less relevant in cell-free or cell culture experiments, in which superphysiological amounts of recombinant or overexpressed proteins are used for experiments (e.g. co-precipitation assays). However, if functional studies require physiological protein expression levels, then the influence of an epitope tag may turn out to affect the results of the study. Despite this important issue, only limited information is currently available with respect to the influence of epitope tags on the fusion protein. Transgenic mice expressing the wild-type P0-glycoprotein, which is important for peripheral nerve myelination, and which was N-terminally tagged by the cMyc epitope, demonstrated clinical symptoms of Charcot-Marie-Tooth disease

solely due to the presence of the cMyc-tag (Previtali, S. C. *et al.*, 2000), although crystallographic studies suggest that the N-terminus of this protein is not involved in *cis* or *trans* interactions (Shapiro, L. *et al.*, 1996). Fusion of the FLAG epitope to the membrane-binding subunit of influenza virus haemagglutinin caused the protein to localize to the cytoplasm of cells rather than to the membrane (Chen, J. *et al.*, 1998). Tagging the small GTPase H-Ras by the FLAG epitope resulted in activity changes as well as in altered mobility in SDS gel electrophoresis (Johnson, K. Y. *et al.*, 2002). As such, potential influences of epitope tags must be taken into account especially in studies regarding proteins with as-of-yet unknown functions. Putative phosphorylation sites as present in the cMyc- and the FLAG-tag amino acids sequences may only be post-translationally modified depending on a particular cellular environment. Regardless, such modifications may have unpredictable impacts on the protein under investigation.

While some background staining is to be expected if an epitope derived from a cellular protein (like the cMyc-tag) is used, epitopes derived from viral proteins should not have matching cellular counterparts and thus the respective antibodies should be less likely to result in background staining. In the present study, this assumption was found to be correct for the influenza hemagglutinin (HA-) tag (Wilson, I. A. *et al.*, 1984) and for the AU1-tag, which is derived from the bovine papilloma virus capsid protein L1 (Lim, P. S. *et al.*, 1990), but not for the EE (or Glu-Glu) tag, which is derived from polyoma virus medium T-antigen (Grussenmeyer, T. *et al.*, 1985). This latter result together with the finding of FLAG - antibody background staining clearly demonstrates the need to evaluate potential epitope tags and their respective antibodies in the tissue under study, since it can not be excluded that epitope tag - specific antibodies bind to unexpected cellular antigens. SFV vectors appear to be an attractive tool for such evaluation due to their property of fast and efficient transduction of broad specificity.

In a proof-of-principle experiment we used an AAV-2 based viral vector for demonstration of the functionality of the AU1-tag in an *in vivo* gene transfer approach. The AAV vector genome was designed in a way that EGFP is co-expressed with calbindin D_{28K}, clearly demarcating the transduced areas. It should be noted that the approach of co-expressing a reporter gene with the transgene under investigation is a valuable, but indirect way of proving transgene expression. It may fail if detailed sub-cellular localisation of the transgene has to be documented, if the transgene is expressed with different kinetics, or if it is processed or secreted. Therefore, epitope-tagging may be a more reliable methodological approach in targeting transgenic protein expression. Despite robust endogenous calbindin D_{28K} expression in several retinal neuron populations, it was possible to unequivocally trace the expression of the

vector derived AU1-tagged calbindin D_{28K}, clearly discriminating endogenous from overexpressed protein. These results demonstrate the usefulness of this epitope and of epitope-tagging techniques for *in vivo* studies in general. However, this data also clearly demonstrated that a careful pre-evaluation of epitope tags and their respective antibodies is necessary for different types of tissues and transduction paradigms, in order to avoid problems with background detection and unexpected influences of the epitope tags on the protein under investigation.

In this study we have chosen to tag the calcium buffering protein calbindin D_{28K} as its role in neurodegeneration has yet to be clarified. It remains unclear whether localized rather than general increase in cytosolic free calcium is critical for cell death (Rizzuto, R. *et al.*, 1999; Mattson, M. P. *et al.*, 2003). In ongoing experiments we aim to investigate the role of calcium and calbindin D_{28K} in two models of neurodegeneration: optic nerve axotomy and 6-OHDA nigrostriatal lesion. Since relatively high expression of calbindin in retina and certain brain regions was detected in a series of preliminary experiments, appropriate detection of overexpressed calbindin by using the AU1-tag may prove to be useful.

4.3. Neuroprotective therapy of PD as evaluated in the complete 6-OHDA lesion model

Neurodegenerative diseases are characterized by slow and multifactorial progression, and potential therapeutic treatment is difficult due to diagnosis at relatively late stages of life. After diagnosis patients have one or more decades of life expectation, which would necessitate a long-lasting therapeutical intervention in order to halt, or at least significantly postpone the neurodegenerative processes. Any potential therapeutic intervention should thus be confirmed to be effective over longer periods of time. Furthermore, the multifactorial nature of neurodegeneration in its later stages suggests that therapeutic approaches targeting more than one neurodegenerative mechanism might be more effective than mono-specific attempts.

In this study we have evaluated such combination gene transfer in a widely used animal model of neurodegeneration induced by oxidative stress, 6-OHDA lesion of the nigrostriatal system. The unilateral 6-OHDA lesion model of PD offers certain advantages in that it allows the immunohistological analysis of the lesioned hemisphere in comparison to the unaffected brain hemisphere of the same animal as an internal control. Furthermore, an easy-to-perform apomorphine induced rotational behaviour test reflects the degree of asymmetry in striatal dopamine content and can be used to verify the successful lesioning surgery. In order to produce the unilateral toxic model of PD, 6-OHDA is typically injected either into the striatum or into the medial forebrain bundle (MFB) (Blum, D. *et al.*, 2001; Deumens, R. *et al.*, 2002). Multiple striatal injections are usually required to induce the degeneration of more than 50-60% of the DA

neurons in SNpc which increase the time and traumatisation of the surgery (Deumens, R. *et al.*, 2002). An alternative way to achieve the selective degeneration of the nigrostriatal DA neurons in SNpc is to deliver the 6-OHDA toxin directly into the nigrostriatal projection, the MFB. Injection of 6-OHDA into the MFB represents a more severe oxidative stress lesion of DA neurons than the striatal 6-OHDA injection or systemic MPTP application (Deumens, R. *et al.*, 2002; Dauer, W. *et al.*, 2003). Therefore, molecules, able to counteract neurodegeneration in this model may have high potential for therapeutic benefit in PD, in which degeneration of DA neurons occurs at much slower rates.

4.4. BclX_L mediated neuroprotection

The data obtained in this study demonstrate that BclX_L overexpression can promote the survival of 61% of dopaminergic neurons at 2 weeks and 31% at 6 weeks after the 6-OHDA lesion of the medial forebrain bundle. The numbers of remaining neurons in AAV-2-BclX_L injected group are significantly higher ($p<0.001$) than those transduced with the AAV-2-EGFP control virus (25% at 2 weeks and 7% at 6 weeks). However, a decline in DA cell numbers from 2 to 6 weeks post-lesion was observed, and thus, stable neuroprotection could not be achieved through BclX_L overexpression alone.

Several studies have focused on the role of bcl-2, another anti-apoptotic protein of the same family as BclX_L, in the protection of CNS neurons from cell death. In the partial 6-OHDA toxicity model of PD, herpes virus mediated overexpression of bcl-2 supported the survival of approximately 50% of nigral neurons at 2 weeks after the lesion (Yamada, M. *et al.*, 1999). Also, transgenic mice expressing human bcl-2 under the neuron-specific enolase promoter have been found to be more resistant to MPTP and 6-OHDA toxicity (Offen, D. *et al.*, 1998). However, both experiments were estimating only the short-term effects of the bcl-2 on DA cell survival. Moreover, the toxic lesions performed in either of the studies were relatively mild as compared to the complete unilateral lesion paradigm (Deumens, R. *et al.*, 2002; Dauer, W. *et al.*, 2003).

In this study, overexpression of BclX_L but not bcl-2 was chosen mainly for two reasons. First, BclX_L has been shown to be more potent in inhibiting mitochondrial membrane potential breakdown than bcl-2 (Kim, R., 2005), probably due to its more efficient targeting to mitochondria (Kaufmann, T. *et al.*, 2003). Second, BclX_L but not bcl-2 can inhibit TNF α -activated TRAIL mediated apoptotic and non-apoptotic cell death (necrosis and autophagy) (Kim, I. K. *et al.*, 2003; Kim, R., 2005; Keogh, S. A. *et al.*, 2000), which play important roles in

several neurodegenerative paradigms (Anglade, P. *et al.*, 1997; Hirsch, E. C. *et al.*, 2003; Cacquevel, M. *et al.*, 2004).

Taken together, BclX_L overexpression failed to finally preserve neurons from degeneration after severe unilateral lesion of nigrostriatal system, with a 50% decrease of surviving neuron numbers late after lesion as compared to the early time of analysis. Moreover, BclX_L failed to preserve the DA neurites, protecting only the cell bodies of DA neurons. Thus, maintenance of mitochondrial integrity may be essential for neuronal survival early after lesion but appeared to be less important for the long-term survival of deafferentiated neurons and insufficient for the maintenance of the functional DA connections.

4.5. Combination of BclX_L and GDNF for neuroprotection of DA neurons

In order to achieve sustained and complete protection of nigrostriatal neurons, a combination of mitochondrial integrity protection by BclX_L overexpression with neurotrophic support by GDNF expression was used. To this purpose a mixture of two AAV-2 vectors each carrying a functional transgene (BclX_L or GDNF) and a fluorescent reporter gene (DsRed or EGFP) was stereotactically applied into the SNpc. The presence of the fluorescent transgenes was required to prove the efficient co-transduction of nigral DA neurons upon co-injection of the AAV vectors. As it has been shown before for retinal ganglion cells (Michel, U. *et al.*, 2005), double transduction of the vast majority of DA neurons (>90%) by two different AAV-2 vectors could be accomplished.

When used in combination, BclX_L and GDNF provided almost complete neuroprotection (96%) in the 6-OHDA lesion paradigm at early time after lesion. The combined effect of these two molecules was found to be additive indicating the important role for targeting multiple pathways in neurodegenerative diseases. The results obtained in the short-term experiments are in coincidence with previous studies demonstrating that a combination of expression of GDNF with the anti-apoptotic bcl-2 or XIAP proteins had additive neuroprotective effects in several other lesion models (Natsume, A. *et al.*, 2002; Natsume, A. *et al.*, 2001; Straten, G. *et al.*, 2002; Eberhardt, O. *et al.*, 2000). Altogether, this strengthens the notion that aiming to prevent neurodegeneration through different pathways may be a more effective approach to slow down the progression of neurodegenerative processes than by targeting single cellular pathways.

In the model system evaluated in this study, the BclX_L plus GDNF co-expression resulted in the most effective short-term prevention from neurodegeneration reported so far. While the mode of action for BclX_L is relatively well-defined (Kim, R., 2005), this does not hold

true for the neurotrophin GDNF. GDNF may exert its beneficial effects through several receptor systems, including its prototype receptors GFR α and Ret, but also NCAM and heparansulphate-proteoglycans like syndecan-3 (Sariola, H. *et al.*, 2003). Dopaminergic neurons of the SNpc express high levels of GDNF receptors (Trupp, M. *et al.*, 1996), and thus may be responsive to the neurotrophin without a delay, explaining the stable and efficient protection mediated by GDNF expression.

Nevertheless, at later time after lesions co-expressed BclX_L and GDNF failed to demonstrate any additive effect of on DA neuronal survival. This outcome may be partially explained by the fact that GDNF may induce the upregulation of bcl-2 and BclX_L expression (Ghribi, O. *et al.*, 2001; Cheng, H. *et al.*, 2002) and further AAV mediated overexpression of BclX_L may not be beneficial. However, immunofluorescence did not reveal any GDNF-induced upregulation of BclX_L or bcl-2 levels in transduced nigral neurons.

In many neurodegenerative paradigms axonal damage precedes the loss of neuronal cell bodies (Dauer, W. *et al.*, 2003; Stokin, G. B. *et al.*, 2005; Li, H. *et al.*, 2001; Gunawardena, S. *et al.*, 2005). This principle is at least partially recapitulated in the model system used in this study, since DA neurons of SNpc are lesioned primarily by the axonal damage. In this paradigm protection of mitochondrial integrity was substantially more effective at early time after lesion, but no stable prevention of neurodegeneration over time was achieved by BclX_L expression. These data suggest that in deafferentiated CNS neurons degeneration can only be postponed by targeting mitochondria mediated pathways. Further neuroprotective signalling by GDNF may then be necessary to inhibit neurodegeneration in its later stages. These results should have important implications for the design of therapeutic neuroprotective approaches.

Taken together, it was demonstrated in this work that BclX_L and GDNF act additively in protecting DA cells of SNpc at early time points after lesion, however loose this combinatorial effect when investigated at later time points. This data suggest that the actual potency of the therapeutic approach could only be revealed over long-term experiments suggesting that studies aiming to define neuroprotective strategies should be generally performed over longer periods of time.

4.6. GDNF mediated neurorestorative therapy

The highly efficient neuroprotection of DA cell bodies in SNpc reported in this study does not, however, preserve their striatal projections. Therefore, the ultimate goal to restore the balance in nigrostriatal DA system could not be achieved due to the model system outlay.

GDNF appears to become the molecule of choice for restoration of the dopaminergic projection network in the striatum. Striatal delivery of GDNF was proven to be effective in protecting both nigral dopamine (DA) neurons and their axons in the striatum accompanied by recovery of spontaneous sensorimotor behaviors in various animal models (Chao, C. C. *et al.*, 2003; Georgievska, B. *et al.*, 2002b; Jollivet, C. *et al.*, 2004; Rosenblad, C. *et al.*, 2000). Sprouting of the lesioned axons was documented along the nigrostriatal pathway, precisely corresponding to the areas containing anterogradely transported GDNF (Georgievska, B. *et al.*, 2002b). First successful phase 1 clinical trials on intraputamenal delivery of GDNF reported to improve motor symptoms and striatal dopamine content in human patients (Nutt, J. G. *et al.*, 2003; Gill, S. S. *et al.*, 2003). However, recent results from a double-controlled clinical study delivering the recombinant GDNF directly into brain did not demonstrate efficacy and safety of such a treatment (Lang, A. E. *et al.*, 2006). Various methodological reasons could contribute to this outcome, such as surgical procedure of peptide delivery, the development of immune response to the recombinant protein, and overall dosage of the GDNF. It may therefore be premature to conclude the ineffectiveness of GDNF trophic support therapy for PD patients. Nevertheless, before proceeding with any further clinical trials, the safety issues regarding the tools for efficient GDNF delivery, the dosages and therapeutic indications have to be carefully re-evaluated. More preclinical studies in animal models will be required to fulfil these requirements. Future approaches, such as gene therapy or cells engineered to produce GDNF (Kishima, H. *et al.*, 2004; Behrstock, S. *et al.*, 2006), or viral vector mediated GDNF expression (Eslamboli, A. *et al.*, 2003) may prove more effective for providing local and sustained delivery of GDNF than simple direct brain infusion.

In this work the question was posed on whether GDNF may contribute to the re-sprouting and behavioural recovery *after* the *complete* nigrostriatal lesion which may reflect the situation at the very late stages of PD, when more than 90% of DA innervation is lost. The appropriate dose of GDNF may be crucial for beneficial outcome. Long-term striatal overexpression of GDNF was shown to selectively downregulate tyrosine hydroxylase in intact nigral neurons (Rosenblad, C. *et al.*, 2003) and may induce aberrant neuritic sprouting (Georgievska, B. *et al.*, 2002a). To avoid the overdose effect, GDNF was expressed from the hSyn1 promoter which typically allows for physiological levels of protein expression (Kügler, S. *et al.*, 2003a).

In contrast to the data showing that delayed delivery of AAV-GDNF promoted functional recovery in the *partial* 6-OHDA lesion of the nigrostriatal system (Wang, L. *et al.*, 2002), it failed to produce such effect in the *complete* lesion model in the study presented here. This result favours the hypothesis that GDNF requires the presence of sufficient remaining DA

projections in the striatum (as in partial lesion model) in order to exert its neurorestorative effect and may therefore be inefficient at late stages of PD.

5. Summary

Gene transfer to the brain is a promising therapeutic strategy for a variety of neurodegenerative disorders including Parkinson's disease (PD). PD is characterized by a progressive degeneration of the nigrostriatal dopaminergic system. By using adeno-associated viral (AAV) vector that allows for long-term and stable transgene expression, a single intervention rather than continuous pharmacological treatment may provide a therapeutic effect. In this study, BclX_L and GDNF have been evaluated separately and in combination as prospective neuroprotective molecules for gene therapy in the complete 6-hydroxydopamine lesion model of PD. Efficiency of gene therapy is dependent on the effective transduction of the selected regions in the brain. AAV-2 serotype is known to preferentially transduce dopaminergic neurons in substantia nigra (SN) and therefore was chosen for BclX_L and/or GDNF gene transfer into this region. Wide-spread transduction of the rat striatum for GDNF delivery could be achieved by cross-packaging of the AAV-2 genome into the AAV-5 capsid. Attempts to restrict GDNF transgene expression to astrocytes, as it is naturally secreted from glial cells, by using murine cytomegalovirus (mCMV) promoter and AAV-5 serotype, were successful *in vitro* but not *in vivo*. In order to facilitate tracing of the transgenic protein expression *in vivo*, epitope-tagging technique has been employed. The first systematic evaluation of six different epitope/antibody combinations for *in vivo* application is presented in this study and reveals the AU1 epitope tag as the best suited for detection of the transgenic protein in the central nervous system.

AAV-2-mediated overexpression of BclX_L in substantia nigra of rat brain mediated the survival of 61% of dopaminergic neurons at 2 weeks and 31% at 6 weeks after the lesion as compared to 25% and 7%, respectively, in the control-virus transduced SN. Co-expression of BclX_L and GDNF resulted in the most effective protection of dopaminergic neurons at 2 weeks after the 6-OHDA lesion reported so far (96% surviving DA neurons). At this time point of analysis, additive neuroprotective effects of BclX_L and GDNF were evident. At 6 weeks after the lesion, however, no additive effect of BclX_L to GDNF-mediated neuroprotection was observed. Therefore, long-term studies should be generally performed to determine the actual potency of particular gene transfer.

Aiming for delayed restoration of dopaminergic projections, AAV-5-GDNF transduction of the striatum was performed *after* the complete lesion of nigrostriatal system. Failure to observe any behavioural or histo-morphological improvement at 3 months after the AAV injection into the lesioned striatum favours the conclusion that sufficient remaining nigrostriatal projections are required as a template for GDNF to induce the resprouting.

6. Acknowledgements

I would like to express my gratitude to all people who have supported me during the work on the PhD thesis, especially to

Dr. Sebastian Kögler, for his excellent supervision, fruitful discussions and guiding me through the every-day-experiments, for creating nice and friendly atmosphere in the laboratory

Prof. Mathias Bähr, for financial and mental support, for closely following my progress on the project

My PhD Committee Members, Prof. Reinhard Jahn and Prof. Markus Missler, for the feedback on the project and supervision during the years of PhD

My colleagues and friends in the laboratory, Dr. Malik Ibrahim, Manuel Garrido, Dr. Uwe Michel, Ulrike Schöll and Veronique Planchamp, for their helping hands and open hearts, for making my time in the laboratory and outside full of great memories

My dear friends, Elena Kvachnina, Rocio Finol and Nataliya Korogod, always being there to share wonderful and sad moments, giving warmth and understanding like only family can give

To all my friends in Göttingen, Ukraine and all-round-the-world for their helping hands and open minds

Last, but not least, I want to thank my parents, for continuous support and love in every moment of my life independent on distance and time that parts me from home.

7. References

- Abou-Sleiman, P. M., Muqit, M. M., and Wood, N. W. (2006). Expanding insights of mitochondrial dysfunction in Parkinson's disease. *Nat.Rev.Neurosci.* **7:** 207-219.
- Addison, C. L., Hitt, M., Kunskon, D., and Graham, F. L. (1997). Comparison of the human versus murine cytomegalovirus immediate early gene promoters for transgene expression by adenoviral vectors. *J.Gen.Viro.* **78 (Pt 7):** 1653-1661.
- Airaksinen, M. S. and Saarma, M. (2002). The GDNF family: signalling, biological functions and therapeutic value. *Nat.Rev.Neurosci.* **3:** 383-394.
- Andersen, J. K. (2004). Oxidative stress in neurodegeneration: cause or consequence? *Nat.Med.* **10 Suppl:** S18-S25.
- Anglade, P., Vyas, S., Javoy-Agid, F., Herrero, M. T., Michel, P. P., Marquez, J., Mouatt-Prigent, A., Ruberg, M., Hirsch, E. C., and Agid, Y. (1997). Apoptosis and autophagy in nigral neurons of patients with Parkinson's disease. *Histol.Histopathol.* **12:** 25-31.
- Arenas, E., Trupp, M., Akerud, P., and Ibanez, C. F. (1995). GDNF prevents degeneration and promotes the phenotype of brain noradrenergic neurons in vivo. *Neuron* **15:** 1465-1473.
- Atkins, G. J., Sheahan, B. J., and Liljestrom, P. (1999). The molecular pathogenesis of Semliki Forest virus: a model virus made useful? *J.Gen.Viro.* **80 (Pt 9):** 2287-2297.
- Auricchio, A., Kobinger, G., Anand, V., Hildinger, M., O'Connor, E., Maguire, A. M., Wilson, J. M., and Bennett, J. (15-12-2001). Exchange of surface proteins impacts on viral vector cellular specificity and transduction characteristics: the retina as a model. *Hum.Mol.Genet.* **10:** 3075-3081.
- Azzouz, M., Hottinger, A., Paterna, J. C., Zurn, A. D., Aebsicher, P., and Bueler, H. (22-3-2000). Increased motoneuron survival and improved neuromuscular function in transgenic ALS mice after intraspinal injection of an adeno-associated virus encoding Bcl-2. *Hum.Mol.Genet.* **9:** 803-811.
- Bantel-Schaal, U., Delius, H., Schmidt, R., and zur, H. H. (1999). Human adeno-associated virus type 5 is only distantly related to other known primate helper-dependent parvoviruses. *J.Viro.* **73:** 939-947.
- Beal, M. F. (2005). Mitochondria take center stage in aging and neurodegeneration. *Ann.Neurol.* **58:** 495-505.
- Bear, M. F., Connors, B. W., and Paradiso, M. A. *Neuroscience: Exploring the Brain.* [2nd ed.]. 2001. Williams and Wilkins.
- Behrstock, S., Ebert, A., McHugh, J., Vosberg, S., Moore, J., Schneider, B., Capowski, E., Hei, D., Kordower, J., Aebsicher, P., and Svendsen, C. N. (2006). Human neural progenitors deliver glial cell line-derived neurotrophic factor to parkinsonian rodents and aged primates. *Gene Ther.* **13:** 379-388.
- Beilina, A., Van Der, B. M., Ahmad, R., Kesavapany, S., Miller, D. W., Petsko, G. A., and Cookson, M. R. (19-4-2005). Mutations in PTEN-induced putative kinase 1 associated with

recessive parkinsonism have differential effects on protein stability.
Proc.Natl.Acad.Sci.U.S.A **102**: 5703-5708.

Ben Shachar, D., Zuk, R., and Glinka, Y. (1995). Dopamine neurotoxicity: inhibition of mitochondrial respiration. J.Neurochem. **64**: 718-723.

Betarbet, R., Sherer, T. B., MacKenzie, G., Garcia-Osuna, M., Panov, A. V., and Greenamyre, J. T. (2000). Chronic systemic pesticide exposure reproduces features of Parkinson's disease. Nat.Neurosci. **3**: 1301-1306.

Björklund, A., Rosenblad, C., Winkler, C., and Kirik, D. (1997). Studies on neuroprotective and regenerative effects of GDNF in a partial lesion model of Parkinson's disease. Neurobiol.Dis. **4**: 186-200.

Blom, N., Sicheritz-Ponten, T., Gupta, R., Gammeltoft, S., and Brunak, S. (2004). Prediction of post-translational glycosylation and phosphorylation of proteins from the amino acid sequence. Proteomics. **4**: 1633-1649.

Blum, D., Torch, S., Lambeng, N., Nissou, M., Benabid, A. L., Sadoul, R., and Verna, J. M. (2001). Molecular pathways involved in the neurotoxicity of 6-OHDA, dopamine and MPTP: contribution to the apoptotic theory in Parkinson's disease. Prog.Neurobiol. **65**: 135-172.

Braak, H. and Braak, E. (2000). Pathoanatomy of Parkinson's disease. J.Neurol. **247 Suppl 2**: II3-10.

Buller, R. M., Janik, J. E., Sebring, E. D., and Rose, J. A. (1981). Herpes simplex virus types 1 and 2 completely help adenovirus-associated virus replication. J.Virol. **40**: 241-247.

Burger, C., Gorbatyuk, O. S., Velardo, M. J., Peden, C. S., Williams, P., Zolotukhin, S., Reier, P. J., Mandel, R. J., and Muzyczka, N. (2004). Recombinant AAV viral vectors pseudotyped with viral capsids from serotypes 1, 2, and 5 display differential efficiency and cell tropism after delivery to different regions of the central nervous system. Mol.Ther. **10**: 302-317.

Cacquevel, M., Lebeurrier, N., Cheenne, S., and Vivien, D. (2004). Cytokines in neuroinflammation and Alzheimer's disease. Curr.Drug Targets. **5**: 529-534.

Cadet, J. L., Zhu, S. M., and Angulo, J. A. (1992). Quantitative in situ hybridization evidence for differential regulation of proenkephalin and dopamine D2 receptor mRNA levels in the rat striatum: effects of unilateral intrastriatal injections of 6-hydroxydopamine. Brain Res.Mol.Brain Res. **12**: 59-67.

Cearley, C. N. and Wolfe, J. H. (2006). Transduction characteristics of adeno-associated virus vectors expressing cap serotypes 7, 8, 9, and Rh10 in the mouse brain. Mol.Ther. **13**: 528-537.

Chang, L. K., Putcha, G. V., Deshmukh, M., and Johnson, E. M., Jr. (2002). Mitochondrial involvement in the point of no return in neuronal apoptosis. Biochimie **84**: 223-231.

Chao, C. C., Ma, Y. L., Chu, K. Y., and Lee, E. H. (2003). Integrin alphav and NCAM mediate the effects of GDNF on DA neuron survival, outgrowth, DA turnover and motor activity in rats. Neurobiol.Aging **24**: 105-116.

Chao, H., Liu, Y., Rabinowitz, J., Li, C., Samulski, R. J., and Walsh, C. E. (2000). Several log increase in therapeutic transgene delivery by distinct adeno-associated viral serotype vectors. *Mol.Ther.* **2**: 619-623.

Chen, J., Skehel, J. J., and Wiley, D. C. (29-9-1998). A polar octapeptide fused to the N-terminal fusion peptide solubilizes the influenza virus HA2 subunit ectodomain. *Biochemistry* **37**: 13643-13649.

Cheng, E. H., Wei, M. C., Weiler, S., Flavell, R. A., Mak, T. W., Lindsten, T., and Korsmeyer, S. J. (2001). BCL-2, BCL-X(L) sequester BH3 domain-only molecules preventing BAX- and BAK-mediated mitochondrial apoptosis. *Mol.Cell* **8**: 705-711.

Cheng, H., Wu, J. P., and Tzeng, S. F. (1-8-2002). Neuroprotection of glial cell line-derived neurotrophic factor in damaged spinal cords following contusive injury. *J.Neurosci.Res.* **69**: 397-405.

Dauer, W. and Przedborski, S. (11-9-2003). Parkinson's disease: mechanisms and models. *Neuron* **39**: 889-909.

Davidson, B. L., Stein, C. S., Heth, J. A., Martins, I., Kotin, R. M., Derksen, T. A., Zabner, J., Ghodsi, A., and Chiorini, J. A. (28-3-2000). Recombinant adeno-associated virus type 2, 4, and 5 vectors: transduction of variant cell types and regions in the mammalian central nervous system. *Proc.Natl.Acad.Sci.U.S.A* **97**: 3428-3432.

Dawson, T. M., Dawson, V. L., Gage, F. H., Fisher, L. J., Hunt, M. A., and Wamsley, J. K. (1991). Functional recovery of supersensitive dopamine receptors after intrastratal grafts of fetal substantia nigra. *Exp.Neurol.* **111**: 282-292.

de Rijk, M. C., Tzourio, C., Breteler, M. M., Dartigues, J. F., Amaducci, L., Lopez-Pousa, S., Manubens-Bertran, J. M., Alperovitch, A., and Rocca, W. A. (1997). Prevalence of parkinsonism and Parkinson's disease in Europe: the EUROPARKINSON Collaborative Study. European Community Concerted Action on the Epidemiology of Parkinson's disease. *J.Neurol.Neurosurg.Psychiatry* **62**: 10-15.

Deumens, R., Blokland, A., and Prickaerts, J. (2002). Modeling Parkinson's disease in rats: an evaluation of 6-OHDA lesions of the nigrostriatal pathway. *Exp.Neurol.* **175**: 303-317.

Dexter, D. T., Carter, C. J., Wells, F. R., Javoy-Agid, F., Agid, Y., Lees, A., Jenner, P., and Marsden, C. D. (1989a). Basal lipid peroxidation in substantia nigra is increased in Parkinson's disease. *J.Neurochem.* **52**: 381-389.

Dexter, D. T., Wells, F. R., Lees, A. J., Agid, F., Agid, Y., Jenner, P., and Marsden, C. D. (1989b). Increased nigral iron content and alterations in other metal ions occurring in brain in Parkinson's disease. *J.Neurochem.* **52**: 1830-1836.

Di Giovanni, S., Knoblach, S. M., Brandoli, C., Aden, S. A., Hoffman, E. P., and Faden, A. I. (2003). Gene profiling in spinal cord injury shows role of cell cycle in neuronal death. *Ann.Neurol.* **53**: 454-468.

Di Pasquale, G., Davidson, B. L., Stein, C. S., Martins, I., Scudiero, D., Monks, A., and Chiorini, J. A. (2003). Identification of PDGFR as a receptor for AAV-5 transduction. *Nat.Med.* **9**: 1306-1312.

- Dong, J. Y., Fan, P. D., and Frizzell, R. A. (10-11-1996). Quantitative analysis of the packaging capacity of recombinant adeno-associated virus. *Hum.Gene Ther.* **7**: 2101-2112.
- Duan, D., Sharma, P., Yang, J., Yue, Y., Dudus, L., Zhang, Y., Fisher, K. J., and Engelhardt, J. F. (1998). Circular intermediates of recombinant adeno-associated virus have defined structural characteristics responsible for long-term episomal persistence in muscle tissue. *J.Virol.* **72**: 8568-8577.
- Duan, D., Yue, Y., and Engelhardt, J. F. (2001). Expanding AAV packaging capacity with trans-splicing or overlapping vectors: a quantitative comparison. *Mol.Ther.* **4**: 383-391.
- Eberhardt, O., Coelln, R. V., Kügler, S., Lindenau, J., Rathke-Hartlieb, S., Gerhardt, E., Haid, S., Isenmann, S., Gravel, C., Srinivasan, A., Bähr, M., Weller, M., Dichgans, J., and Schulz, J. B. (15-12-2000). Protection by synergistic effects of adenovirus-mediated X-chromosome-linked inhibitor of apoptosis and glial cell line-derived neurotrophic factor gene transfer in the 1-methyl-4-phenyl-1,2,3,6-tetrahydropyridine model of Parkinson's disease. *J.Neurosci.* **20**: 9126-9134.
- Ehrengruber, M. U., Renggli, M., Raineteau, O., Hennou, S., Vähä-Koskela, M. J., Hinkkanen, A. E., and Lundstrom, K. (2003). Semliki Forest virus A7(74) transduces hippocampal neurons and glial cells in a temperature-dependent dual manner. *J.Neurovirol.* **9**: 16-28.
- Elston, T., Wang, H., and Oster, G. (29-1-1998). Energy transduction in ATP synthase. *Nature* **391**: 510-513.
- Eslamboli, A., Cummings, R. M., Ridley, R. M., Baker, H. F., Muzyczka, N., Burger, C., Mandel, R. J., Kirik, D., and Annett, L. E. (2003). Recombinant adeno-associated viral vector (rAAV) delivery of GDNF provides protection against 6-OHDA lesion in the common marmoset monkey (*Callithrix jacchus*). *Exp.Neurol.* **184**: 536-548.
- Esselink, R. A., de Bie, R. M., de Haan, R. J., Lenders, M. W., Nijssen, P. C., Staal, M. J., Smeding, H. M., Schuurman, P. R., Bosch, D. A., and Speelman, J. D. (27-1-2004). Unilateral pallidotomy versus bilateral subthalamic nucleus stimulation in PD: a randomized trial. *Neurology* **62**: 201-207.
- Ewing, B. and Green, P. (2000). Analysis of expressed sequence tags indicates 35,000 human genes. *Nat.Genet.* **25**: 232-234.
- Feany, M. B. and Bender, W. W. (23-3-2000). A Drosophila model of Parkinson's disease. *Nature* **404**: 394-398.
- Fearnley, J. M. and Lees, A. J. (1991). Ageing and Parkinson's disease: substantia nigra regional selectivity. *Brain* **114 (Pt 5)**: 2283-2301.
- Fleming, S. M., Fernagut, P. O., and Chesselet, M. F. (2005). Genetic mouse models of parkinsonism: strengths and limitations. *NeuroRx.* **2**: 495-503.
- Floor, E. and Wetzel, M. G. (1998). Increased protein oxidation in human substantia nigra pars compacta in comparison with basal ganglia and prefrontal cortex measured with an improved dinitrophenylhydrazine assay. *J.Neurochem.* **70**: 268-275.

Flotte, T. R., Afione, S. A., and Zeitlin, P. L. (1994). Adeno-associated virus vector gene expression occurs in nondividing cells in the absence of vector DNA integration. *Am.J.Respir.Cell Mol.Biol.* **11**: 517-521.

Flotte, T. R., Solow, R., Owens, R. A., Afione, S., Zeitlin, P. L., and Carter, B. J. (1992). Gene expression from adeno-associated virus vectors in airway epithelial cells. *Am.J.Respir.Cell Mol.Biol.* **7**: 349-356.

Foley, P. and Riederer, P. (1999). Pathogenesis and preclinical course of Parkinson's disease. *J.Neural Transm.Suppl* **56**: 31-74.

Fornai, F., Schluter, O. M., Lenzi, P., Gesi, M., Ruffoli, R., Ferrucci, M., Lazzeri, G., Busceti, C. L., Pontarelli, F., Battaglia, G., Pellegrini, A., Nicoletti, F., Ruggieri, S., Paparelli, A., and Sudhof, T. C. (1-3-2005). Parkinson-like syndrome induced by continuous MPTP infusion: convergent roles of the ubiquitin-proteasome system and alpha-synuclein. *Proc.Natl.Acad.Sci.U.S.A* **102**: 3413-3418.

Forno, L. S. (1996). Neuropathology of Parkinson's disease. *J.Neuropathol.Exp.Neurol.* **55**: 259-272.

Fuxe, K., Chadi, G., Tinne, B., Agnati, L. F., Pettersson, R., and David, G. (4-2-1994). On the regional distribution of heparan sulfate proteoglycan immunoreactivity in the rat brain. *Brain Res.* **636**: 131-138.

Gagnon, C., Bedard, P. J., Rioux, L., Gaudin, D., Martinoli, M. G., Pelletier, G., and Di Paolo, T. (6-9-1991). Regional changes of striatal dopamine receptors following denervation by 6-hydroxydopamine and fetal mesencephalic grafts in the rat. *Brain Res.* **558**: 251-263.

Gandhi, S. and Wood, N. W. (15-9-2005). Molecular pathogenesis of Parkinson's disease. *Hum.Mol.Genet.* **14**: 2749-2755.

Georgievska, B., Kirik, D., and Björklund, A. (2002a). Aberrant sprouting and downregulation of tyrosine hydroxylase in lesioned nigrostriatal dopamine neurons induced by long-lasting overexpression of glial cell line derived neurotrophic factor in the striatum by lentiviral gene transfer. *Exp.Neurol.* **177**: 461-474.

Georgievska, B., Kirik, D., Rosenblad, C., Lundberg, C., and Björklund, A. (21-1-2002b). Neuroprotection in the rat Parkinson model by intrastriatal GDNF gene transfer using a lentiviral vector. *Neuroreport* **13**: 75-82.

Gerdes, C. A., Castro, M. G., and Löwenstein, P. R. (2000). Strong promoters are the key to highly efficient, noninflammatory and noncytotoxic adenoviral-mediated transgene delivery into the brain in vivo. *Mol.Ther.* **2**: 330-338.

Ghribi, O., Herman, M. M., Forbes, M. S., DeWitt, D. A., and Savory, J. (2001). GDNF protects against aluminum-induced apoptosis in rabbits by upregulating Bcl-2 and Bcl-XL and inhibiting mitochondrial Bax translocation. *Neurobiol.Dis.* **8**: 764-773.

Gill, S. S., Patel, N. K., Hotton, G. R., O'Sullivan, K., McCarter, R., Bunnage, M., Brooks, D. J., Svendsen, C. N., and Heywood, P. (2003). Direct brain infusion of glial cell line-derived neurotrophic factor in Parkinson disease. *Nat.Med.* **9**: 589-595.

Gotz, M. E., Dirr, A., Burger, R., Janetzky, B., Weinmuller, M., Chan, W. W., Chen, S. C., Reichmann, H., Rausch, W. D., and Riederer, P. (15-2-1994). Effect of lipoic acid on redox

state of coenzyme Q in mice treated with 1-methyl-4-phenyl-1,2,3,6-tetrahydropyridine and diethyldithiocarbamate. *Eur.J.Pharmacol.* **266:** 291-300.

Graham, D. G., Tiffany, S. M., Bell, W. R., Jr., and Gutknecht, W. F. (1978). Autoxidation versus covalent binding of quinones as the mechanism of toxicity of dopamine, 6-hydroxydopamine, and related compounds toward C1300 neuroblastoma cells in vitro. *Mol.Pharmacol.* **14:** 644-653.

Grondin, R. and Gash, D. M. (1998). Glial cell line-derived neurotrophic factor (GDNF): a drug candidate for the treatment of Parkinson's disease. *J.Neurol.* **245:** 35-42.

Grussenmeyer, T., Scheidtmann, K. H., Hutchinson, M. A., Eckhart, W., and Walter, G. (1985). Complexes of polyoma virus medium T antigen and cellular proteins. *Proc.Natl.Acad.Sci.U.S.A* **82:** 7952-7954.

Gunawardena, S. and Goldstein, L. S. (2005). Polyglutamine diseases and transport problems: deadly traffic jams on neuronal highways. *Arch.Neurol.* **62:** 46-51.

Hald, A. and Lotharius, J. (2005). Oxidative stress and inflammation in Parkinson's disease: is there a causal link? *Exp.Neurol.* **193:** 279-290.

Hauck, B., Chen, L., and Xiao, W. (2003). Generation and characterization of chimeric recombinant AAV vectors. *Mol.Ther.* **7:** 419-425.

Henderson, C. E., Phillips, H. S., Pollock, R. A., Davies, A. M., Lemeulle, C., Armanini, M., Simmons, L., Moffet, B., Vandlen, R. A., Simpson LC [corrected to Simmons, and . (11-11-1994)]. GDNF: a potent survival factor for motoneurons present in peripheral nerve and muscle. *Science* **266:** 1062-1064.

Hengartner, M. O. (12-10-2000). The biochemistry of apoptosis. *Nature* **407:** 770-776.

Hildinger, M., Auricchio, A., Gao, G., Wang, L., Chirmule, N., and Wilson, J. M. (2001). Hybrid vectors based on adeno-associated virus serotypes 2 and 5 for muscle-directed gene transfer. *J.Virol.* **75:** 6199-6203.

Hirsch, E. C., Breidert, T., Rousselet, E., Hunot, S., Hartmann, A., and Michel, P. P. (2003). The role of glial reaction and inflammation in Parkinson's disease. *Ann.N.Y.Acad.Sci.* **991:** 214-228.

Hristova, A. H. and Koller, W. C. (2000). Early Parkinson's disease: what is the best approach to treatment. *Drugs Aging* **17:** 165-181.

Hughes, A. J., Ben Shlomo, Y., Daniel, S. E., and Lees, A. J. (2001). What features improve the accuracy of clinical diagnosis in Parkinson's disease: a clinicopathologic study. *1992. Neurology* **57:** S34-S38.

Ibanez, C. F. (1998). Emerging themes in structural biology of neurotrophic factors. *Trends Neurosci.* **21:** 438-444.

Jin, J., Meredith, G. E., Chen, L., Zhou, Y., Xu, J., Shie, F. S., Lockhart, P., and Zhang, J. (24-3-2005). Quantitative proteomic analysis of mitochondrial proteins: relevance to Lewy body formation and Parkinson's disease. *Brain Res.Mol.Brain Res.* **134:** 119-138.

- Johnson, K. Y., Liu, L., and Vincent, T. S. (2002). Minimal FLAG sequence useful in the functional epitope tagging of H-Ras. *Biotechniques* **32**: 1270, 1272-6, 1278, 1280.
- Jollivet, C., Aubert-Pouessel, A., Clavreul, A., Venier-Julienne, M. C., Remy, S., Montero-Menei, C. N., Benoit, J. P., and Menei, P. (2004). Striatal implantation of GDNF releasing biodegradable microspheres promotes recovery of motor function in a partial model of Parkinson's disease. *Biomaterials* **25**: 933-942.
- Juraska, J. M., Wilson, C. J., and Groves, P. M. (15-4-1977). The substantia nigra of the rat: a Golgi study. *J.Comp Neurol.* **172**: 585-600.
- Kaludov, N., Brown, K. E., Walters, R. W., Zabner, J., and Chiorini, J. A. (2001). Adeno-associated virus serotype 4 (AAV4) and AAV5 both require sialic acid binding for hemagglutination and efficient transduction but differ in sialic acid linkage specificity. *J.Virol.* **75**: 6884-6893.
- Kandel, E. R., Schwartz, J. H., and Jessell, T. M. *Principles of Neural Science*. [4th ed.]. 2000. New York, McGraw-Hill.
- Kaufmann, T., Schlipf, S., Sanz, J., Neubert, K., Stein, R., and Borner, C. (6-1-2003). Characterization of the signal that directs Bcl-x(L), but not Bcl-2, to the mitochondrial outer membrane. *J.Cell Biol.* **160**: 53-64.
- Keogh, S. A., Walczak, H., Bouchier-Hayes, L., and Martin, S. J. (7-4-2000). Failure of Bcl-2 to block cytochrome c redistribution during TRAIL-induced apoptosis. *FEBS Lett.* **471**: 93-98.
- Kermer, P., Klöcker, N., and Bähr, M. (1999). Long-term effect of inhibition of ced 3-like caspases on the survival of axotomized retinal ganglion cells in vivo. *Exp.Neurol.* **158**: 202-205.
- Kim, I. K., Jung, Y. K., Noh, D. Y., Song, Y. S., Choi, C. H., Oh, B. H., Masuda, E. S., and Jung, Y. K. (24-3-2003). Functional screening of genes suppressing TRAIL-induced apoptosis: distinct inhibitory activities of Bcl-XL and Bcl-2. *Br.J.Cancer* **88**: 910-917.
- Kim, R. (29-7-2005). Unknotting the roles of Bcl-2 and Bcl-xL in cell death. *Biochem.Biophys.Res.Commun.* **333**: 336-343.
- Kirik, D., Annett, L. E., Burger, C., Muzyczka, N., Mandel, R. J., and Björklund, A. (4-3-2003). Nigrostriatal alpha-synucleinopathy induced by viral vector-mediated overexpression of human alpha-synuclein: a new primate model of Parkinson's disease. *Proc.Natl.Acad.Sci.U.S.A* **100**: 2884-2889.
- Kirik, D., Georgievska, B., and Björklund, A. (2004). Localized striatal delivery of GDNF as a treatment for Parkinson disease. *Nat.Neurosci.* **7**: 105-110.
- Kirik, D., Rosenblad, C., and Björklund, A. (1998). Characterization of behavioral and neurodegenerative changes following partial lesions of the nigrostriatal dopamine system induced by intrastriatal 6-hydroxydopamine in the rat. *Exp.Neurol.* **152**: 259-277.
- Kirik, D., Rosenblad, C., Burger, C., Lundberg, C., Johansen, T. E., Muzyczka, N., Mandel, R. J., and Björklund, A. (1-4-2002). Parkinson-like neurodegeneration induced by targeted overexpression of alpha-synuclein in the nigrostriatal system. *J.Neurosci.* **22**: 2780-2791.

Kish, S. J., Morito, C., and Hornykiewicz, O. (5-8-1985). Glutathione peroxidase activity in Parkinson's disease brain. *Neurosci.Lett.* **58**: 343-346.

Kishima, H., Poyot, T., Bloch, J., Dauguet, J., Conde, F., Dolle, F., Hinnen, F., Pralong, W., Palfi, S., Deglon, N., Aebischer, P., and Hantraye, P. (2004). Encapsulated GDNF-producing C2C12 cells for Parkinson's disease: a pre-clinical study in chronic MPTP-treated baboons. *Neurobiol.Dis.* **16**: 428-439.

Klein, R. L., King, M. A., Hamby, M. E., and Meyer, E. M. (20-3-2002). Dopaminergic cell loss induced by human A30P alpha-synuclein gene transfer to the rat substantia nigra. *Hum.Gene Ther.* **13**: 605-612.

Kügler, S., Kilic, E., and Bähr, M. (2003a). Human synapsin 1 gene promoter confers highly neuron-specific long-term transgene expression from an adenoviral vector in the adult rat brain depending on the transduced area. *Gene Ther.* **10**: 337-347.

Kügler, S., Lingor, P., Schöll, U., Zolotukhin, S., and Bähr, M. (20-6-2003b). Differential transgene expression in brain cells in vivo and in vitro from AAV-2 vectors with small transcriptional control units. *Virology* **311**: 89-95.

Kügler, S., Meyn, L., Holzmuller, H., Gerhardt, E., Isenmann, S., Schulz, J. B., and Bähr, M. (2001). Neuron-specific expression of therapeutic proteins: evaluation of different cellular promoters in recombinant adenoviral vectors. *Mol.Cell Neurosci.* **17**: 78-96.

Lang, A. E., Gill, S., Patel, N. K., Lozano, A., Nutt, J. G., Penn, R., Brooks, D. J., Hotton, G., Moro, E., Heywood, P., Brodsky, M. A., Burchiel, K., Kelly, P., Dalvi, A., Scott, B., Stacy, M., Turner, D., Wooten, V. G., Elias, W. J., Laws, E. R., Dhawan, V., Stoessl, A. J., Matcham, J., Coffey, R. J., and Traub, M. (2006). Randomized controlled trial of intraputamenal glial cell line-derived neurotrophic factor infusion in Parkinson disease. *Ann.Neurol.* **59**: 459-466.

Lang, A. E. and Lozano, A. M. (15-10-1998). Parkinson's disease. Second of two parts. *N Engl.J.Med.* **339**: 1130-1143.

Leroy, E., Boyer, R., Auburger, G., Leube, B., Ulm, G., Mezey, E., Harta, G., Brownstein, M. J., Jonnalagada, S., Chernova, T., Dehejia, A., Lavedan, C., Gasser, T., Steinbach, P. J., Wilkinson, K. D., and Polymeropoulos, M. H. (1-10-1998). The ubiquitin pathway in Parkinson's disease. *Nature* **395**: 451-452.

Li, H., Li, S. H., Yu, Z. X., Shelbourne, P., and Li, X. J. (1-11-2001). Huntingtin aggregate-associated axonal degeneration is an early pathological event in Huntington's disease mice. *J.Neurosci.* **21**: 8473-8481.

Liljestrom, P. and Garoff, H. (1991). A new generation of animal cell expression vectors based on the Semliki Forest virus replicon. *Biotechnology (N.Y.)* **9**: 1356-1361.

Lim, P. S., Jenson, A. B., Cowser, L., Nakai, Y., Lim, L. Y., Jin, X. W., and Sundberg, J. P. (1990). Distribution and specific identification of papillomavirus major capsid protein epitopes by immunocytochemistry and epitope scanning of synthetic peptides. *J.Infect.Dis.* **162**: 1263-1269.

Lin, L. F., Doherty, D. H., Lile, J. D., Bektesh, S., and Collins, F. (21-5-1993). GDNF: a glial cell line-derived neurotrophic factor for midbrain dopaminergic neurons. *Science* **260**: 1130-1132.

- Liu, S. and Altman, R. B. (15-8-2003). Large scale study of protein domain distribution in the context of alternative splicing. *Nucleic Acids Res.* **31**: 4828-4835.
- Lo, B. C., Deglon, N., Pralong, W., and Aebsicher, P. (2004). Lentiviral nigral delivery of GDNF does not prevent neurodegeneration in a genetic rat model of Parkinson's disease. *Neurobiol. Dis.* **17**: 283-289.
- Lomri, N., Perret, C., Gouhier, N., and Thomasset, M. (1-8-1989). Cloning and analysis of calbindin-D28K cDNA and its expression in the central nervous system. *Gene* **80**: 87-98.
- Lotharius, J. and Brundin, P. (1-10-2002a). Impaired dopamine storage resulting from alpha-synuclein mutations may contribute to the pathogenesis of Parkinson's disease. *Hum.Mol.Genet.* **11**: 2395-2407.
- Lotharius, J. and Brundin, P. (2002b). Pathogenesis of Parkinson's disease: dopamine, vesicles and alpha-synuclein. *Nat.Rev.Neurosci.* **3**: 932-942.
- Love, S., Plaha, P., Patel, N. K., Hotton, G. R., Brooks, D. J., and Gill, S. S. (2005). Glial cell line-derived neurotrophic factor induces neuronal sprouting in human brain. *Nat.Med.* **11**: 703-704.
- Lundstrom, K. (2005). Biology and application of alphaviruses in gene therapy. *Gene Ther.* **12 Suppl 1**: S92-S97.
- Lundstrom, K., Abenavoli, A., Malgaroli, A., and Ehrengruber, M. U. (2003). Novel Semliki Forest virus vectors with reduced cytotoxicity and temperature sensitivity for long-term enhancement of transgene expression. *Mol.Ther.* **7**: 202-209.
- Malik, J. M., Shevtsova, Z., Bähr, M., and Kügler, S. (2005). Long-term in vivo inhibition of CNS neurodegeneration by Bcl-XL gene transfer. *Mol.Ther.* **11**: 373-381.
- Marini, P., Jendrossek, V., Durand, E., Gruber, C., Budach, W., and Belka, C. (2003). Molecular requirements for the combined effects of TRAIL and ionising radiation. *Radiother.Oncol.* **68**: 189-198.
- Marjama-Lyons, J. M. and Koller, W. C. (2001). Parkinson's disease. Update in diagnosis and symptom management. *Geriatrics* **56**: 24-30, 33.
- Mastakov, M. Y., Baer, K., Symes, C. W., Leichtlein, C. B., Kotin, R. M., and During, M. J. (2002). Immunological aspects of recombinant adeno-associated virus delivery to the mammalian brain. *J.Viro.* **76**: 8446-8454.
- Mattson, M. P. and Chan, S. L. (2003). Calcium orchestrates apoptosis. *Nat.Cell Biol.* **5**: 1041-1043.
- Melov, S. (2004). Modeling mitochondrial function in aging neurons. *Trends Neurosci.* **27**: 601-606.
- Michel, U., Malik, I., Ebert, S., Bähr, M., and Kügler, S. (14-1-2005). Long-term in vivo and in vitro AAV-2-mediated RNA interference in rat retinal ganglion cells and cultured primary neurons. *Biochem.Biophys.Res.Commun.* **326**: 307-312.
- Moskalenko, M., Chen, L., van Roey, M., Donahue, B. A., Snyder, R. O., McArthur, J. G., and Patel, S. D. (2000). Epitope mapping of human anti-adeno-associated virus type 2

neutralizing antibodies: implications for gene therapy and virus structure. *J.Virol.* **74:** 1761-1766.

Motoyama, N., Wang, F., Roth, K. A., Sawa, H., Nakayama, K., Nakayama, K., Negishi, I., Senju, S., Zhang, Q., Fujii, S., and . (10-3-1995). Massive cell death of immature hematopoietic cells and neurons in Bcl-x-deficient mice. *Science* **267:** 1506-1510.

Nakajima, A., Kataoka, K., Hong, M., Sakaguchi, M., and Huh, N. H. (25-11-2003). BRPK, a novel protein kinase showing increased expression in mouse cancer cell lines with higher metastatic potential. *Cancer Lett.* **201:** 195-201.

Natsume, A., Mata, M., Goss, J., Huang, S., Wolfe, D., Oligino, T., Glorioso, J., and Fink, D. J. (2001). Bcl-2 and GDNF delivered by HSV-mediated gene transfer act additively to protect dopaminergic neurons from 6-OHDA-induced degeneration. *Exp.Neurol.* **169:** 231-238.

Natsume, A., Mata, M., Wolfe, D., Oligino, T., Goss, J., Huang, S., Glorioso, J., and Fink, D. J. (2002). Bcl-2 and GDNF delivered by HSV-mediated gene transfer after spinal root avulsion provide a synergistic effect. *J.Neurotrauma* **19:** 61-68.

Newmeyer, D. D. and Ferguson-Miller, S. (21-2-2003). Mitochondria: releasing power for life and unleashing the machineries of death. *Cell* **112:** 481-490.

Nutt, J. G., Burchiel, K. J., Comella, C. L., Jankovic, J., Lang, A. E., Laws, E. R., Jr., Lozano, A. M., Penn, R. D., Simpson, R. K., Jr., Stacy, M., and Wooten, G. F. (14-1-2003). Randomized, double-blind trial of glial cell line-derived neurotrophic factor (GDNF) in PD. *Neurology* **60:** 69-73.

Offen, D., Beart, P. M., Cheung, N. S., Pascoe, C. J., Hochman, A., Gorodin, S., Melamed, E., Bernard, R., and Bernard, O. (12-5-1998). Transgenic mice expressing human Bcl-2 in their neurons are resistant to 6-hydroxydopamine and 1-methyl-4-phenyl-1,2,3,6-tetrahydropyridine neurotoxicity. *Proc.Natl.Acad.Sci.U.S.A* **95:** 5789-5794.

Olanow, C. W. and Stocchi, F. (13-1-2004). COMT inhibitors in Parkinson's disease: can they prevent and/or reverse levodopa-induced motor complications? *Neurology* **62:** S72-S81.

Opie, S. R., Warrington, K. H., Jr., Agbandje-McKenna, M., Zolotukhin, S., and Muzyczka, N. (2003). Identification of amino acid residues in the capsid proteins of adeno-associated virus type 2 that contribute to heparan sulfate proteoglycan binding. *J.Virol.* **77:** 6995-7006.

Paratcha, G., Ledda, F., and Ibanez, C. F. (27-6-2003). The neural cell adhesion molecule NCAM is an alternative signaling receptor for GDNF family ligands. *Cell* **113:** 867-879.

Parker, W. D., Jr., Boyson, S. J., and Parks, J. K. (1989). Abnormalities of the electron transport chain in idiopathic Parkinson's disease. *Ann.Neurol.* **26:** 719-723.

Passini, M. A., Watson, D. J., Vite, C. H., Landsburg, D. J., Feigenbaum, A. L., and Wolfe, J. H. (2003). Intraventricular brain injection of adeno-associated virus type 1 (AAV1) in neonatal mice results in complementary patterns of neuronal transduction to AAV2 and total long-term correction of storage lesions in the brains of beta-glucuronidase-deficient mice. *J.Virol.* **77:** 7034-7040.

- Patel, N. K., Bunnage, M., Plaha, P., Svendsen, C. N., Heywood, P., and Gill, S. S. (2005). Intraputamenal infusion of glial cell line-derived neurotrophic factor in PD: a two-year outcome study. *Ann.Neurol.* **57**: 298-302.
- Paterna, J. C., Feldon, J., and Bueler, H. (2004). Transduction profiles of recombinant adeno-associated virus vectors derived from serotypes 2 and 5 in the nigrostriatal system of rats. *J.Virol.* **78**: 6808-6817.
- Peel, A. L. and Klein, R. L. (1-6-2000). Adeno-associated virus vectors: activity and applications in the CNS. *J.Neurosci.Methods* **98**: 95-104.
- Peel, A. L., Zolotukhin, S., Schrimsher, G. W., Muzyczka, N., and Reier, P. J. (1997). Efficient transduction of green fluorescent protein in spinal cord neurons using adeno-associated virus vectors containing cell type-specific promoters. *Gene Ther.* **4**: 16-24.
- Perrelet, D., Ferri, A., MacKenzie, A. E., Smith, G. M., Korneluk, R. G., Liston, P., Sagot, Y., Terrado, J., Monnier, D., and Kato, A. C. (2000). IAP family proteins delay motoneuron cell death in vivo. *Eur.J.Neurosci.* **12**: 2059-2067.
- Picada, J. N., Roesler, R., and Henriques, J. A. (2005). Genotoxic, neurotoxic and neuroprotective activities of apomorphine and its oxidized derivative 8-oxo-apomorphine. *Braz.J.Med.Biol.Res.* **38**: 477-486.
- Previtali, S. C., Quattrini, A., Fasolini, M., Panzeri, M. C., Villa, A., Filbin, M. T., Li, W., Chiu, S. Y., Messing, A., Wrabetz, L., and Feltri, M. L. (27-11-2000). Epitope-tagged P(0) glycoprotein causes Charcot-Marie-Tooth-like neuropathy in transgenic mice. *J.Cell Biol.* **151**: 1035-1046.
- Qin, Z. H., Chen, R. W., Wang, Y., Nakai, M., Chuang, D. M., and Chase, T. N. (15-5-1999). Nuclear factor kappaB nuclear translocation upregulates c-Myc and p53 expression during NMDA receptor-mediated apoptosis in rat striatum. *J.Neurosci.* **19**: 4023-4033.
- Qing, K., Mah, C., Hansen, J., Zhou, S., Dwarki, V., and Srivastava, A. (1999). Human fibroblast growth factor receptor 1 is a co-receptor for infection by adeno-associated virus 2. *Nat.Med.* **5**: 71-77.
- Rabinowitz, J. E., Bowles, D. E., Faust, S. M., Ledford, J. G., Cunningham, S. E., and Samulski, R. J. (2004). Cross-dressing the virion: the transcapsidation of adeno-associated virus serotypes functionally defines subgroups. *J.Virol.* **78**: 4421-4432.
- Ramer, M. S., Priestley, J. V., and McMahon, S. B. (20-1-2000). Functional regeneration of sensory axons into the adult spinal cord. *Nature* **403**: 312-316.
- Rideout, H. J. and Stefanis, L. (2001). Caspase inhibition: a potential therapeutic strategy in neurological diseases. *Histol.Histopathol.* **16**: 895-908.
- Riederer, P. and Wuketich, S. (1976). Time course of nigrostriatal degeneration in parkinson's disease. A detailed study of influential factors in human brain amine analysis. *J.Neural Transm.* **38**: 277-301.
- Rioux, L., Gaudin, D. P., Gagnon, C., Di Paolo, T., and Bedard, P. J. (1991). Decrease of behavioral and biochemical denervation supersensitivity of rat striatum by nigral transplants. *Neuroscience* **44**: 75-83.

- Rizzuto, R., Pinton, P., Brini, M., Chiesa, A., Filippin, L., and Pozzan, T. (1999). Mitochondria as biosensors of calcium microdomains. *Cell Calcium* **26**: 193-199.
- Rosenblad, C., Georgievska, B., and Kirik, D. (2003). Long-term striatal overexpression of GDNF selectively downregulates tyrosine hydroxylase in the intact nigrostriatal dopamine system. *Eur.J.Neurosci.* **17**: 260-270.
- Rosenblad, C., Kirik, D., and Björklund, A. (2000). Sequential administration of GDNF into the substantia nigra and striatum promotes dopamine neuron survival and axonal sprouting but not striatal reinnervation or functional recovery in the partial 6-OHDA lesion model. *Exp.Neurol.* **161**: 503-516.
- Sambrook, J., Fritsch, E. F., and Maniatis, T. Molecular Cloning: A Laboratory Manual. [2nd ed.]. 1989. Cold Spring Harbor, Cold Spring Harbor Laboratory Press.
- Samulski, R. J., Chang, L. S., and Shenk, T. (1989). Helper-free stocks of recombinant adeno-associated viruses: normal integration does not require viral gene expression. *J.Viro.* **63**: 3822-3828.
- Sariola, H. and Saarma, M. (1-10-2003). Novel functions and signalling pathways for GDNF. *J.Cell Sci.* **116**: 3855-3862.
- Sattler, M., Liang, H., Nettesheim, D., Meadows, R. P., Harlan, J. E., Eberstadt, M., Yoon, H. S., Shuker, S. B., Chang, B. S., Minn, A. J., Thompson, C. B., and Fesik, S. W. (14-2-1997). Structure of Bcl-xL-Bak peptide complex: recognition between regulators of apoptosis. *Science* **275**: 983-986.
- Schaar, D. G., Sieber, B. A., Dreyfus, C. F., and Black, I. B. (1993). Regional and cell-specific expression of GDNF in rat brain. *Exp.Neurol.* **124**: 368-371.
- Schapira, A. H. (1994). Evidence for mitochondrial dysfunction in Parkinson's disease--a critical appraisal. *Mov Disord.* **9**: 125-138.
- Schapira, A. H., Cooper, J. M., Dexter, D., Clark, J. B., Jenner, P., and Marsden, C. D. (1990). Mitochondrial complex I deficiency in Parkinson's disease. *J.Neurochem.* **54**: 823-827.
- Schapira, A. H., Cooper, J. M., Dexter, D., Jenner, P., Clark, J. B., and Marsden, C. D. (3-6-1989). Mitochondrial complex I deficiency in Parkinson's disease. *Lancet* **1**: 1269.
- Schmidt, R. H., Björklund, A., Stenevi, U., Dunnett, S. B., and Gage, F. H. (1983). Intracerebral grafting of neuronal cell suspensions. III. Activity of intrastriatal nigral suspension implants as assessed by measurements of dopamine synthesis and metabolism. *Acta Physiol Scand.Supp* **522**: 19-28.
- Seniuk, N. A., Tatton, W. G., and Greenwood, C. E. (10-9-1990). Dose-dependent destruction of the coeruleus-cortical and nigral-striatal projections by MPTP. *Brain Res.* **527**: 7-20.
- Shapiro, L., Doyle, J. P., Hensley, P., Colman, D. R., and Hendrickson, W. A. (1996). Crystal structure of the extracellular domain from P0, the major structural protein of peripheral nerve myelin. *Neuron* **17**: 435-449.

- Shevtsova, Z., Malik, J. M., Michel, U., Bähr, M., and Kügler, S. (2005). Promoters and serotypes: targeting of adeno-associated virus vectors for gene transfer in the rat central nervous system in vitro and in vivo. *Exp.Physiol* **90**: 53-59.
- Shindler, K. S., Latham, C. B., and Roth, K. A. (1-5-1997). Bax deficiency prevents the increased cell death of immature neurons in bcl-x-deficient mice. *J.Neurosci.* **17**: 3112-3119.
- Sian, J., Dexter, D. T., Lees, A. J., Daniel, S., Agid, Y., Javoy-Agid, F., Jenner, P., and Marsden, C. D. (1994). Alterations in glutathione levels in Parkinson's disease and other neurodegenerative disorders affecting basal ganglia. *Ann.Neurol.* **36**: 348-355.
- Sofic, E., Lange, K. W., Jellinger, K., and Riederer, P. (17-8-1992). Reduced and oxidized glutathione in the substantia nigra of patients with Parkinson's disease. *Neurosci.Lett.* **142**: 128-130.
- Sofic, E., Riederer, P., Heinsen, H., Beckmann, H., Reynolds, G. P., Hebenstreit, G., and Youdim, M. B. (1988). Increased iron (III) and total iron content in post mortem substantia nigra of parkinsonian brain. *J.Neural Transm.* **74**: 199-205.
- Srivastava, A., Lusby, E. W., and Berns, K. I. (1983). Nucleotide sequence and organization of the adeno-associated virus 2 genome. *J.Viro.* **45**: 555-564.
- Staniek, K., Gille, L., Kozlov, A. V., and Nohl, H. (2002). Mitochondrial superoxide radical formation is controlled by electron bifurcation to the high and low potential pathways. *Free Radic.Res.* **36**: 381-387.
- Stieger, K., Le Meur, G., Lasne, F., Weber, M., Deschamps, J. Y., Nivard, D., Mendes-Madeira, A., Provost, N., Martin, L., Moullier, P., and Rolling, F. (24-1-2006). Long-term doxycycline-regulated transgene expression in the retina of nonhuman primates following subretinal injection of recombinant AAV vectors. *Mol.Ther.*
- Stokes, A. H., Hastings, T. G., and Vrana, K. E. (15-3-1999). Cytotoxic and genotoxic potential of dopamine. *J.Neurosci.Res.* **55**: 659-665.
- Stokin, G. B., Lillo, C., Falzone, T. L., Brusch, R. G., Rockenstein, E., Mount, S. L., Raman, R., Davies, P., Masliah, E., Williams, D. S., and Goldstein, L. S. (25-2-2005). Axonopathy and transport deficits early in the pathogenesis of Alzheimer's disease. *Science* **307**: 1282-1288.
- Straten, G., Schmeer, C., Kretz, A., Gerhardt, E., Kügler, S., Schulz, J. B., Gravel, C., Bähr, M., and Isenmann, S. (2002). Potential synergistic protection of retinal ganglion cells from axotomy-induced apoptosis by adenoviral administration of glial cell line-derived neurotrophic factor and X-chromosome-linked inhibitor of apoptosis. *Neurobiol.Dis.* **11**: 123-133.
- Strauss, J. H. and Strauss, E. G. (1994). The alphaviruses: gene expression, replication, and evolution. *Microbiol.Rev.* **58**: 491-562.
- Strauss, K. M., Martins, L. M., Plun-Favreau, H., Marx, F. P., Kautzmann, S., Berg, D., Gasser, T., Wszolek, Z., Muller, T., Bornemann, A., Wolburg, H., Downward, J., Riess, O., Schulz, J. B., and Krüger, R. (1-8-2005). Loss of function mutations in the gene encoding Omi/HtrA2 in Parkinson's disease. *Hum.Mol.Genet.* **14**: 2099-2111.

- Strelau, J. and Unsicker, K. (1999). GDNF family members and their receptors: expression and functions in two oligodendroglial cell lines representing distinct stages of oligodendroglial development. *Glia* **26**: 291-301.
- Sulzer, D., Sonders, M. S., Poulsen, N. W., and Galli, A. (2005). Mechanisms of neurotransmitter release by amphetamines: a review. *Prog.Neurobiol.* **75**: 406-433.
- Sulzer, D. and Zecca, L. (2000). Intraneuronal dopamine-quinone synthesis: a review. *Neurotox.Res.* **1**: 181-195.
- Summerford, C., Bartlett, J. S., and Samulski, R. J. (1999). AlphaVbeta5 integrin: a co-receptor for adeno-associated virus type 2 infection. *Nat.Med.* **5**: 78-82.
- Sun, L., Li, J., and Xiao, X. (2000). Overcoming adeno-associated virus vector size limitation through viral DNA heterodimerization. *Nat.Med.* **6**: 599-602.
- Takahashi, M. (2001). The GDNF/RET signaling pathway and human diseases. *Cytokine Growth Factor Rev.* **12**: 361-373.
- Tenenbaum, L., Chtarto, A., Lehtonen, E., Velu, T., Brotchi, J., and Levivier, M. (2004). Recombinant AAV-mediated gene delivery to the central nervous system. *J.Gene Med.* **6 Suppl 1**: S212-S222.
- Terpe, K. (2003). Overview of tag protein fusions: from molecular and biochemical fundamentals to commercial systems. *Appl.Microbiol.Biotechnol.* **60**: 523-533.
- Thress, K., Kornbluth, S., and Smith, J. J. (1999). Mitochondria at the crossroad of apoptotic cell death. *J.Bioenerg.Biomembr.* **31**: 321-326.
- Tretter, L., Sipos, I., and Adam-Vizi, V. (2004). Initiation of neuronal damage by complex I deficiency and oxidative stress in Parkinson's disease. *Neurochem.Res.* **29**: 569-577.
- Trupp, M., Arenas, E., Fainzilber, M., Nilsson, A. S., Sieber, B. A., Grigoriou, M., Kilkenny, C., Salazar-Grueso, E., Pachnis, V., and Arumae, U. (27-6-1996). Functional receptor for GDNF encoded by the c-ret proto-oncogene. *Nature* **381**: 785-789.
- Trupp, M., Scott, R., Whittemore, S. R., and Ibanez, C. F. (23-7-1999). Ret-dependent and -independent mechanisms of glial cell line-derived neurotrophic factor signaling in neuronal cells. *J.Biol.Chem.* **274**: 20885-20894.
- Ungerstedt, U. (1968). 6-Hydroxy-dopamine induced degeneration of central monoamine neurons. *Eur.J.Pharmacol.* **5**: 107-110.
- Ungerstedt, U. and Arbuthnott, G. W. (18-12-1970). Quantitative recording of rotational behavior in rats after 6-hydroxy-dopamine lesions of the nigrostriatal dopamine system. *Brain Res.* **24**: 485-493.
- Unoki, M. and Nakamura, Y. (27-7-2001). Growth-suppressive effects of BPOZ and EGR2, two genes involved in the PTEN signaling pathway. *Oncogene* **20**: 4457-4465.
- Valente, E. M., Abou-Sleiman, P. M., Caputo, V., Muqit, M. M., Harvey, K., Gispert, S., Ali, Z., Del Turco, D., Bentivoglio, A. R., Healy, D. G., Albanese, A., Nussbaum, R., Gonzalez-Maldonado, R., Deller, T., Salvi, S., Cortelli, P., Gilks, W. P., Latchman, D. S., Harvey, R. J.,

Dallapiccola, B., Auburger, G., and Wood, N. W. (21-5-2004). Hereditary early-onset Parkinson's disease caused by mutations in PINK1. *Science* **304**: 1158-1160.

van Adel, B. A., Kostic, C., Deglon, N., Ball, A. K., and Arsenijevic, Y. (20-1-2003). Delivery of ciliary neurotrophic factor via lentiviral-mediated transfer protects axotomized retinal ganglion cells for an extended period of time. *Hum.Gene Ther.* **14**: 103-115.

Van Den Eeden, S. K., Tanner, C. M., Bernstein, A. L., Fross, R. D., Leimpeter, A., Bloch, D. A., and Nelson, L. M. (1-6-2003). Incidence of Parkinson's disease: variation by age, gender, and race/ethnicity. *Am.J.Epidemiol.* **157**: 1015-1022.

von Bohlen und Halbach O., Schober, A., and Kriegstein, K. (2004). Genes, proteins, and neurotoxins involved in Parkinson's disease. *Prog.Neurobiol.* **73**: 151-177.

Wagenknecht, B., Glaser, T., Naumann, U., Kügler, S., Isenmann, S., Bähr, M., Korneluk, R., Liston, P., and Weller, M. (1999). Expression and biological activity of X-linked inhibitor of apoptosis (XIAP) in human malignant glioma. *Cell Death.Differ.* **6**: 370-376.

Walters, R. W., Yi, S. M., Keshavjee, S., Brown, K. E., Welsh, M. J., Chiorini, J. A., and Zabner, J. (8-6-2001). Binding of adeno-associated virus type 5 to 2,3-linked sialic acid is required for gene transfer. *J.Biol.Chem.* **276**: 20610-20616.

Wang, H. Y., Baxter, C. F., Jr., and Schulz, H. (1991). Regulation of fatty acid beta-oxidation in rat heart mitochondria. *Arch.Biochem.Biophys.* **289**: 274-280.

Wang, L., Muramatsu, S., Lu, Y., Ikeguchi, K., Fujimoto, K., Okada, T., Mizukami, H., Hanazono, Y., Kume, A., Urano, F., Ichinose, H., Nagatsu, T., Nakano, I., and Ozawa, K. (2002). Delayed delivery of AAV-GDNF prevents nigral neurodegeneration and promotes functional recovery in a rat model of Parkinson's disease. *Gene Ther.* **9**: 381-389.

Weise, J., Isenmann, S., Klöcker, N., Kügler, S., Hirsch, S., Gravel, C., and Bähr, M. (2000). Adenovirus-mediated expression of ciliary neurotrophic factor (CNTF) rescues axotomized rat retinal ganglion cells but does not support axonal regeneration in vivo. *Neurobiol.Dis.* **7**: 212-223.

Wilson, I. A., Niman, H. L., Houghten, R. A., Cherenson, A. R., Connolly, M. L., and Lerner, R. A. (1984). The structure of an antigenic determinant in a protein. *Cell* **37**: 767-778.

Wong, L. F., Ralph, G. S., Walmsley, L. E., Bienemann, A. S., Parham, S., Kingsman, S. M., Uney, J. B., and Mazarakis, N. D. (2005). Lentiviral-mediated delivery of Bcl-2 or GDNF protects against excitotoxicity in the rat hippocampus. *Mol.Ther.* **11**: 89-95.

Woo, Y. J., Zhang, J. C., Taylor, M. D., Cohen, J. E., Hsu, V. M., and Sweeney, H. L. (28-4-2005). One year transgene expression with adeno-associated virus cardiac gene transfer. *Int.J.Cardiol.* **100**: 421-426.

Yamada, M., Oligino, T., Mata, M., Goss, J. R., Glorioso, J. C., and Fink, D. J. (30-3-1999). Herpes simplex virus vector-mediated expression of Bcl-2 prevents 6-hydroxydopamine-induced degeneration of neurons in the substantia nigra in vivo. *Proc.Natl.Acad.Sci.U.S.A* **96**: 4078-4083.

Zhang, J., Perry, G., Smith, M. A., Robertson, D., Olson, S. J., Graham, D. G., and Montine, T. J. (1999). Parkinson's disease is associated with oxidative damage to cytoplasmic DNA and RNA in substantia nigra neurons. *Am.J.Pathol.* **154**: 1423-1429.

Zhang, L., Shimoji, M., Thomas, B., Moore, D. J., Yu, S. W., Marupudi, N. I., Torp, R., Torgner, I. A., Ottersen, O. P., Dawson, T. M., and Dawson, V. L. (15-7-2005). Mitochondrial localization of the Parkinson's disease related protein DJ-1: implications for pathogenesis. *Hum.Mol.Genet.* **14**: 2063-2073.

Curriculum vitae

Personal details:

Name: Zinayida Shevtsova

Citizenship: Ukrainian

Date of birth: 12 August 1978

Place of birth: Dnipropetrovsk, Ukraine

Marital status: Single

Education:

1993-1995 High school N 23, Dnipropetrovsk, Ukraine

Graduation with honours

1995-2001 Dnipropetrovsk State Medical Academy, Dnipropetrovsk, Ukraine

Diploma in general medicine with honours

1999/ Oct-Dec Clinical clerkship rotation, University of Rochester

School of Medicine and Dentistry, USA

2001-2002 International MSc/MD/PhD program in Neurosciences, Göttingen, Germany

Completion of the 1st MSc year, admission to the PhD

2002-2006 Department of Neurology, University Hospital, Göttingen, Germany

PhD project in the framework of the International MSc/MD/PhD
program in Neurosciences

Publications

Shevtsova, Z., Malik, I. J. M., Michel, U., Bähr, M., and Kügler, S. (2005). Promoters and serotypes: targeting of adeno-associated virus vectors for gene transfer in the rat central nervous system in vitro and in vivo. *Exp.Physiol* **90**: 53-59.

Shevtsova, Z., Malik, J. M. I., Michel, U., Schöll, U., Bähr, M., Kügler, S. (2006). Evaluation of epitope tags for protein detection after *in vivo* CNS gene transfer. *EJN* (accepted for publication, Feb 2006)

Shevtsova, Z., Malik, I. J. M., Garrido, M., Schöll, U., Bähr, M., and Kügler, S. (2006). Potentiation of *in vivo* neuroprotection by BclX_L and GDNF co-expression depends on post-lesion time in deafferentiated CNS neurons. (submitted)

Malik, J. M., **Shevtsova, Z.**, Bähr, M., and Kügler, S. (2005). Long-term *in vivo* inhibition of CNS neurodegeneration by Bcl-XL gene transfer. *Mol.Ther.* **11**: 373-381.